



SOLERAS

**Solar Energy Water Desalination Project**

---

**PILOT PLANT  
FINAL REPORT**

**Martin Marietta Corporation**

---

**Midwest Research Institute, Operating Agent**

MRI/SOL 0406  
Distribution Category UC-62b and 62c

**Solar Energy Water Desalination Project**

---

**PILOT PLANT FINAL REPORT**

**Martin Marietta Corporation**

---

Published for the  
United States – Saudi Arabian Joint Program  
for Cooperation in the Field of Solar Energy  
SOLERAS

by the Program Operating Agent  
Midwest Research Institute  
425 Volker Boulevard  
Kansas City, Missouri 64110 USA

Available from the National Technical Information Service, U.S. Department of Commerce, Springfield, Virginia 22161.

Price: Printed Copy A08

Microfiche A01

Codes are used for pricing all publications. The code is determined by the number of pages in the publication. Information pertaining to the pricing codes can be found in the current issues of the following publications, which are generally available in most libraries: *Energy Research Abstracts (ERA)*; *Government Reports Announcements and Index (GRA and I)*; *Scientific and Technical Abstract Reports (STAR)*; and publication NTIS-PR-360 available from NTIS at the above address.

#### NOTICE

This report was prepared as an account of work sponsored by the United States Department of Energy and by the Saudi Arabian National Center for Science and Technology. Neither the Kingdom of Saudi Arabia nor the United States nor any agency thereof, nor any of their employees, makes any warranty, expressed or implied, or assumes any legal liability or responsibility for any third party's use or the results of such use of any information, apparatus, product, or process disclosed in this report, or represents that its use by such third party would not infringe privately-owned rights.

# FOREWORD

## THE SOLERAS PROGRAM: A UNIQUE EFFORT IN COOPERATIVE SOLAR ENERGY RESEARCH

In October 1977, Saudi Arabia and the United States signed a Program Agreement for Cooperation in the Field of Solar Energy. The Program, named SOLERAS, is the first of its kind in purpose, funding, organization, and results. It is based on the respective commitments of the United States and Saudi Arabia to advance the development of solar energy as a viable cost-competitive energy alternative, by combining the technical and other unique resources of each country. SOLERAS has made significant progress in demonstrating the effectiveness of solar energy—progress that would have been difficult for either country to achieve on its own.

SOLERAS is sponsored by the government agencies responsible for energy research and development in each country: the Saudi Arabian National Center for Science and Technology (SANCST) and the United States Department of Energy. The Program is under the auspices of the United States-Saudi Arabian Joint Commission on Economic Cooperation, formed in 1974 by the Saudi Arabian Ministry of Finance and National Economy and the United States Department of the Treasury.

Although SOLERAS is only one of more than 30 such projects under the direction of the Joint Commission, it is the only one that is funded by both countries. All other projects are funded completely by Saudi Arabia. This jointly funded program is evidence, therefore, that both countries recognize the mutually beneficial results expected to be generated by the cooperative research projects undertaken by SOLERAS.

The administration of SOLERAS also reflects the philosophy of cooperation underlying this unique Program. Senior officials from SANCST, the Ministry of Finance and National Economy, the U.S. Department of Energy, and the U.S. Department of the Treasury comprise an eight-member Executive Board which governs all aspects of the SOLERAS Program. The Board establishes the goals, objectives, and policies of SOLERAS and oversees the technical and financial management of the projects undertaken to implement those goals and objectives.

A four-member Project Selection Committee, with two members from each government, assists the Executive Board in selecting and evaluating projects. Its members combine their technical expertise and experience in renewable energy technologies and demonstration projects to review proposals, designs, plans, reports, operations, and data for the various projects.

The daily technical and administrative management of the SOLERAS projects is the responsibility of Midwest Research Institute, an independent, not-for-profit research organization, which has been designated as the SOLERAS Operating Agent. MRI utilizes technical and managerial personnel from both countries in fulfilling its responsibility for implementing the decisions of the Executive Board and in managing the individual technical projects. This includes contracting with various companies and research organizations in both countries to design and install state-of-the-art solar systems. SOLERAS program offices are located at MRI's Kansas City, Missouri, headquarters, and in Riyadh and Yanbu, Saudi Arabia.

SOLERAS has initiated several major research projects: converting solar energy into electricity for everyday use by the inhabitants of several rural villages; testing solar energy as a source for space cooling and water treatment; developing agricultural systems using solar energy to control the entire growing environment; undertaking fundamental photovoltaic and solar thermal research; establishing high technology laboratories for advanced solar research at Saudi Arabian universities; and sponsoring basic solar energy research in universities in the United States.

In addition, SOLERAS has contributed to the dissemination of scientific and technical solar information through its sponsorship of technology workshops, short courses, and the publication of technical reports. These have provided an important means of informing the scientific research community about the solar energy technologies developed under SOLERAS and other relevant projects throughout the world.

## تقديم

### «البرنامج السعودي الأمريكي المشترك» للتعاون في ميدان أبحاث الطاقة الشمسية

وقعت المملكة العربية السعودية والولايات المتحدة الأمريكية في عام ١٩٧٧م اتفاقية برنامج التعاون في ميدان أبحاث الطاقة الشمسية . وكان هذا البرنامج الذي سُمِّي «سوليراس» الأول من نوعه من حيث الغرض والتمويل والتنظيم والنتائج . وهو معتمد على الالتزام المتبادل بين الولايات المتحدة الأمريكية والمملكة العربية السعودية بالعمل على تنمية الطاقة الشمسية ، بوصفها طاقة بديلة متجددة وذات كلفة منافسة ، عن طريق الجمع للموارد الفنية وغيرها من المصادر الطبيعية لكل من البلدين . ولقد حقق برنامج «سوليراس» تقدماً ملحوظاً ببيان فعالية الطاقة الشمسية ، وهو تقدّم قد يكون من الصعب تحقيقه على أي من البلدين منفرداً .

يتم إنجاز برنامج «سوليراس» تحت رعاية الهيئات الحكومية المسؤولة عن أبحاث وتنمية الطاقة في كل من البلدين ، أي المركز الوطني السعودي للعلوم والتكنولوجيا ووزارة الطاقة الأمريكية . وتشرف على البرنامج اللجنة الأمريكية السعودية المشتركة للتعاون الاقتصادي المكوّنة عام ١٩٧٤م من قبل وزارة المالية والاقتصاد الوطني في المملكة العربية السعودية ووزارة المالية في الولايات المتحدة الأمريكية .

بالرغم من أن برنامج «سوليراس» هو واحد من بين ما يزيد عن ٣٠ مشروعاً تديرها اللجنة المشتركة فإنه البرنامج الوحيد الذي يموله البلدان ، في حين أن جميع البرامج الأخرى تمولها المملكة العربية السعودية كلياً . فيبرهن هذا البرنامج ، المشترك التمويل ، على أن كلا البلدين يعترفان بالفوائد المتبادلة المتوقع تحقيقها من خلال مشاريع البحث التعاوني التي يتداولها برنامج «سوليراس» .

وتعكس إدارة «سوليراس» أيضاً فلسفة التعاون التي يستند عليها هذا البرنامج . فيشكل مسؤولون من المركز الوطني السعودي للعلوم والتكنولوجيا ومن وزارة المالية والاقتصاد الوطني ومن وزارة الطاقة الأمريكية ووزارة المالية الأمريكية مجلساً تنفيذياً يضم ثمانية أعضاء ويدير جميع جوانب برنامج «سوليراس» . فيحدّد هذا المجلس أهداف وغايات وسياسة «سوليراس» كما يشرف على الإدارة الفنية والمالية للمشاريع المباشرة لتحقيق هذه الأهداف والغايات .

تقوم لجنة اختيار المشاريع المكوّنة من أربعة أعضاء ، اثنان من كل جانب بمساعدة المجلس التنفيذي في اختيار وتقييم المشاريع . فيجمع أعضاء هذه اللجنة خبرتهم الفنية وتجربتهم في مجال تكنولوجيا الطاقة المتجددة والمشاريع النموذجية لمراجعة المقترحات والتصاميم والمخططات والتقارير والعمليات والبيانات المتعلقة بالمشاريع المتنوعة .

أما الإدارة الفنيّة والإدارية اليومية لمشاريع «سوليراس» فهي تحت مسؤولية «مدوست ريسيرتش انستيتوت» (معهد «مدوست» للبحوث) . وهو معهد أبحاث مستقل ليس ذا صبغة تجارية ، تم تعيينه كوكيل تشغيل لبرنامج «سوليراس» . ويستخدم معهد «مدوست للبحوث» فنيين وإداريين من كلا البلدين للقيام بمسؤولية تنفيذ قرارات المجلس التنفيذي وإدارة المشاريع الفنية الفردية . ويشمل ذلك التعاقد مع مختلف الشركات ومعاهد الأبحاث في كلا البلدين لتصميم وتركيب أنظمة طاقة شمسية من أحدث تكنولوجيا . وتقع مكاتب برنامج «سوليراس» في المقر الرئيسي لمعهد «مدوست للبحوث» بمدينة كنساس سيتي بولاية ميسوري وكذلك في الرياض وينبع بالمملكة العربية السعودية .

انبعث من برنامج «سوليراس» العديد من مشاريع الأبحاث الكبرى ، منها تحويل الطاقة الشمسية الى كهرباء للاستعمال اليومي لسكان العديد من القرى الريفية واختبار الطاقة الشمسية كمصدر طاقة للتبريد والتدفئة وتحلية المياه وتطوير أنظمة زراعية باستعمال الطاقة الشمسية للتحكم في كامل بيئة الانماء ، والقيام بأبحاث نظرية حول الخلايا الكهروضوئية والحرارة الشمسية وانشاء مختبرات تكنولوجيا عالية للبحوث الشمسية المتقدمة في الجامعات السعودية ورعاية أبحاث أساسية في الطاقة الشمسية في جامعات بالولايات المتحدة الأمريكية .

كما أن برنامج «سوليراس» ساهم في نشر المعلومات العلمية والفنية المتعلقة بالطاقة الشمسية من خلال رعايته للندوات العلمية والدورات القصيرة ونشر التقارير الفنية . ولقد كان ذلك وسيلة لنقل معلومات هامة لمجموعة الباحثين العلميين حول تكنولوجيا الطاقة الشمسية المطوّرة من خلال برنامج «سوليراس» والمشاريع الأخرى المرتبطة به عبر بلدان العالم .

TABLE OF CONTENTS

	<u>Page</u>
FORWORD . . . . .	i
TABLE OF CONTENTS . . . . .	11
1. INTRODUCTION . . . . .	1
2. BASELINE SYSTEM . . . . .	5
3. COST REDUCTION ANALYSIS . . . . .	6
4. 75-HELIOSTAT PLANT DESIGN . . . . .	21
4.1 System Description and Operation . . . . .	21
4.2 System Performance . . . . .	25
4.3 Heliostat Field . . . . .	32
4.3.1 DELSOL 2 Program . . . . .	32
4.3.2 Field Optimization . . . . .	33
4.3.3 STEAC Input . . . . .	37
4.4 Heliostat . . . . .	38
4.4.1 Heliostat Foundations. . . . .	38
4.4.2 Other Design Improvements. . . . .	41
4.4.3 Heliostat Array Controller . . . . .	42
4.5 Receiver . . . . .	47
4.5.1 Cavity Configuration Design. . . . .	47
4.5.2 Aperture Sizing . . . . .	49
4.5.3 Receiver Cavity Design Tradeoffs . . . . .	54
4.5.4 Thermal and Hydraulic Design . . . . .	55
4.5.5 Receiver Emergency Protection . . . . .	60
4.5.6 Operating Modes. . . . .	61
4.5.7 Receiver Control . . . . .	63
4.5.8 Receiver Fabrication . . . . .	64
4.5.9 Receiver Structural Design . . . . .	68
4.5.10 Receiver Tower . . . . .	72
4.6 Steam Generating Equipment . . . . .	74
4.6.1 Configuration. . . . .	75
4.6.2 Design . . . . .	81
4.7 Energy Storage . . . . .	91
4.7.1 Configuration . . . . .	91
4.7.2 Design . . . . .	93
4.8 Reverse Osmosis . . . . .	97
4.9 Multiple Effect Distillation Unit . . . . .	98
4.10 Turbine Generator . . . . .	98
4.11 Master Control . . . . .	100
4.11.1 Receiver Control . . . . .	100
4.11.2 Steam Generation Control . . . . .	107
4.11.3 Thermal Storage Control. . . . .	116
4.11.4 Turbine Generator, RO and MED Control. . . . .	116
4.11.5 Baseline MCS . . . . .	130
4.11.6 Other MCS Configuration. . . . .	130
4.11.7 Electrical Systems . . . . .	143

## 1. INTRODUCTION

This report documents the technical effort of Martin Marietta Corporation, in association with Black and Veatch International as a subcontractor for the trade studies performed to design a Solar Desalination Pilot Plant. The final system configuration utilizes existing technology to convert seawater to potable water. This technology includes the collection of solar energy, storage of this energy in a fluid heat transfer medium, generation of steam and electricity from this stored energy, utilization of low pressure turbine exhaust steam as a source of energy to distill salt water, and also generation of potable water through the use of a reverse osmosis unit.

Figure 1-1 shows a simplified schematic of the proposed pilot plant. This system is comprised of 75 tracking heliostats. These heliostats, located in a field to the north of a tower, reflect the sun's energy to a receiver at the top of the tower. The receiver is designed to absorb this radiant energy and transfer it to the circulating molten salt heat transfer fluid. The selected heat transfer fluid is a salt comprised of 60%  $\text{NaNO}_3$  and 40%  $\text{KNO}_3$  by weight and operates in the 288°C (550°F) to 538°C (1000°F) temperature range. The molten salt is stored in externally insulated hot storage tanks at 538°C (1000°F) and will be used as the energy source to generate the high temperature and high pressure steam in the salt steam heat exchanger. The steam at 427°C (800°F) and 5.5 MP (800 psia) enters the turbine generator which converts the thermal energy to electrical energy. The exhaust steam from the turbine is used as the energy source to distill seawater in a multiple effect distillation (MED) unit which converts seawater to potable water. The electricity which is generated by the turbine generator set provides the power to operate a reverse osmosis (RO) unit which also provides potable water. The solar portion of the plant and the turbine generator set is run by a master control subsystem consisting of operational control and supervisory control equipment for each major subsystem. All plant data is collected displayed and stored by a separate data acquisition subsystem.

Each component of the proposed system utilizes either existing hardware or technologies which have been proven successful by years of research and development. This plant will demonstrate for the first time all of these existing technologies integrated into a solar energy powered desalination facility.

Once the combination of solar technology with the existing desalination technologies has been successfully demonstrated, it can then be applied in larger more efficient plants to displace fossil fuel as the energy source to desalinate water.

The location of the proposed site is approximately 35 kilometers south of Yanbu, Saudi Arabia, near the existing site of the Saline Water Conversion Company (SWCC). This existing plant transforms seawater to potable water, and provides power to the local grid. The existing plant will provide many of the solar plant utilities, such as water, power and waste water discharge, for the demonstration plant during construction and operation.

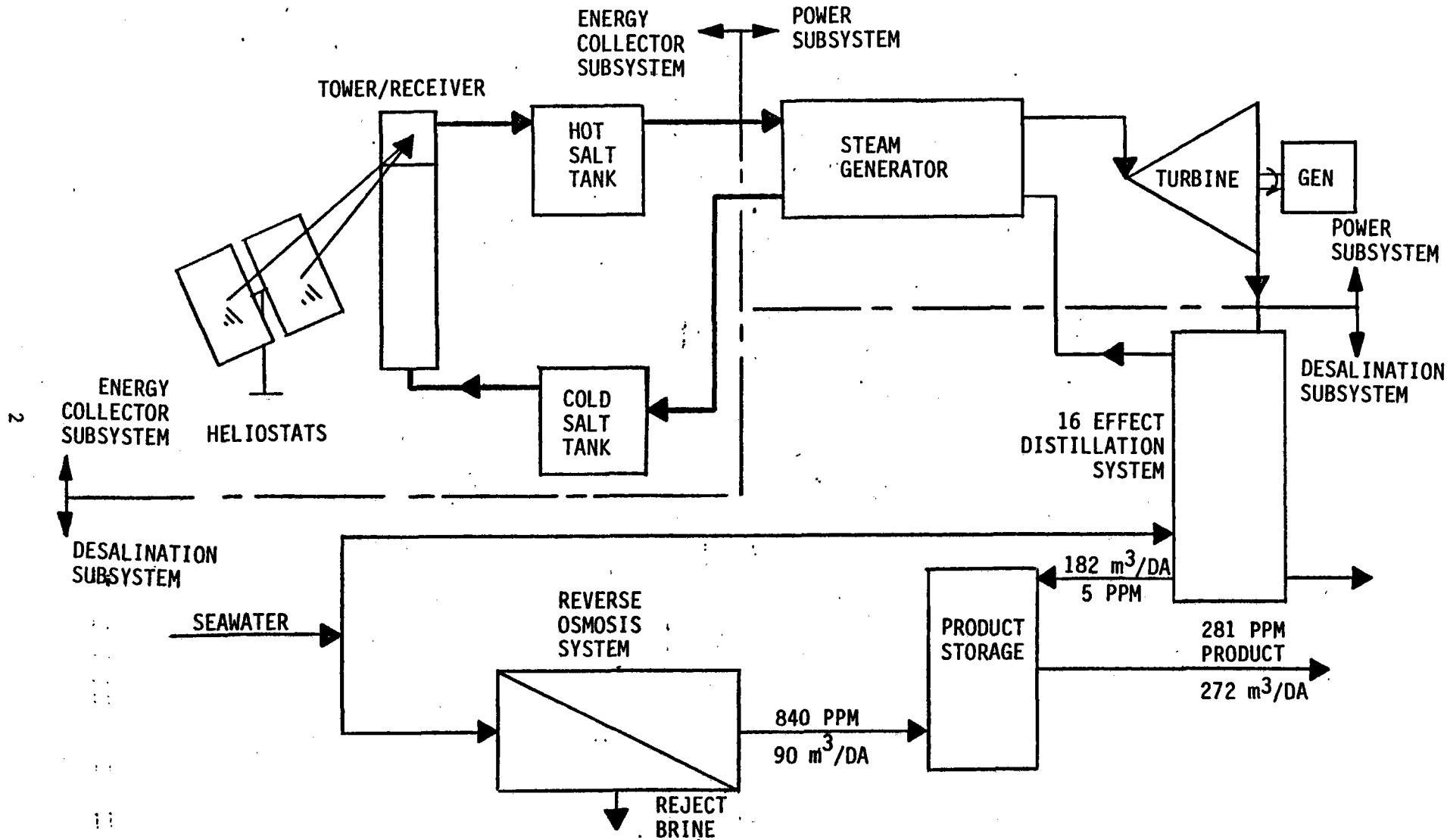


Figure 1-1 Simplified Flow Diagram



## PROGRAM DESCRIPTION

In 1977, under the auspices of the United States/Saudi Arabian joint Commission on Economic Cooperation, the Project Agreement for Cooperation in the Field of Solar Energy (SOLERAS) was signed between the United States and Saudi Arabia. The objectives of the agreement were to:

- o Enhance cooperation in the field of solar energy technology for the mutual benefit of both countries,
- o Advance the development of solar energy technology, and,
- o Facilitate solar technology transfer between the U.S. and Saudi Arabia.

A five-year technical program plan was developed and approved by the SOLERAS Executive Board. The Solar Energy Research Institute (SERI), acting as the program's operating agent, was delegated the responsibility for implementing the program plan in accordance with directives issued by the SOLERAS Executive Board.

As part of the technical program plan, a general area of Industrial Solar Applications was identified, under which an application utilizing solar technology could be developed. The matching of a solar technology(ies) to a desalination technology(ies) was selected as the demonstration to be carried out under this general area.

Demand in Saudi Arabia for desalination, a highly energy intensive technology, is largely derived from municipal and agricultural needs. River salinity control, enhancement of municipal water quality and relief from regional water shortages has similarly created a demand for desalination in the United States.

## PROJECT BACKGROUND

Exxon Research and Engineering Company and The Solar Thermal Project of Exxon Enterprises led a design team supported by Badger Energy Co., Martin Marietta Corporation, the Permutit Co., Ecodyne and the Saudi Investment and Development Center, in the preliminary design of a solar powered desalination system.

Two solar desalination designs were developed under the contract--a conceptual baseline plant capable of producing an average daily product water output of 6000 m<sup>3</sup>/day, and a pilot plant for the evaluation of the design features of the conceptual baseline plant.

The baseline plant design was powered by a solar central receiver-heliostat field consisting of 395 Martin Marietta Corporation second generation heliostats.

The Exxon pilot plant design was similar to the baseline design, but produced an approximate maximum of 1100 m<sup>3</sup>/day. The thermal energy was provided by a hybrid energy system consisting of 100 Barstow heliostats and three fossil fuel furnaces. A 500 kWe, one-stage turbine generator set was used to furnish electricity. The solar energy system supplied only a fraction of the total energy consumed by the plant, with the remainder being supplied by fossil fuel.

In 1981, Martin Marietta Corporation presented a conceptual description of a 111 heliostat desalination pilot plant to the Solar Energy Research Institute. The plant design was revised so that the product water output was reduced to 330 m<sup>3</sup>/day, with nearly all the energy consumed by the plant being derived from solar energy. In early 1982, Martin Marietta Corporation was awarded a study contract for the preliminary design of the 111 heliostat desalination pilot plant as the baseline plant.

### Program Objectives

The demonstration of the effective use of solar energy to desalinate sea water is the major objective of this program. The pilot plant is designed to provide maximum design and operational information needed to verify methods to be used for a commercial sized plant. An effort was made to minimize the cost of the plant while achieving this objective. The selected plant size (75 heliostats) represents the smallest system that is considered workable and representative of current technology.

Molten salt (60% NaNO<sub>3</sub>, 40% KNO<sub>3</sub> by weight) was selected as the working fluid for the receiver and steam generator, and also as the energy storage medium. Molten salt has been proven safe and reliable in past industrial applications, and is an efficient heat transfer and storage medium. Design and operation of the molten salt components for the pilot plant will provide valuable experience for later applications to a commercial scale plant.

The selected central receiver system configuration consists of a North heliostat field and a single cavity type solar receiver. Based on past studies, a north field is the most efficient configuration for the pilot plant. The cavity type receiver was selected over an exposed receiver because of the reduced thermal losses, and therefore the increased performance that can be achieved.

### Summary of Program Tasks

In addition to the necessary management, direction and control of the program, Martin Marietta Corporation was contracted to perform a verification of the Solar Desalination Pilot Plant Feasibility Design dated January 1982. This analysis included the following:

1. Analysis of steam requirements of the multiple effect distillation (MED) system and the power requirements of the reverse osmosis (RO) unit.
2. Analysis of the power available from the power subsystem.
3. Verification of the operating strategy of the plant requirements on the energy storage system.
4. Summary of the heliostat field and receiver tower layout and description of the control system and operational procedures.

In order to minimize the pilot plant construction costs Martin Marieta Corporation analyzed means of reducing the cost of the baseline plant. This included analysis to reduce the product water output to the minimum output compatible with the availability of key subsystem components.

The final task encompassed the design of the reduced capacity pilot plant. This design is summarized in the technical volume of the Phase II proposal.

## 2. BASELINE SYSTEM

The original 111 heliostat baseline system is very similar to the final plant selected which consists of 75 heliostats. Most of the plant components are directly scalable by the number of heliostats. The system uses solar energy to heat molten salt to be used either to store energy or to be pumped through a series of heat exchangers to generate steam. This steam drives a turbine and its exhaust is then used as a heat source for a distillation unit. The electricity from the turbine driven generator is used for the pump in a reverse osmosis unit and for the electrical needs of the balance of the plant. The product streams of the RO unit and the MED unit are blended to give the final product water purity measured by total dissolved solids (TDS).

The baseline and final plant configurations are shown in Table 2-1.

Table 2-1 Plant Configuration at Design Point Conditions

	<u>Baseline Plant</u>	<u>Final Plant</u>
Water Output Average	330 m <sup>3</sup> /day	272 m <sup>3</sup> /day
Expected Water Purity (TDS)	500 PPM	281 PPM
Sea Water Inlet (TDS)	44,000 PPM	44,000 PPM
Number of Heliostats	111	75
Hours of Storage	21	28
Storage Capacity	16.8 MWh <sub>t</sub>	13.52 MWh <sub>t</sub>
Generator Output	100 kWe	54 KWe
Salt Composition by Weight	60/40 NaNO <sub>3</sub> /KNO <sub>3</sub>	60/40 NaNO <sub>3</sub> /KNO <sub>3</sub>

The plant supplies 100% of its normal energy requirements from solar. However, certain peak electric power demands would be supplied from the local power grid.

The plant is designed to operate continuously 24 hours per day with normal insolation conditions. The system includes an automatic control system to minimize operator requirements.

### 3. COST REDUCTION ANALYSIS

Under Task 3 of the desalination program an analysis was performed to determine means of reducing the capital cost of the plant. An effort was made to reduce the size of the solar energy collection subsystem to the minimum compatible with producing the energy required for essential desalination processes. The minimum product water output compatible with availability of key subsystem components in standard sizes was determined.

The original conceptual plant design consisted of 111 heliostats along with the RO, MED, and the associated equipment. Two smaller plants were investigated in the cost reduction analysis, a 75 heliostat plant, and a 50 heliostat plant. The size of the desalination equipment was scaled down with the energy available from the heliostat field. Each plant was then analyzed to determine the subsystem component sizes, the product water output, and the plant cost.

The first step in the analysis was to determine the effect of the heliostat field size reduction on the receiver design. This was accomplished by first laying out a 50, 75, and 111 heliostat field. The fields were simple wedge shaped 90° north fields. The heliostat coordinates were determined with a simple technique that avoids all heliostat blocking. Tower heights of 23 m, 28 m, and 35 m respectively were determined from data derived from the DELSOL optimization program. The TRASYS radiation analysis program was used to produce design point flux maps at the plane of the aperture for each plant. This information was used to determine spillage for various aperture sizes.

Figure 3-1 is a comparison of the aperture flux profile for each plant. The size of the image at the aperture remains the same as the number of heliostats is reduced. This occurs because the minimum image size a single heliostat can produce remains constant even though the total field size is reduced. The lower limit on image size from the heliostats has been reached. The only effect of reducing the number of heliostats below 111 is a reduction in flux intensity.

Figures 3-2 through 3-4 show the method used to optimize the aperture size for each plant. Thermal losses (conduction, convection, reradiation, and reflection) were calculated as a function of aperture area. Test data from the Alternate Central Receiver Subsystem Research Experiment 5 MWt molten salt receiver was used as a basis for these calculations. (The test data is discussed in Section 4.5 Receiver).

The aperture size was optimized by calculating the combination of spillage and thermal losses from the receiver for various aperture sizes. The aperture size that minimizes the total losses is the optimum aperture. Because the image size is relatively constant for the three receivers, the optimized aperture size is fairly constant. Therefore, the thermal losses from the receivers are fairly constant. The amount of energy absorbed from the receiver panel is reduced as the heliostat field size is reduced. This is because the flux intensity is lower. The fact that the thermal losses from the receiver are constant with field size reduction, but the amount of energy absorbed is reduced, causes a severe reduction in receiver efficiency for the smaller plants. This effect can be seen on Figure 3-5.

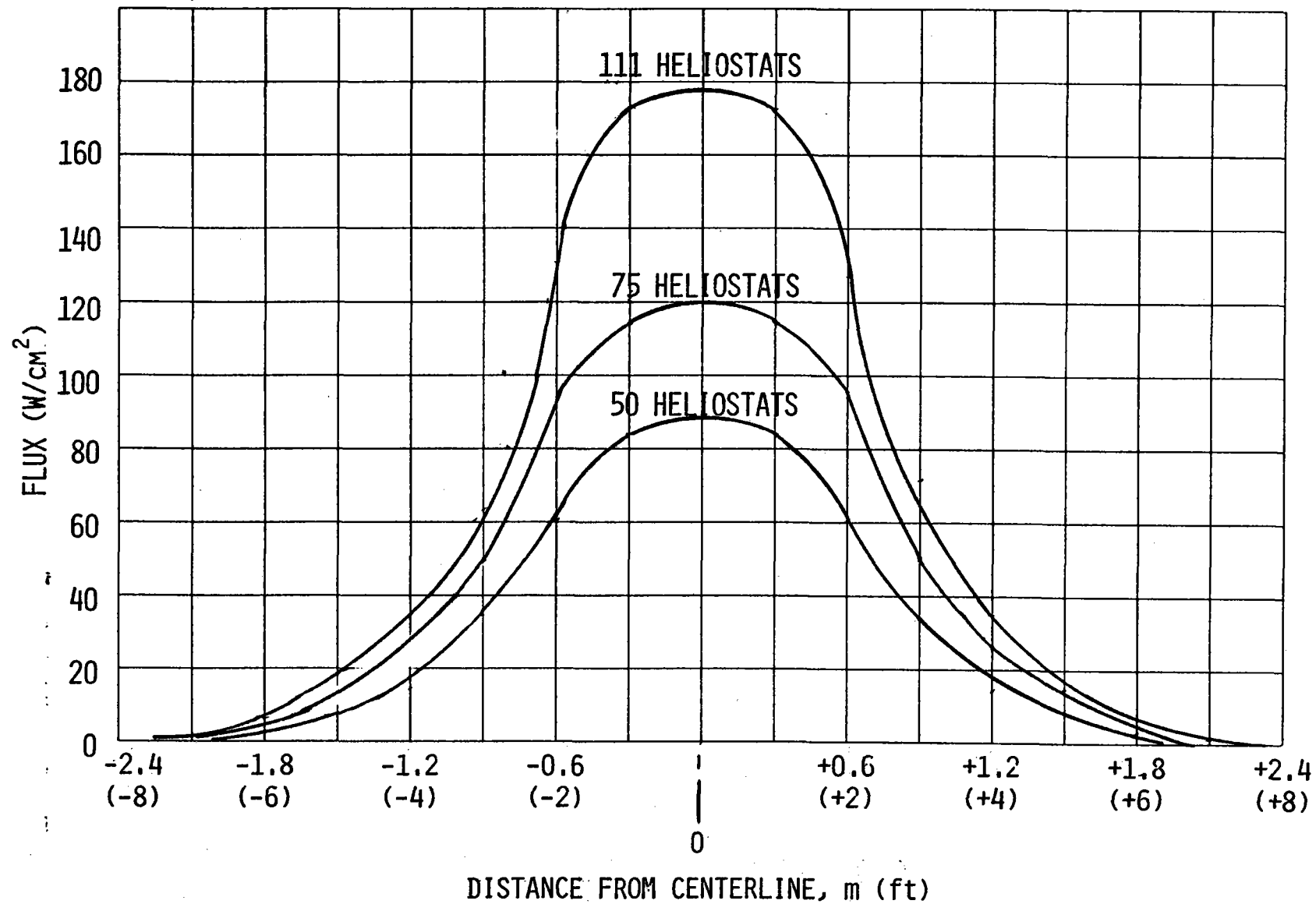


Figure 3-1 Aperture Flux Profile

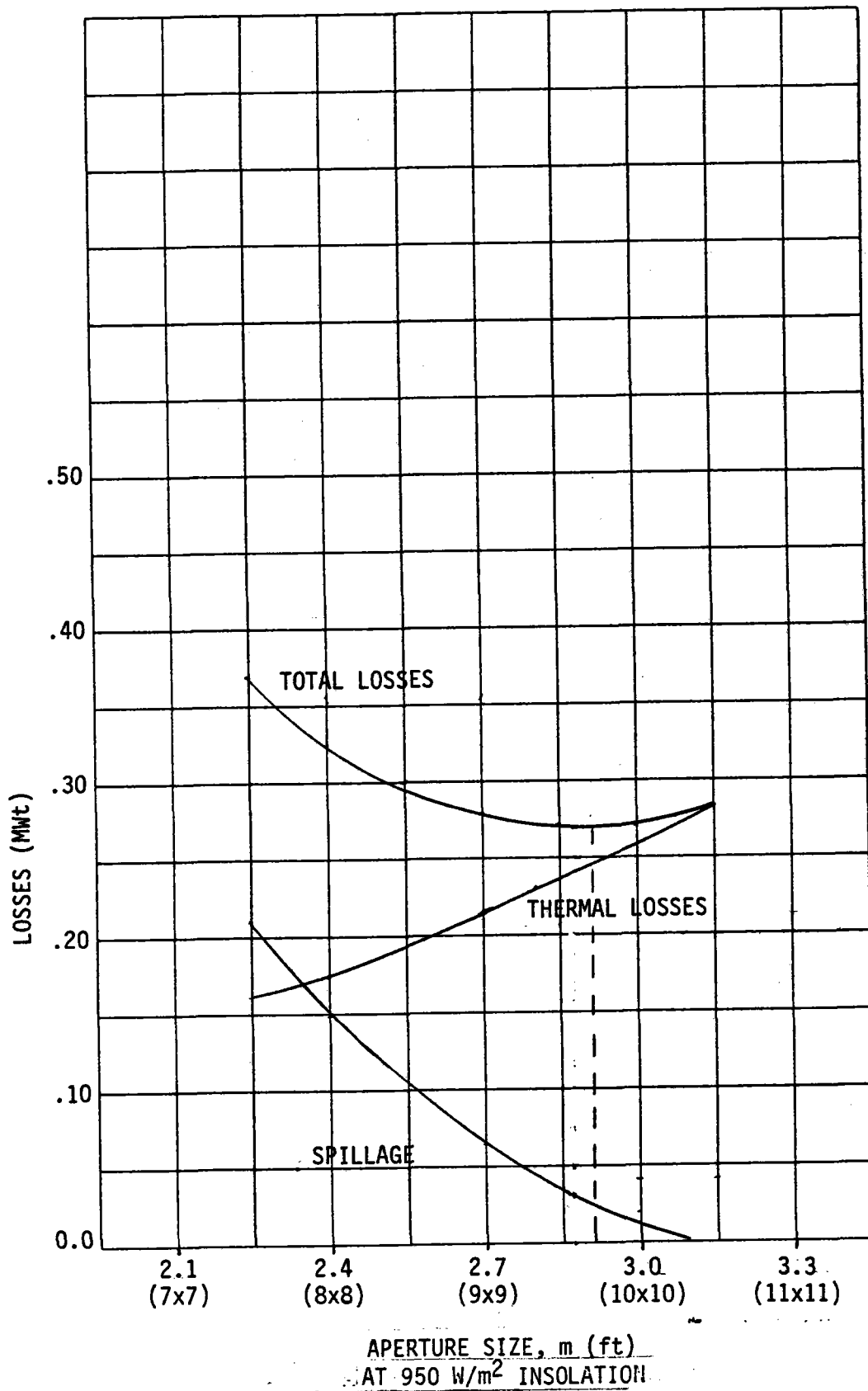


Figure 3-2 50 Heliostat Field Aperture Sizing

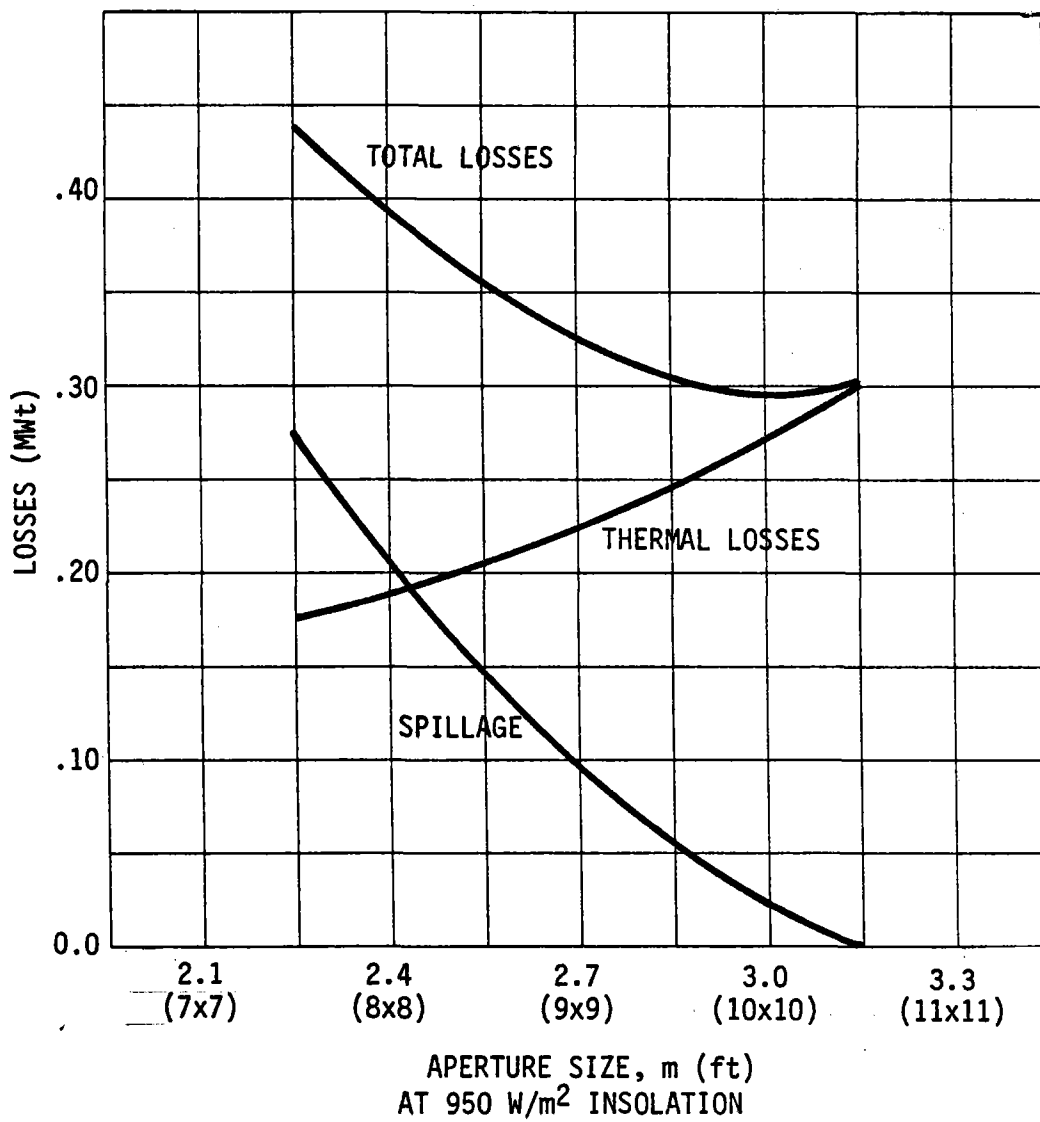
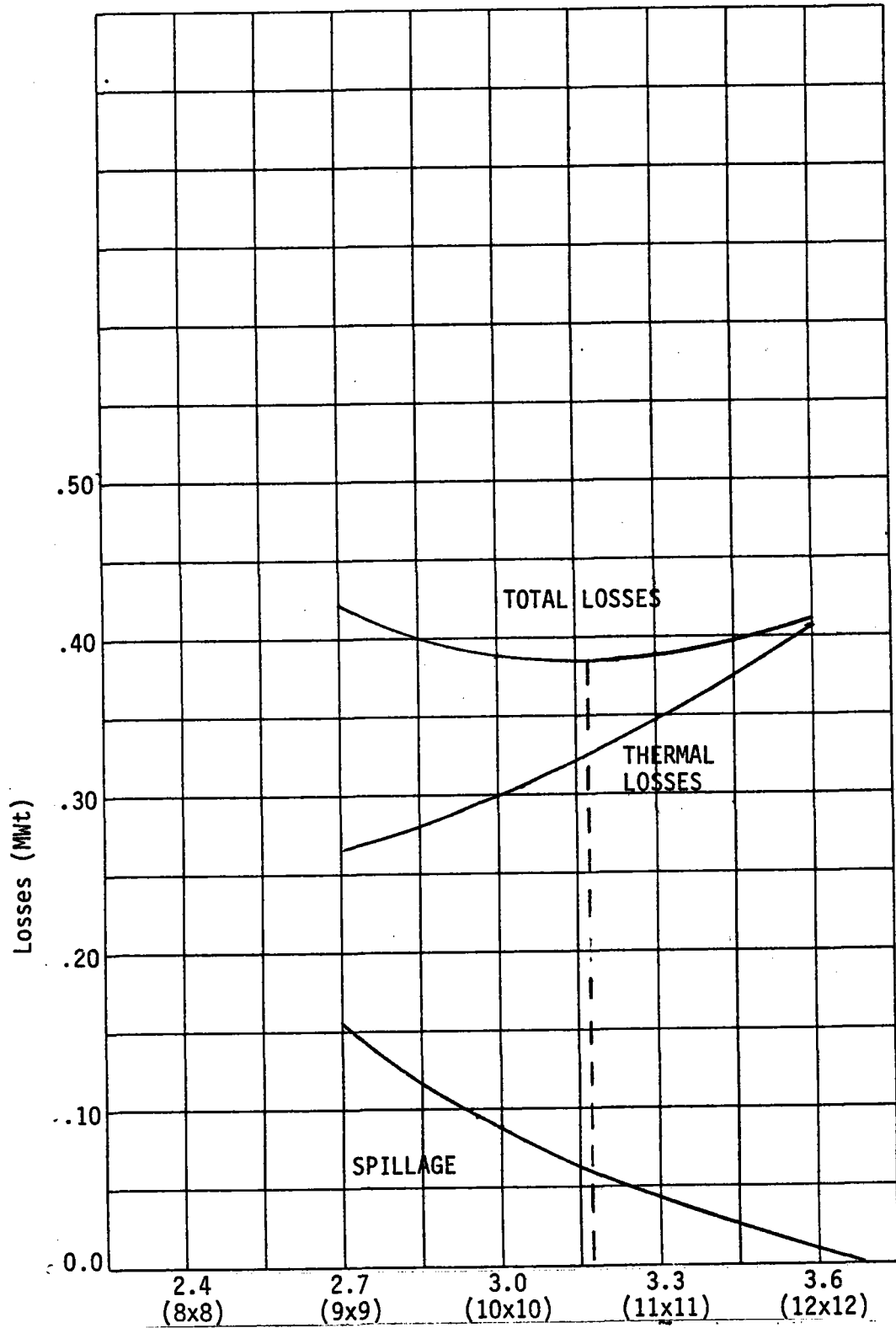


Figure 3-3 75 Heliostat Field Aperture Sizing



APERTURE SIZE, m (ft)  
 AT 950 W/m<sup>2</sup> INSOLATION

Figure 3-4 111 Heliostat Field Aperture Sizing



### EFFECT OF HELIOSTAT FIELD SIZE REDUCTION ON RECEIVER

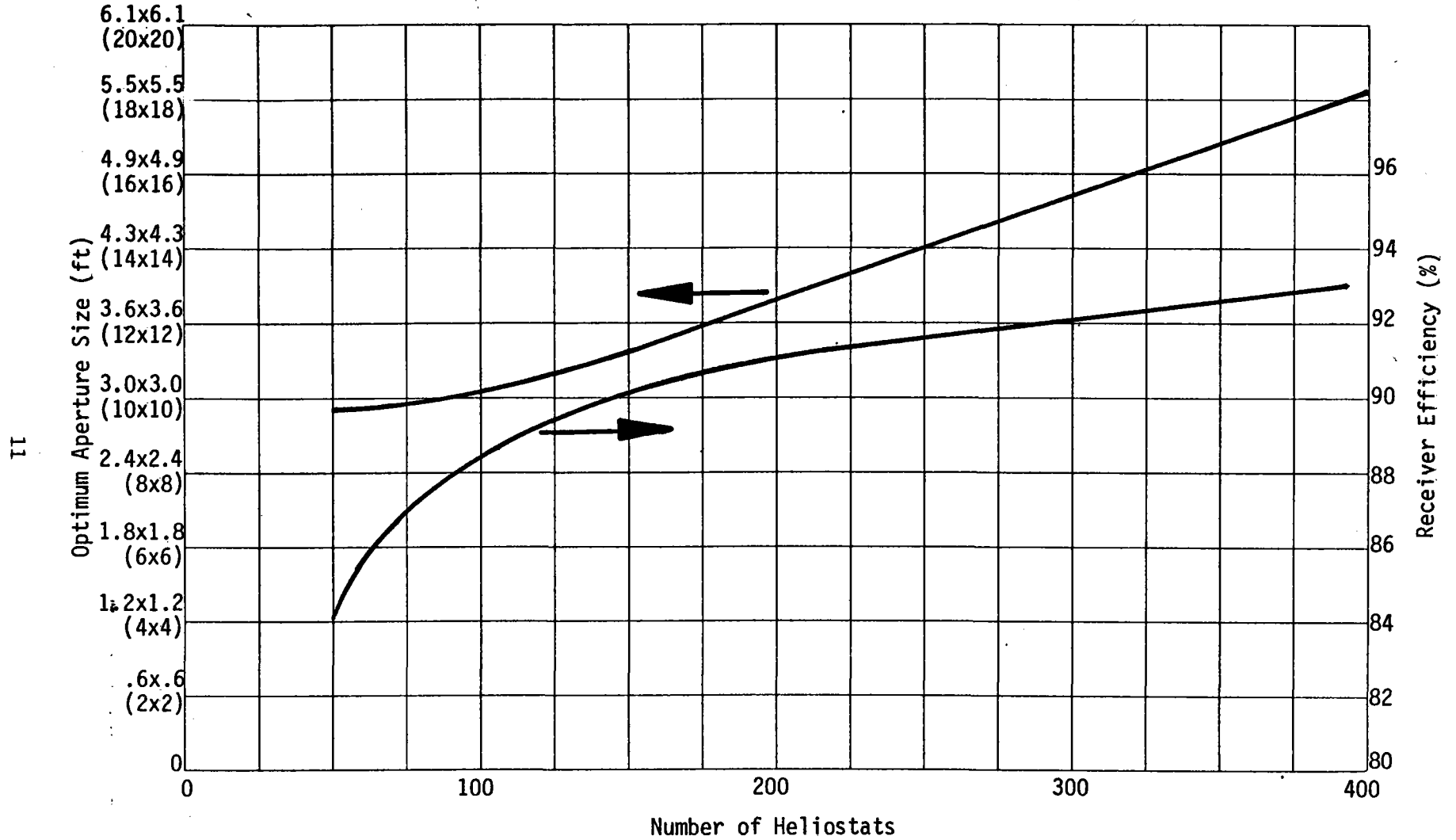


Figure 3-5 Effect of Heliostat Field Size Reduction on Receiver

The next step in the analysis was to determine the electricity and water output of the steam cycle for each plant. Figure 3-6 shows the chosen configuration of the steam cycle. The energy balance and water output for the 50, 75 and 111 heliostat plants are shown in Tables 3-1 through 3-3 respectively. Turbine efficiencies are for Terry single stage turbines. The turbine shown on Figure 3-6 (29 KWe) is not available with the 427°C/5.5MPa (800°F/800) psia inlet conditions. The turbine-generator efficiency decreases as the plant size decreases, therefore, the amount of electricity generated does not decrease proportionally with the energy delivered to the MED as turbine exhaust steam. This fact makes it difficult to balance the RO-MED water output, since the RO is a major electricity consumer.

The cost of each plant was determined by breaking the plant into subsystems and pricing each subsystem. The original cost estimate for the 111 heliostat plant was used as a basis for costing the smaller plants.

Collector Field Receiver Storage	STCR Computer Model (receiver cost is held constant)
Engineering (includes architect and engineering services, and program management)	Estimate for 330 m <sup>3</sup> /day plant held constant for all plant sizes
Construction, Installation and Checkout	Estimate for 330 m <sup>3</sup> /day plant held constant except for heliostat installation cost
Desalination Equipment	Cref ( $\frac{\# \text{ heliostats}}{111 \text{ heliostats}}$ ).6 Cref is the reference cost of the desalination equipment for the 330m <sup>3</sup> /day plant (Desalination equipment - \$1,575,900)
Controls	Estimate for 330 m <sup>3</sup> /day plant held constant for all plant sizes

Figure 3-7 is a graph of estimated subsystem cost vs. plant size. The main drivers in plant cost are the engineering, construction, and installation. These costs are nearly constant with plant size. Therefore the amount of money saved with the smaller plants is small.

111 heliostat plant	\$15.3M
75 heliostat plant	\$14.4M
50 heliostat plant	\$13.6M



Table 3-1 50 Heliostat Plant Energy Balance

Flow Diagram Point	Fluid	Pressure MPa (psia)	Temperature °C (°F)	Flow kg/hr (lbm/hr)
1	Salt		510 (950)	2922 (6442)
2	Salt		280 (536)	2922 (6442)
3	Salt		260 (500)	2922 (6442)
4	Liq	0.04 (6.5)	78.3 (173)	423 (933)
5	Liq	5.52 (800)	156 (312)	423 (933)
6	Sat Liq	5.52 (800)	270 (518)	512 (1128)
7	Liq	5.52 (800)	169 (337)	88.5 (195)
8	Sat Liq	5.52 (800)	270 (518)	512 (1128)
9	Sat Vap	5.52 (800)	270 (518)	512 (1128)
10	Sat Vap	5.52 (800)	270 (518)	423 (933)
11	S.H. Steam	5.52 (800)	427 (800)	423 (933)
12	S.H. Steam	0.04 (6.5)	262 (504)	423 (933)
13	S.H. Steam	0.04 (6.5)	93.3 (200)	423 (933)
14	Sat Vap	5.52 (800)	270 (518)	12.7 (28)
15	MED Product			69 m <sup>3</sup> /day
16	RO Product			91 m <sup>3</sup> /day

$\eta_{\text{Turbine}} = 26\%$

$\eta_{\text{Cycle}} = 9.3\%$

Electric Output: 29 kWe

RO Consumption: 18 kWe

Table 3-2 75 Heliostat Plant Energy Balance

<u>Flow Diagram Point</u>	<u>Fluid</u>	<u>Pressure MPa (psia)</u>	<u>Temperature °C (°F)</u>	<u>Flow kg/hr (lbm/hr)</u>
1	Salt		510 (950)	4539 (10006)
2	Salt		279 (534)	4539 (10006)
3	Salt		260 (500)	4539 (10006)
4	Liq	0.04 (6.5)	78.3 (173)	645 (1422)
5	Liq	5.52 (800)	143 (290)	645 (1422)
6	Sat Liq	5.52 (800)	270 (518)	798 (1760)
7	Liq	5.52 (800)	157 (315)	153 (338)
8	Sat Liq	5.52 (800)	270 (518)	645 (1422)
9	Sat Vap	5.52 (800)	270 (518)	645 (1422)
10	Sat Vap	5.52 (800)	270 (518)	645 (1422)
11	S.H. Steam	5.52 (800)	427 (800)	645 (1422)
12	S.H. Steam	0.04 (6.5)	236 (457)	645 (1422)
13	S.H. Steam	0.04 (6.5)	93.3 (200)	645 (1422)
14	Sat Vap	5.52 (800)	270 (518)	19.5 (43)
15	MED Product			106 m <sup>3</sup> /day
16	RO Product			139 m <sup>3</sup> /day

$\eta_{\text{Turbine}} = 32\%$

$\eta_{\text{Cycle}} = 11.2\%$

Electrical Output = 54 kWe

RO Consumption = 27 kWe

Table 3-3 111 Heliostat Plant Energy Balance

Flow Diagram Point	Fluid	Pressure MPa (psia)	Temperature °C (°F)	Flow kg/hr (lbm/hr)
1	Salt		510 (950)	6880 (15168)
2	Salt		278 (533)	6880 (15168)
3	Salt		260 (500)	6880 (15168)
4	Liq	0.04 (6.5)	78.3 (173)	959 (2113)
5	Liq	5.52 (800)	131 (267)	959 (2113)
6	Sat Liq	5.52 (800)	270 (518)	1217 (2682)
7	Liq	5.52 (800)	144 (292)	258 (569)
8	Sat Liq	5.52 (800)	270 (518)	1217 (2682)
9	Sat Vap	5.52 (800)	270 (518)	1217 (2682)
10	Sat Vap	5.52 (800)	270 (518)	959 (2113)
11	S.H. Steam	5.52 (800)	427 (800)	959 (2113)
12	S.H. Steam	0.04 (6.5)	208 (406)	959 (2113)
13	S.H. Steam	0.04 (6.5)	93.3 (200)	959 (2113)
14	Sat Vap	5.52 (800)	270 (518)	28.6 (63)
15	MED Product			175 m <sup>3</sup> /day
16	RO Product			207 m <sup>3</sup> /day

$\eta_{\text{Turbine}} = 38\%$

$\eta_{\text{Cycle}} = 13\%$

Electrical Output = 95 kWe

RO Consumption = 41 kWe

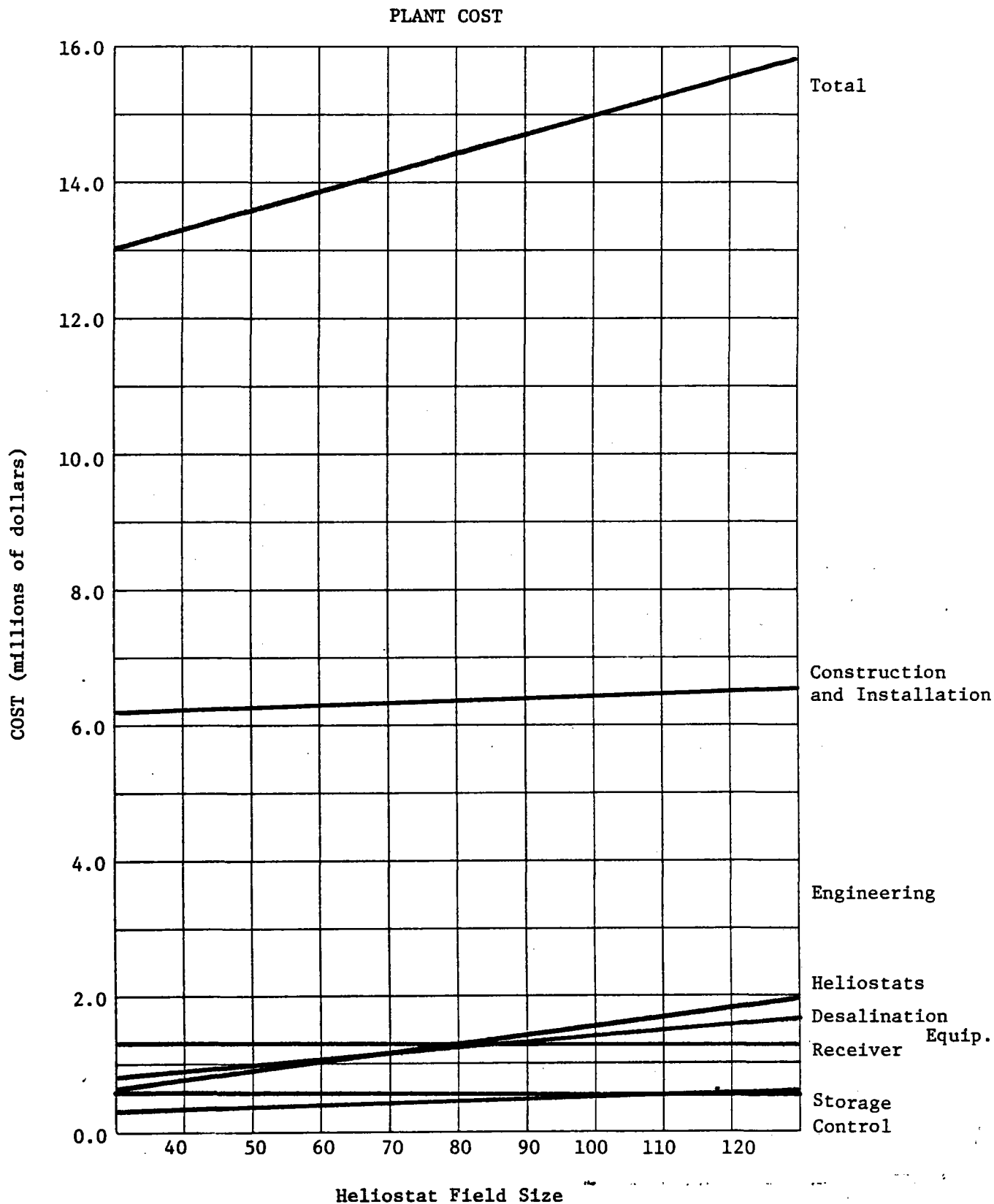
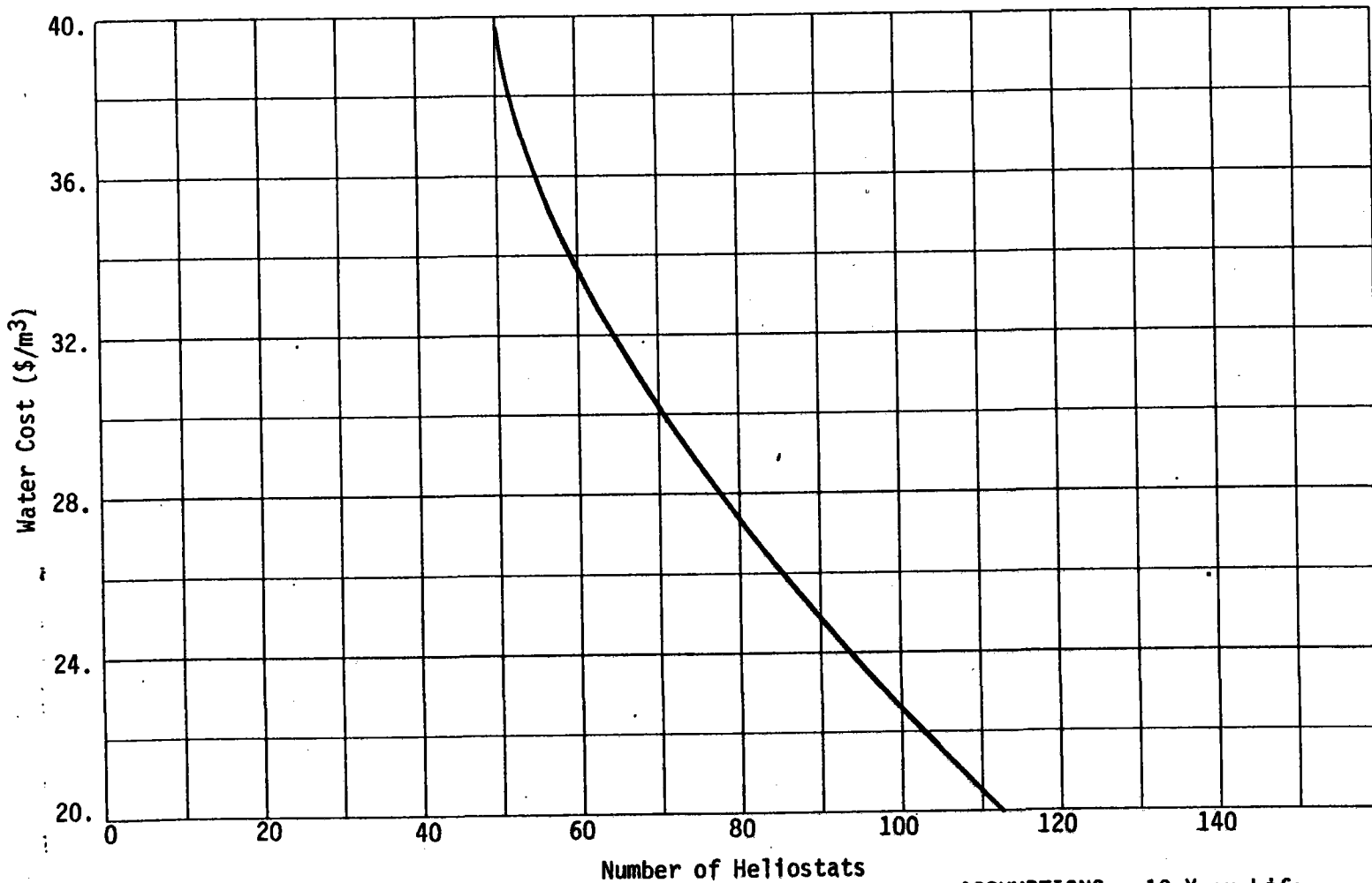


Figure 3-7 Estimated Subsystem Cost vs. Plant Size

### PRODUCT WATER COST



18

Figure 3-8 Product Water Cost

ASSUMPTIONS: 10 Year Life  
10% Cost of Capital  
O&M is 3% of Capital Cost  
8% Esc on O&M



COST OF ELECTRICITY FROM TURBINE-GENERATOR

6T

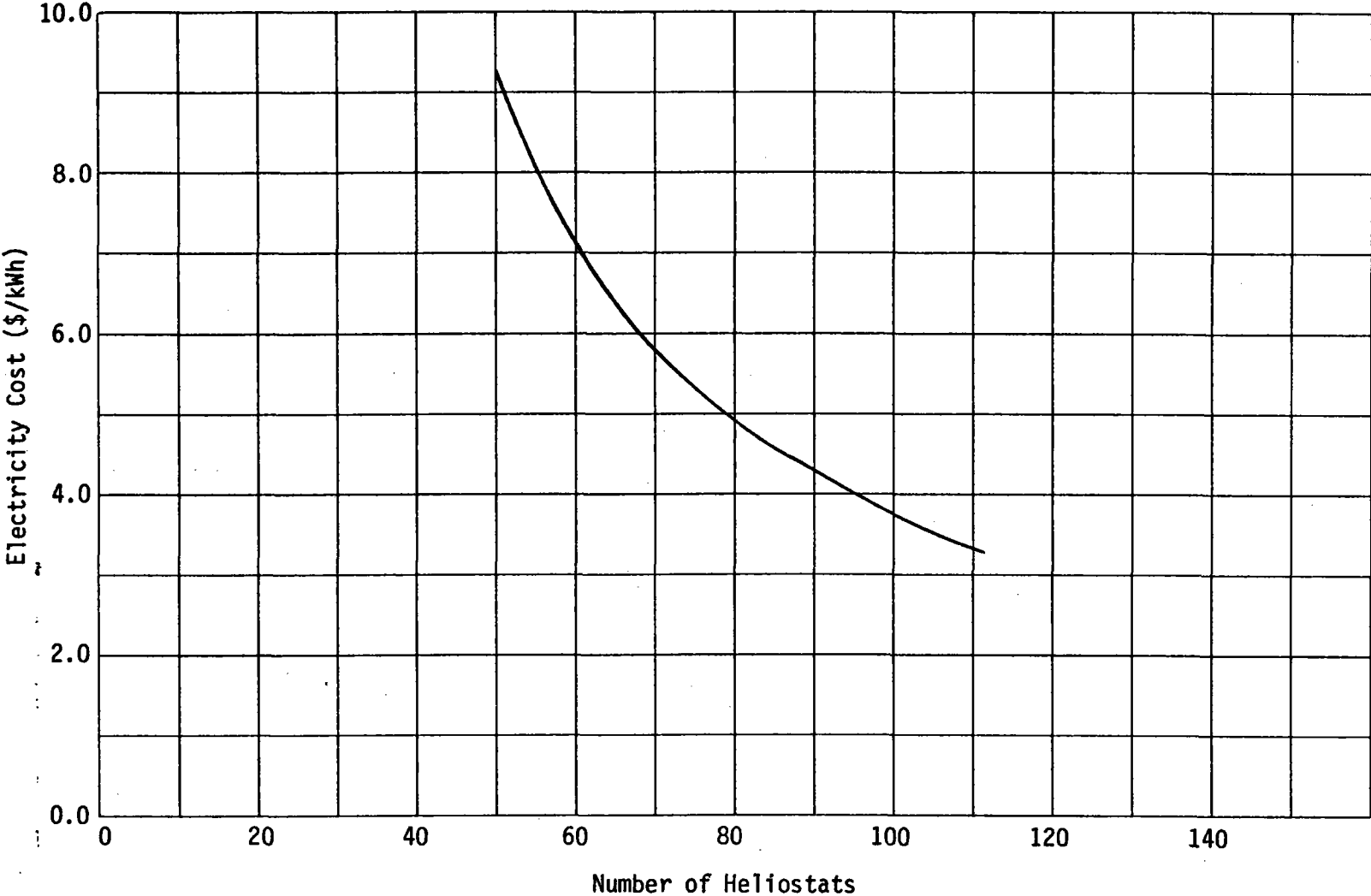


Figure 3-9 Cost of Electricity from Turbine-Generator

ASSUMPTIONS: 20 Year Life  
10% Cost of Capital  
O&M is 3% of Capital Cost  
8% Esc on O&M

The product water output, electricity output, and the cost of each plant was used to determine the water cost ( $\$/\text{m}^3$ ) and electricity cost ( $\$/\text{kWh}$ ) shown on Figures 3-8 and 3-9. The nearly constant plant cost drives these costs up sharply as plant size is decreased. However, water and electricity costs are not significant factors in choosing the plant size for a pilot plant.

Because a turbine was not available for the 50 heliostat plant, this plant was eliminated from consideration. Because the basis for plant selection is the capital cost, the 75 heliostat plant was chosen even though the cost savings is relatively small. Although there will be a penalty in receiver performance with the 75 heliostat plant, the overall design is considered workable.

#### 4. 75-HELIOSTAT PLANT DESIGN

##### 4.1 SYSTEM DESCRIPTION AND OPERATION

The desalination pilot plant designed by the Martin Marietta Denver Aerospace team consists of three major systems tied together by two steam generating heat exchangers and the plant control system. These major systems are the Solar Energy Collection and Storage (EC&S) System and the Desalination and Power Systems. The solar EC&S System collects the solar energy, transfers it to a molten salt fluid state, stores the hot fluid and makes it available on demand. The Power and Desalination Systems convert the hot fluid heat to steam and uses the steam to both desalinate water directly through a distillation process and indirectly by generating electrical power for a reverse osmosis process. Residual electrical power may be used for partial plant operation. The Solar EC&S System represents recent technology which has been proven over the past five years through a series of pilot plant installations and system, subsystem and component level tests. The heat exchangers and the Desalination and Power Systems represent current commercial technology.

The Solar EC&S System is made up of three principal subsystems as illustrated in Figure 4-1. These consist of the heliostats, solar receiver, tower and the thermal storage equipment. Each of these subsystems has some level of independent control but overall control is achieved through the plant master control system. The collector subsystem is made up of 75 Martin Marietta Corporation mirrored heliostats of the type used in Almeria, Spain at the International Energy Agency Small Solar Power Station. These heliostats will concentrate the solar energy from an active area of approximately 2,950 m<sup>2</sup> (31,720 sq ft) onto the receiver at the top of a 30.17 m (99 ft) high tower. The heliostats will be located to the north of the tower within an angle of +55° from a north to south centerline.

The solar receiver is a single cavity receiver that absorbs the radiant solar energy and transfers the resultant heat to a molten salt heat exchange fluid. This is accomplished by pumping the molten salt through pipes arranged to form a single wall across the back of the receiver cavity. To heat the salt from a 288°C (550°F) inlet temperature to 538°C (1000°F) outlet temperature, the fluid makes 14 passes across the active solar heated area before exiting the receiver. The hot fluid then flows down the tower into a hot salt tank where it is stored until required.

The hot salt tank is insulated and is designed to maintain the fluid at close to the receiver exit temperature. The Solar EC&S System is designed with the capacity to provide sufficient thermal fluid for continuous desalination for 24 hours per day based on an average insolation level derived from the Solar Irradiance Model (SIM) data. To extract heat from the system, the hot fluid is simply pumped through steam generating heat exchangers where the hot liquid salt is used to make 427°C (800°F) steam.

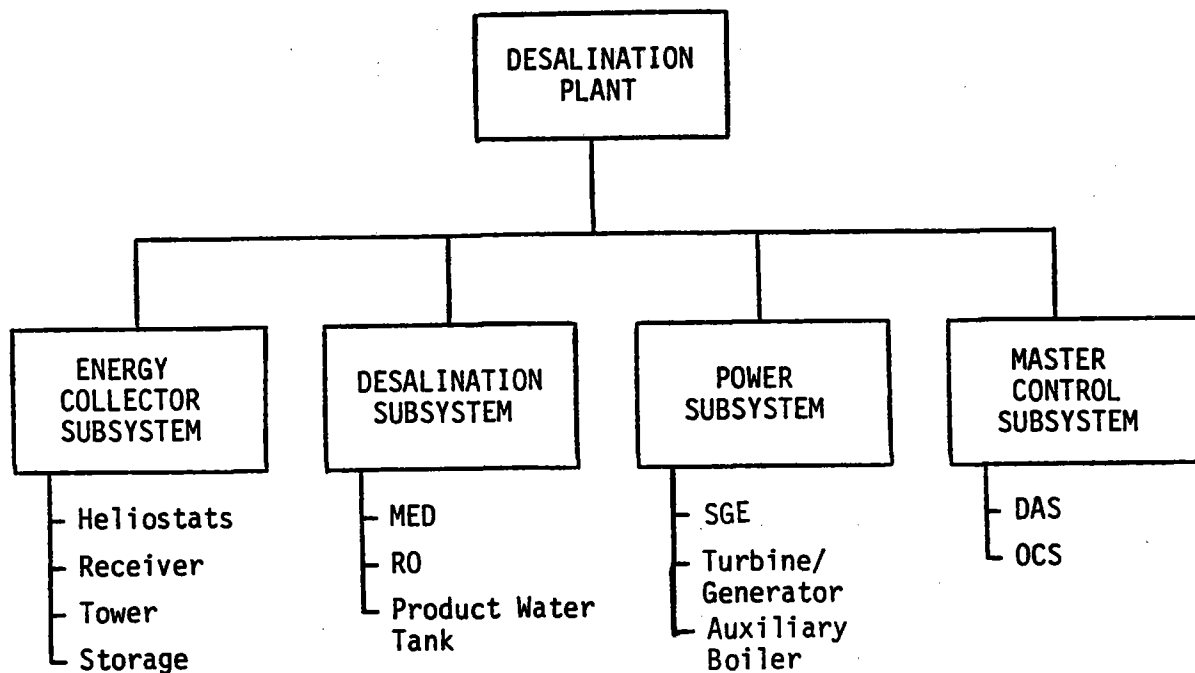


Figure 4-1 Plant Subsystems

This results in reducing the liquid salt temperature to 288°C (550°F). Since this cooled discharge salt can only be returned to the solar receiver for reheat during periods when solar heating can be accomplished, the liquid salt discharge from the steam generated is collected in a discharge cold storage tank. When solar heating conditions are available, the discharge salt is pumped up the tower to be reheated and complete the cycle. Electric salt melters are provided to supply the initial charge of molten salt. Because of the importance of preventing the salt from freezing in the equipment, all interconnecting salt lines are electrically heat traced and are sloped so that in the event of a pump failure they drain into salt sumps. Two pumps are provided to transport the salt from the sumps: a cold salt pump and a hot salt pump.

The Power System ties the EC&S System to the Desalination System. The Power System consist of three principal subsystems as illustrated in Figure 4-1. These are the steam generating equipment (SGE) the turbine generator and the auxiliary boiler.

The selected heat transfer fluid for use by the SGE is a salt comprised of 60% NaNO<sub>3</sub> and 40% KNO<sub>3</sub> by weight and operated in the 288°C (550°F) to 538°C (1000°F) temperature range. The SGE produces steam at 427°C (800°F) and 5,516 kPa (800 psia) for use by the turbine generator. This high temperature/pressure steam enters the turbine generator which converts this thermal energy to electrical energy. The electrical energy is used to power the RO while the exhaust steam from the turbine is used as an energy source for the MED.

The Desalination System consists of an RO unit which utilizes a high pressure reverse osmosis process to produce fresh water from seawater. treated seawater is pumped through an energy recovery turbine, is degasified and pumped to storage. The energy recovery turbine shares a common shaft with the high pressure pump.

The MED system is a desalination unit which utilizes the multi-effect evaporation concept to produce fresh water from seawater with minimum energy consumption. The multi-effect evaporation concept is the separation of the constituents of a liquid mixture by partial vaporization of the mixture and separate recovery of vapor and residue. The constituents are obtained in increased concentration in the residue by vaporizing feed in each effect and feeding the remaining residue to the next effect. The condensed vapors are collected from each effect and leave as product water.

The System Flow Schematic is shown in Figure 4-2.



## 4.2 System Performance

The pilot plant central receiver system has been designed and integrated to fulfill the functional requirement that the energy for essential desalination processes are to be derived from solar energy. This was accomplished by performing trade studies to determine the best overall plant configuration and then optimizing each subsystem to obtain the best possible system performance. The subsystem components that require definition are: 1) heliostat field, 2) receiver (and tower equipment), 3) energy storage equipment, 4) steam generator equipment.

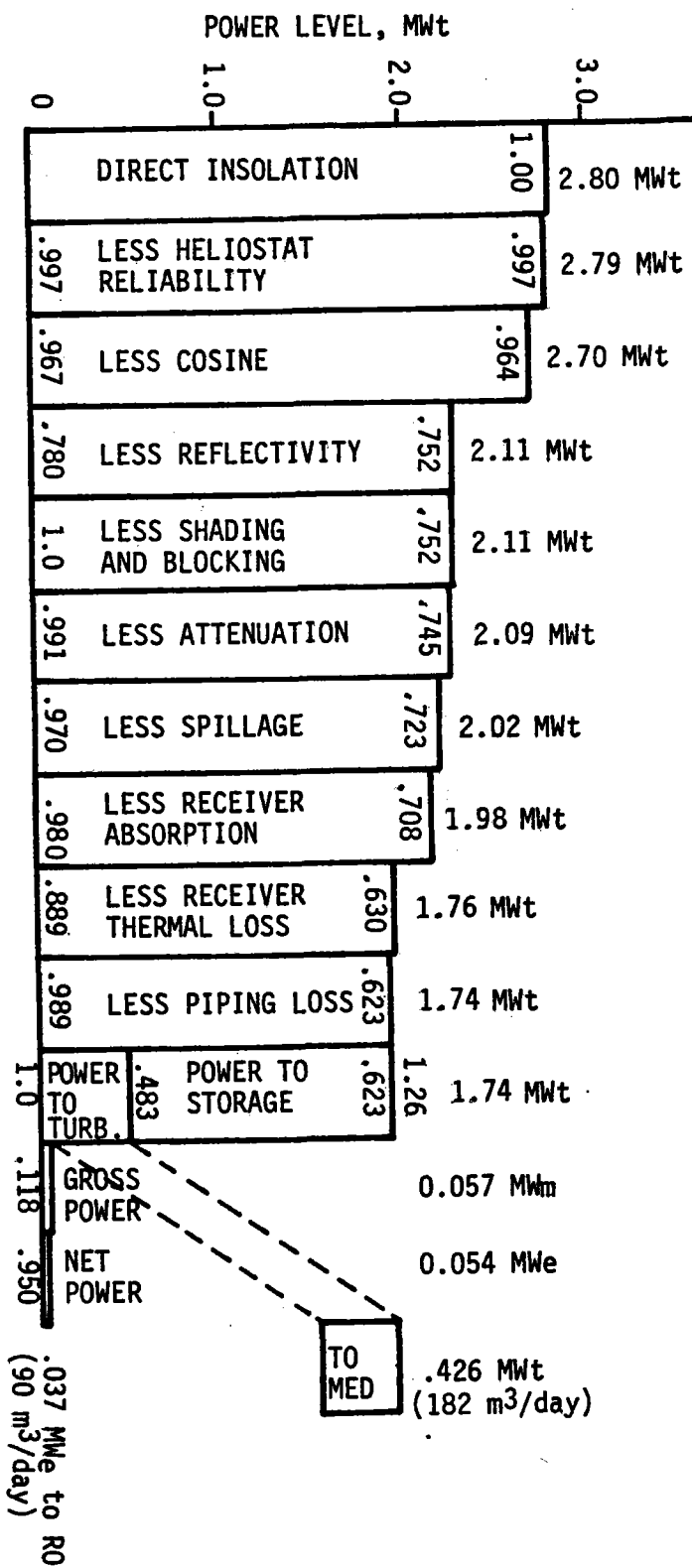
The plant design sequence did not begin with a specific product water output goal, but rather with minimizing the size of the highest cost component of the system - the heliostat field. Figure 4-3 is a Design Point (Day 355, 12:00 solar noon, 950 w/m<sup>2</sup> insolation) staircase efficiency chart showing the energy available to the 75 heliostat field and the subsequent system losses that determine the amount of energy finally delivered to the desalination process.

The field efficiency losses shown occur in the process of delivering the available insolation to the receiver. The receiver is designed to absorb the incident radiation from the collector field at the design point, therefore, the size of the receiver is proportional to the number of heliostats. Of the 202 MWt incident on the receiver, 1.76 MWt is actually absorbed into the circulating molten salt. The other .26 MWt are lost in the form of reflection, reradiation, and convection from the receiver. The molten salt is then delivered to the hot salt storage tank with some associated thermal losses. The optimum storage size was found to be 28 hours (13.52 MWht). The use of a relatively large storage system effectively decouples the collection of solar energy from the use of that energy in the turbine-generator and distillation process. Therefore, the amount of thermal power delivered from storage to the steam generator subsystem can be selected, to some extent, independently from the receiver power output.

The nominal thermal power input to the steam generator equipment was determined to be .483 MWt or 28% of the design point receiver output. This value was selected to allow a large fraction of the energy collected on clear days to be stored for cloudy days and nighttime use. The desalination process can usually be run at full capacity 24 hrs/day from solar energy alone with this design.

The .483 MWt is used to generate steam at 5.5MP/427°C (800°F/800 psia) to be input to the turbine. With a turbine cycle efficiency of 11.8%, the final generator output is .054 MW electric. Of that, .037 MWe is used for the essential desalination processes (RO, MED) and the remainder is used for other auxiliary systems. The turbine exhaust steam contains .426 MWt of useable energy which is used to distill 182 m<sup>3</sup>/day of product water in the MED.

Figure 4-3 Design Point Stairstep (Day 355, Noon, 950 W/m<sup>2</sup> Insolation)





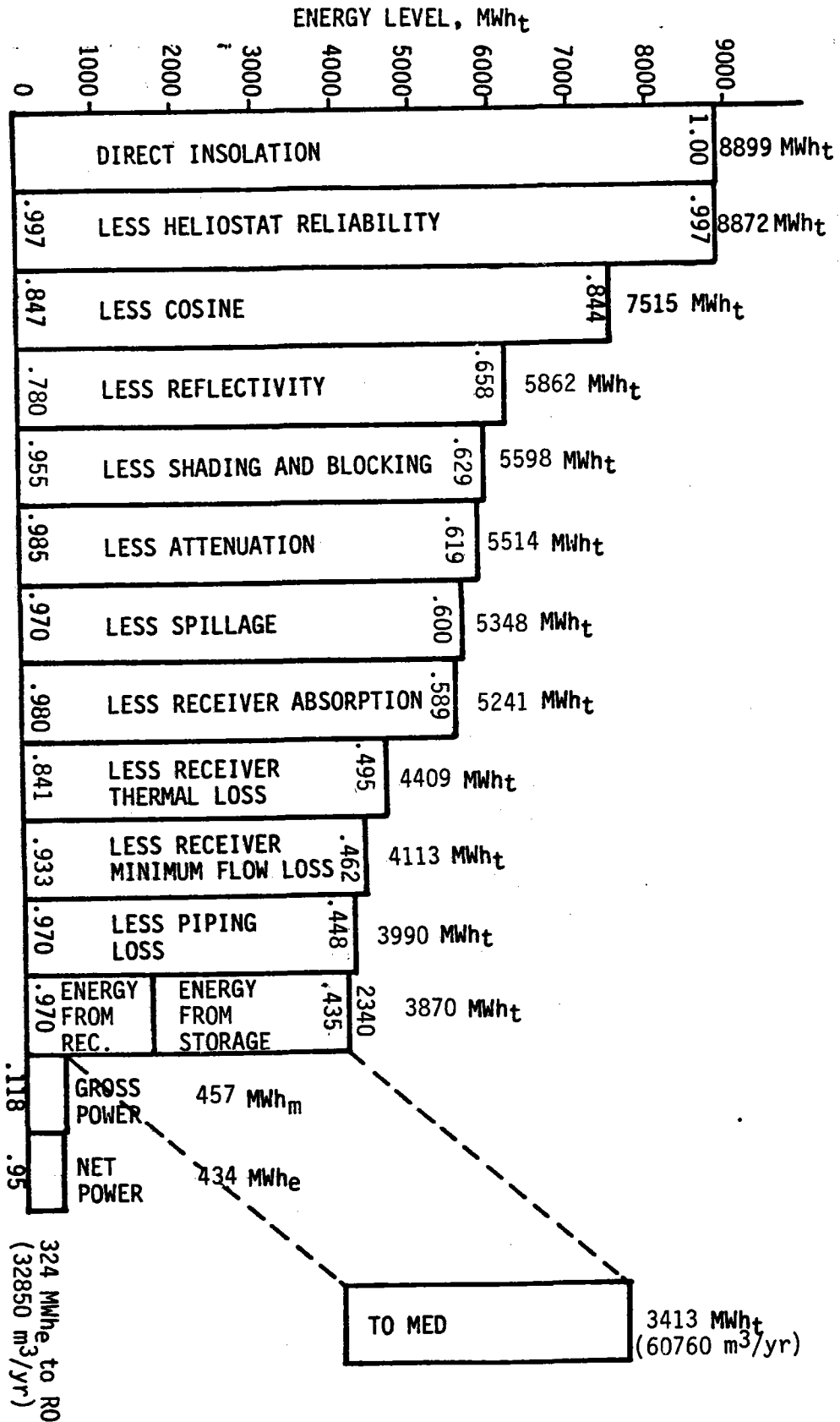
The heliostat collector equipment performance was evaluated using the DELSOL 2 computer program. DELSOL 2 is a revised and extended version of the DELSOL program for calculating collector field performance and layout, and optimal system design for central receiver plants. Receiver losses were evaluated using the TRASYS thermal radiation analysis program for the design point and off-design cases. The results of the individual solar subsystem performance calculations were put into the STEAEC system simulation program, together with solar insolation and weather data, to model the annual performance of the system. The STEAEC program simulates the performance of the system using 15 minute time steps for an entire year.

The STEAEC computer model annual performance stairstep with predictions of various subsystem losses is shown on Figure 4-4. The annual component efficiencies shown are generally lower than their design point counterpart. The "Receiver Minimum Flow Losses" of 6.7% occurs during periods of low insolation levels. The receiver cannot operate at a salt flowrate below 30% of the design point flowrate, therefore, all insolation insufficient to run the receiver at the 30% power level or above is lost (this is also discussed in section 4.5, Receiver Design). The 3% loss in "Energy From Storage" refers to energy that is dumped during periods of high insolation because the storage is fully charged and the receiver is producing more energy than the process can consume. In actual operation, some heliostats will be "turned down" (moved off of the receiver) when this occurs, with the remaining heliostats being enough to produce only what the process can consume at the time.

The annual turbine-generator electrical output of 433 MWhe is more electricity than the essential desalination processes consume ( $.037 \text{ MWe} \times 8760 \text{ hrs/yr} = 324 \text{ MWhe/yr}$ ) in a year. Therefore, the requirement that all electrical power for desalination must come from solar energy is fulfilled. However, the 433 MWhe/yr is less than the amount of power that could be generated if the turbine ran at full capacity all year ( $.054 \text{ MWe} \times 8760 \text{ hrs/yr} = 473 \text{ MWhe/yr}$ ). By supplementing the solar steam flow with steam from the auxiliary boiler during periods of low insolation, the full capacity of the turbine can be maintained all year. The 3413 MWht/yr shown on the stairstep as going to the MED is also not sufficient to run the MED at full capacity all year. Again, the additional 319 MWht/yr required to produce  $182 \text{ m}^3/\text{day}$  all year can be supplied by the auxiliary boiler.

The periods of the year when excess insolation causes energy to be dumped, and the periods of the year when auxiliary energy is required to run at full capacity, can be seen on Figure 4-5. Each bar on the graph represents the daily average energy incident on the collector field for that month. The dotted line represents the average energy level that is required to run the process 24 hrs/day at full capacity. The dotted line varies because the collector field efficiency is higher in the winter than in the summer. The cross-hatched area represents the amount

Figure 4-4 Annual Energy Stairstep



SUFFICIENT ENERGY  
FOR 24 HR/DAY OPERATION  
FROM SOLAR

HELIOSTATS TURNED DOWN

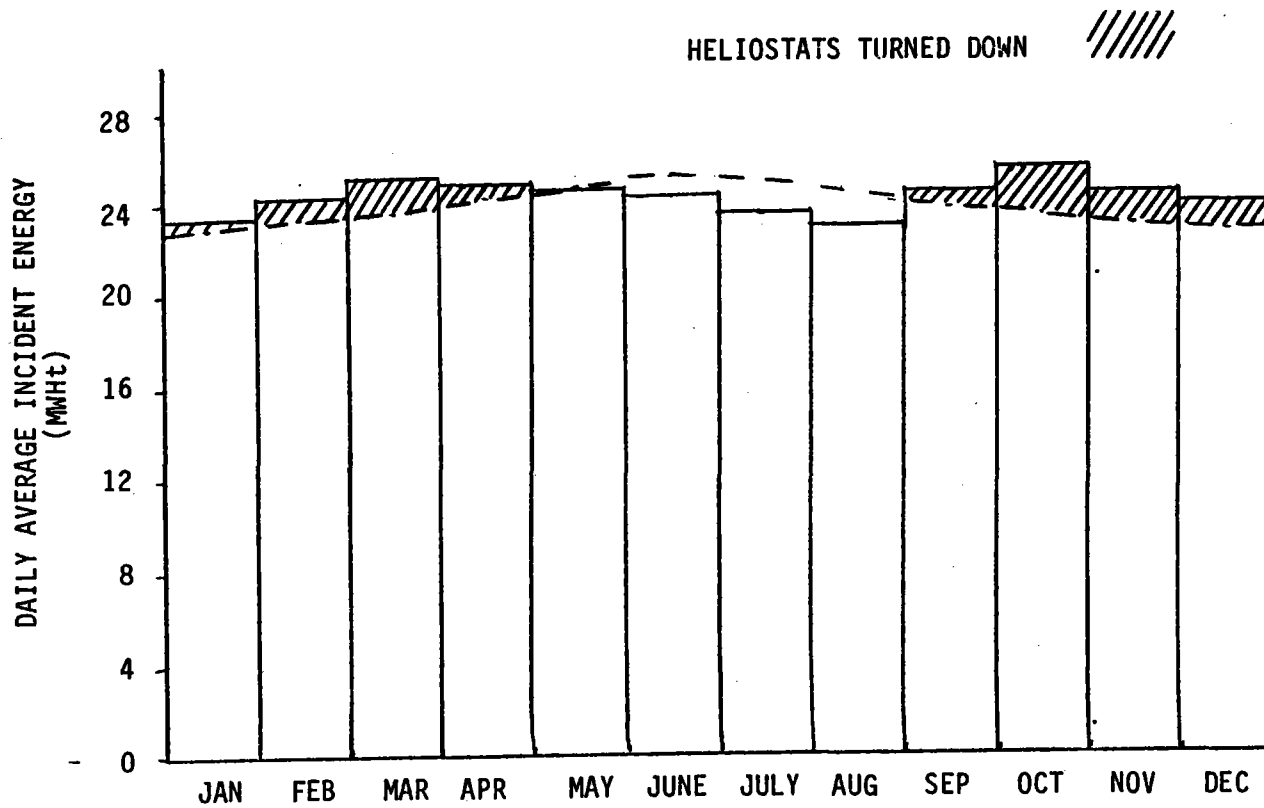


Figure 4-5 Daily Average Energy Incident on Collector Field

of energy that is dumped during periods of high insolation (3% of the annual potential receiver output). The months that fall below the dotted line (June, July, August) are when the auxiliary boiler will be regularly needed to maintain full capacity. An alternative operational strategy is to throttle back the process and reduce the water output during these months in order to reduce the auxiliary energy requirement. In either case, this is a true solar desalination plant as nearly all the energy used for desalination annually is derived from solar energy.

#### Insolation Data

Insolation data used in the analysis was obtained by searching data published by the Kingdom of Saudi Arabia Ministry of Agriculture and Water's Hydrology division for the years 1971-1975. These reports contain monthly mean solar radiation and sunlight duration data for a number of different locations throughout the country. As there was no data recorded at Yanbu, information from a nearby weather station, Mudaylif, was used in its place. (See Figure 4-6.)

The recorded daily sunlight duration data was input to the Solar Irradiance Model (SIM) computer program, which then calculated the theoretical average daily energy collected by a non-tracking horizontal solar collector per month. The measured data for Mudaylif was divided by these results to give a monthly clearness number (CN), a term representing the effective transmissivity of the atmosphere to sunlight. This term was input to SIM, resulting in horizontal data matching the measured insolation values. The corresponding direct normal insolation for Mudaylif was also obtained from SIM. SIM was then used to generate the instantaneous insolation data required as input for the Solar Thermal Electric Annual Energy Calculator (STEAEC) program.

During the contract, 33 days of intermittent insolation data from the plant site at Yanbu became available. The data is from November and December of 1981, and January of 1982. The direct normal insolation from the actual data is lower than the direct normal insolation on the SIM computer model tape.

Average Daily Direct Normal	SIM Synthesized 8.08 KWh/m <sup>2</sup> -day
Insolation for Nov., Dec., Jan	Actual Measured 6.16 KWh/m <sup>2</sup> -day

The 33 days of data is not a sufficient basis for the design of the plant. There is also some question about the instrumentation accuracy at the recording station. However, further investigation into insolation at the site is in order since this is important design information. If the actual insolation is in fact, lower than the SIM data used in the analysis, the plant is adaptable to the lower insolation and the functional requirements of the plant can still be fulfilled.

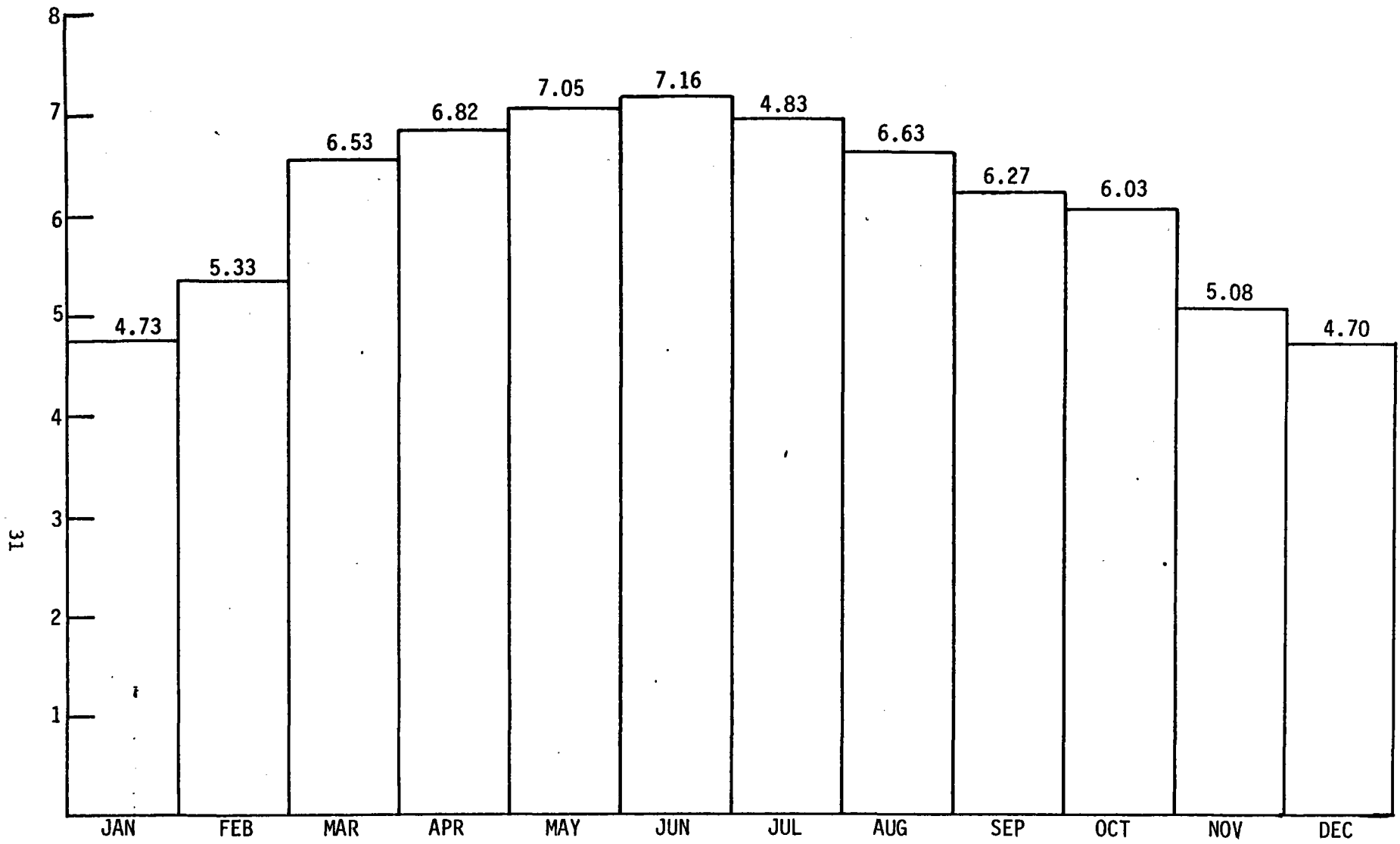


Figure 4-6 Average Values of Recorded Horizontal Plate Insolation (kW-hr/m<sup>2</sup>-day); Mudaylif, S.A.

### 4.3 HELIOSTAT FIELD

The collector field size of 75 Barstow type heliostats (reflective area = 39.31 m<sup>2</sup>) was determined under Task 3 of the program - Cost Reduction Analysis. This field size was identified as the smallest compatible with conventional component sizes and design techniques. The primary driver in the cost-effectiveness of small central receiver systems is the geometric limits on the receiver. Based on the characteristics of the heliostat design and the apparent size of the sun, a minimum aperture size for a cavity receiver is approximately 3m x 3m. (This is also discussed in section 4.5 - Receiver).

#### 4.3.1 DELSOL 2 Program

Once the number of heliostats was selected, the process of optimizing the heliostat field and tower height was begun, using the DELSOL 2 program developed by Sandia National Laboratories - Livermore. DELSOL 2 is a revised and extended version of the DELSOL computer program for calculating collector field performance and layout, and optimal system design for central receiver plants. The code consists of a detailed model of optical performance, a simpler model of the non-optical performance, an algorithm for field layout, and a searching algorithm to find the best system design. The latter two features are coupled to a cost model of central receiver components and an economic model for calculating energy costs. The code can handle flat, focused and/or canted heliostats, and external cylindrical, single, and multi-aperture cavities, and flat plate receivers. The program can optimize the tower height, receiver size, field layout, heliostat spacings, and tower position at user specified power levels subject to flux limits on the receiver and land constraints for field layout.

The size of the image produced by a heliostat on the receiver is determined by the finite size of the sun, the heliostat performance errors, and the size of the heliostat. Reducing the contribution of heliostat size can lead to a smaller image size, and in turn, lower spillage, smaller receivers, and lower receiver radiation and convection losses. DELSOL 2 simulates two methods, focusing and canting, employed to reduce image size by decreasing the contribution from heliostat size.

In focusing, the mirror panels are concave in a manner such that rays from the center of the sun reflected from any point on the mirror panel hit the same point on the receiver. A canted heliostat is divided into a number of submirrors or facets. Each facet is displaced relative to the others such that rays from the center of the sun reflected from analogous points of the facets all converge to the same point on the receiver. Thus, perfect focusing results in the minimum size image by eliminating the contribution of heliostat size to the reflected image. Perfect canting approximates perfect focusing by reducing the total heliostat size to that of a single submirror. The greater the number of canted facets for a given size heliostat, the smaller the contribution of heliostat size to the image. In other words, canting is a Fresnel approximation to focusing.

For the pilot plant, each mirror will not be manufactured for perfect focusing from a given point in the field. The mirrors will be manufactured with three different focal lengths - 77m, 101m, and 132m, (253 ft, 331 ft and 433 ft), with each heliostat position matched with the focal length that will yield the smallest image size. The greater the difference between the focal length and the actual slant range (distance from heliostat to receiver), the greater the focusing error will be, resulting in a larger image size. Each of the 12 facets will be manually canted during installation of the heliostats using a "sun cant" method at 12:00 noon, on or near the spring equinox.

#### 4.3.2 Field Optimization

A previous analysis has indicated a tower height of between 20 to 34m, so the DELSOL 2 program was utilized to optimize collector fields for 20m, 22m, etc., through 34m tower heights. The 28m tower height resulted in the required number of heliostats, 75, in a north field defined by  $+ 55^\circ$  from north. The 28m tower height is measured from the horizontal centerline of the heliostats to the center of the aperture.

The technique used by DELSOL 2 to determine the optimum field shape is to determine a local heliostat efficiency for various locations in the potential field area. Figure 4-7 shows the annual field efficiencies calculated for various zones of the heliostat field. The program determines the land area required for the 75 heliostats, then draws a field boundary (shown as dark line) which will yield the highest total field efficiency. The method used to determine the individual heliostat coordinates with larger fields in the past was to run the RCELL and LAYOUT programs developed by the University of Houston. These programs are not accurate for a very small field, however, so a simple method of determining the heliostat coordinates was used. The radial spacing of the heliostats was calculated in a manner that avoids all heliostat blocking for any time of the year. The tangential spacing was determined with a conventional radial stagger method. The final heliostat field is shown on Figure 4-8 and the heliostat coordinates are shown on Table 4-1. The annual field efficiency breakdown for the 75 heliostat field is as follows:

Heliostat Reliability	.997
Cosine	.847
Reflectivity	.780
Shading and Blocking	.955
Atmospheric Attenuation	.985
Spillage	.970

The reflectivity shown is based on test data from the IEA 93 heliostat field in Almeria, Spain. The glass used is the normal iron content glass as opposed to the low iron glass used for most of field at the Solar One plant near Barstow. The shading and blocking includes tower shadow, and as discussed earlier, the blocking component is actually 0. The atmospheric attenuation shown is based on a 20 mile visibility, although the small field has little sensitivity to this parameter.

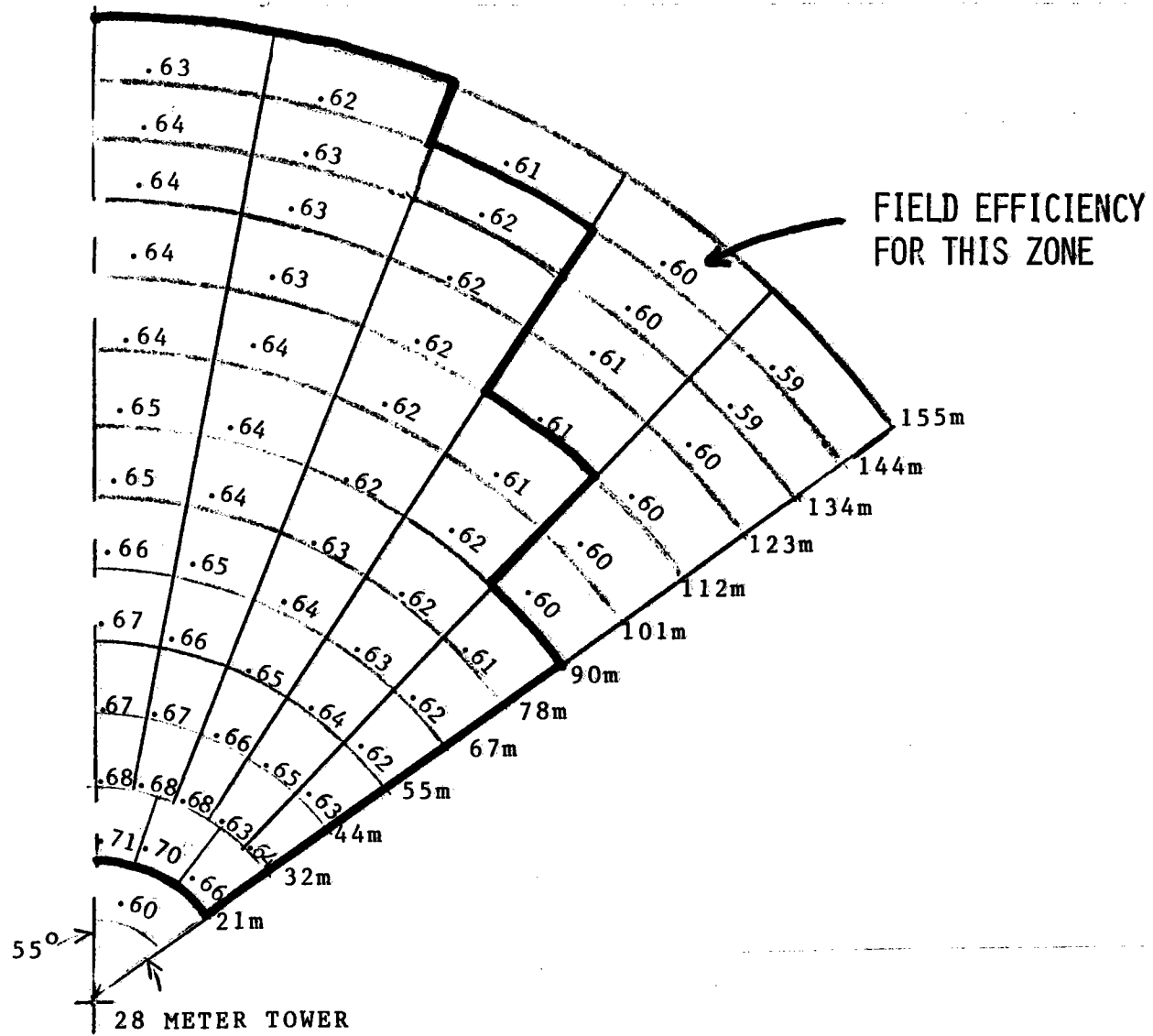


Figure 4-7 DELSOL 2 Field Optimization



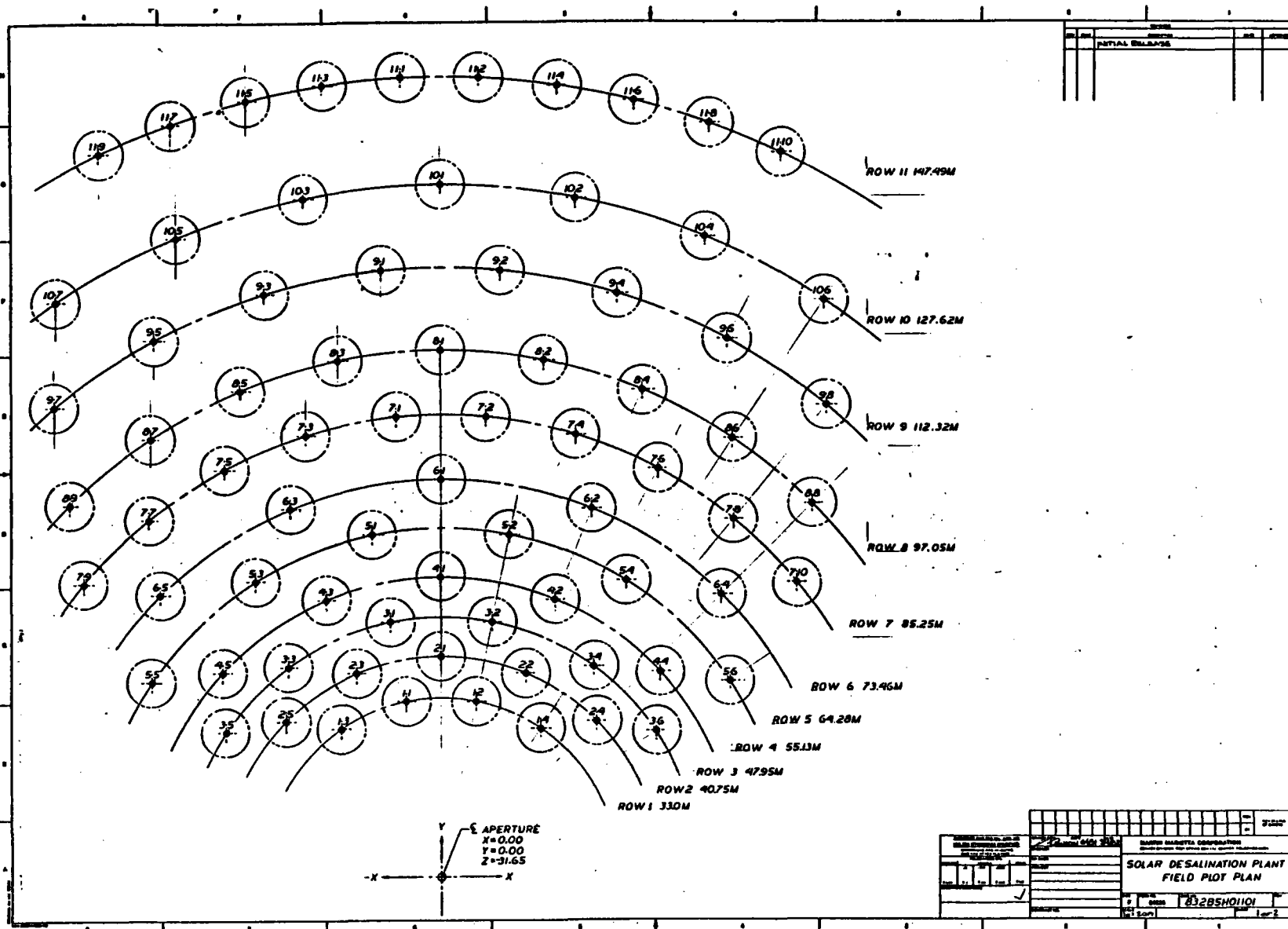


Figure 4-8 Heliostat Field Layout

Table 4-1 Heliostat Coordinantes

Coord. Heliostat X			Coord. Y		Heliostat ID No.	Coord. X		Coord. Y	
ID No.	Meters	Ft.	Meters	Ft.		Meters	Ft.	Meters	Ft.
11	-6.44	-21.1	32.36	106.2	81	0.00	0.0	97.05	318.4
12	6.44	21.1	32.36	106.2	82	18.93	62.1	95.19	312.3
13	-18.33	-60.1	27.44	90.0	83	-18.93	-62.1	95.19	312.3
14	18.33	60.1	27.44	90.0	84	37.14	121.9	89.67	294.2
					85	37.14	121.9	87.67	294.2
21	0.00	0.0	40.75	133.7	86	53.92	176.9	89.69	294.3
22	15.60	51.2	37.65	123.5	87	-53.92	-176.9	80.69	294.3
23	-15.60	-51.2	37.65	123.5	88	68.63	225.2	68.63	225.2
24	28.82	94.6	28.82	94.6	89	-68.63	-225.2	68.63	225.2
25	-28.82	-94.6	28.82	94.6					
					91	-11.00	-36.1	111.80	366.8
31	-9.35	-30.7	47.02	154.3	92	11.00	36.1	111.80	366.8
32	9.35	30.7	47.02	154.3	93	-32.60	-107.0	107.50	352.7
33	-26.63	-87.4	39.86	130.8	94	32.60	107.0	107.50	352.7
34	26.63	87.4	39.86	130.8	95	-52.95	-173.7	99.07	325.0
35	-39.83	130.7	26.67	87.5	96	52.95	173.7	99.07	325.0
36	39.83	130.7	26.67	87.5	97	-71.26	-233.8	86.84	284.9
					98	71.26	233.8	86.84	284.9
41	0.00	0.0	55.13	180.9					
42	21.09	69.2	50.90	167.0	101	0.00	0.0	127.62	418.7
43	-21.09	-69.2	50.90	167.0	102	24.09	79.0	125.17	410.7
44	38.98	127.9	38.98	127.9	103	-24.09	-79.0	125.17	410.7
45	-38.98	-127.9	38.98	127.9	104	48.84	160.2	117.90	386.8
					105	-48.84	-160.2	117.90	386.8
51	-12.54	-41.1	63.05	206.9	106	70.90	232.6	106.10	348.1
52	12.54	41.1	63.05	206.9	107	-70.90	-232.6	106.10	348.1
53	-35.72	-117.2	53.45	175.4					
54	35.72	117.2	53.45	175.4	111	-7.23	-23.7	147.30	483.3
55	-53.42	-175.3	35.76	117.3	112	7.23	23.7	147.30	483.3
56	53.42	175.3	35.76	117.3	113	-21.65	-71.0	145.90	478.7
					114	21.65	71.0	145.90	478.7
61	0.00	0.0	73.46	241.0	115	-35.81	-117.5	143.10	467.5
62	28.11	92.2	63.87	209.6	116	35.81	117.5	143.10	467.5
63	-28.11	-92.2	63.87	209.6	117	-49.69	-163.0	138.80	455.4
64	51.94	170.4	51.94	170.4	118	49.69	163.0	138.80	455.4
65	-51.94	-170.4	51.94	170.4	119	-63.06	-206.9	133.30	437.3
					1110	63.06	206.9	133.30	437.3
71	-8.35	-27.4	84.85	278.4					
72	8.35	27.4	84.85	278.4					
73	-24.74	-81.2	81.59	267.7					
74	24.74	81.2	81.59	267.7					
75	-40.18	-131.8	75.21	246.8					
76	40.18	131.8	75.21	246.8					
77	-54.08	-177.4	65.91	216.2					
78	54.08	177.4	65.91	216.2					
79	-65.88	-216.1	54.11	177.5					
710	65.88	216.1	54.11	177.5					

### 4.3.3 STEAEC Input

The collector field performance excluding heliostat reliability was first evaluated for a matrix of 7 sun azimuth angles and 6 elevation angles to generate the field efficiency matrix for input to the STEAEC system simulation model. The results of this analysis are given in Table 4.2. Using this efficiency matrix in STEAEC, with insolation data from the SIM data tape, the annual receiver output of 3990 MWht was calculated.

Table 4-2 Collector Subsystem Field Efficiency Matrix

Elevation Angle Degrees	0	15	30	45	75	90	120
5	.324	.296	.288	.277	.204	.190	.190
15	.649	.630	.603	.556	.481	.416	.324
25	.760	.768	.751	.686	.593	.529	.482
45	.788	.799	.768	.732	.676	.621	.584
65	.742	.742	.723	.713	.676	.639	.621
95	.658	.640	.641	.629	.619	.620	.612

#### 4.4 HELIOSTAT

The 75 heliostats that will be used for the Solar Desalination Pilot Plant will be of the same design as used for the 93 heliostat field in Almeria, Spain and for the 1818 heliostat field at Solar One near Barstow, California.

The heliostat consists of twelve (12) mirror assemblies, a structural rack assembly, a drive mechanism, a stationary pedestal and the electrical and controls installation. Each heliostat is mounted on an individual foundation as described in C.1 below.

The 12 mirror assemblies are each 3.1m (120.3 in) long by 1.1m (43.3 in) wide for a total heliostat reflective area of 39.3 m<sup>2</sup> (423.1 ft<sup>2</sup>). The mirror assembly consists of a second surface glass mirror bonded to an aluminum honeycomb core. The core is bonded to a steel enclosure pan and sealed with an environmental mirror edge seal.

The mirror assemblies are individually mounted to the structural rack assembly which consists of four bar joists rivited to the elevation beam (a 305 mm (12 in) diameter tube). Each mirror assembly is mounted to the bar joists with a three point mount. This mounting allows the mirrors to be canted so that the centroid of the reflected beam of each of the 12 mirrors fall on the heliostat aiming axis.

The elevation beam of the rack assembly is connected to the drive mechanism by two control arms. The drive mechanism consists of a single housing that encloses both the azimuth axis drive and the elevation axis drive. Each axis is driven by a DC motor with the axis position identified by a 13 bit incremental encoder. Electrical limit switches are mounted on each axis to prevent the heliostat from being driven beyond its mechanical limits.

The drive mechanism is located such that the azimuth and elevation axes are near the centroid of the total reflective surface. The drive mechanism is mounted on the stationary pedestal which in turn is mounted on the foundation.

The pedestal also provides an environmentally protected housing for the individual heliostat controllers (HC). One HC is required for each heliostat and is provided as a component of the electrical installation which also includes the wiring for the motor power and for the encoder signal lines.

##### 4.4.1 Heliostat Foundations

The foundations for the Solar Desalination Pilot Plant heliostats were , designed and analyzed by Black & Veatch Consulting Engineers of Kansas City, Mo under subcontract. The foundation requirements, as established by Martin Marietta Corporation, were compared to the site soil conditions as reported by Saudi Tech Geology and Engineering Consultants of Riyadh, Saudi Arabia.

As a result of the detailed foundation analysis the driven pile foundation system as shown on Figure 4.9 was selected and recommended for the heliostats of the collector subsystem. This system utilizes a cluster of three 305 mm (12") dia piles driven to a depth of approximately 6100 mm (20') and tied together with a cast-in-place concrete cap. The driven pile foundation system combines the least relative cost with the least sensitivity to construction operations.

Heliostat foundation design is primarily controlled by lateral and torsional loading imposed by wind loads on the heliostat structure. The single most important criteria is to meet the system established elastic deflection limits followed closely by the requirement to meet plastic deflection limitations.

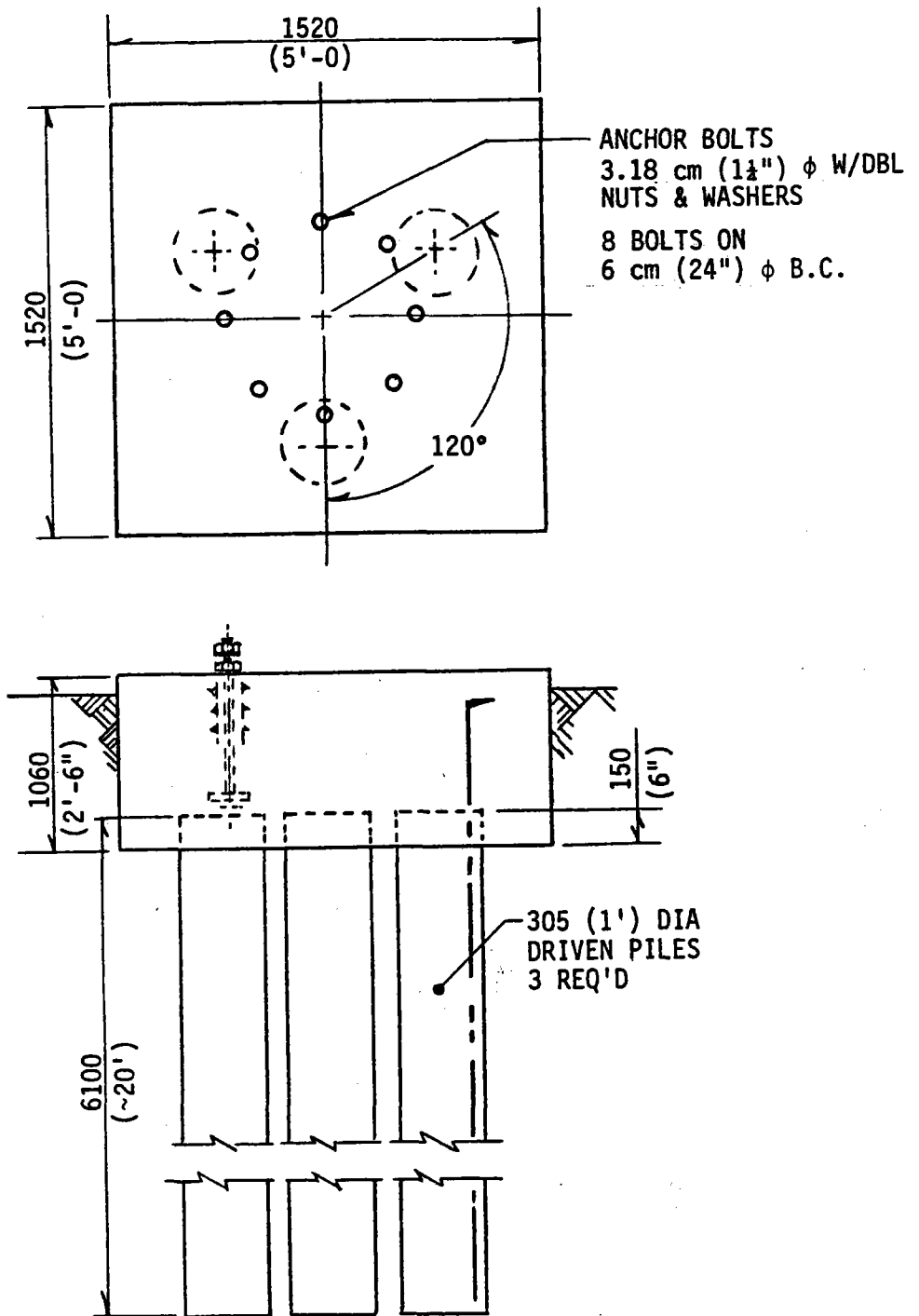
As a result three items directly affect the choice of the foundation system for heliostat support.

- o System Rigidity
- o System Sensitivity to Construction Operations
- o Soil Improvement Requirements

For this study, 3 foundation designs were considered and analyzed: These were 1) spread footings, 2) drilled pier and 3) pile foundation.

System Rigidity - The system rigidity is related to soil-structure interaction. The least rigid system is the spread footing, followed by the drilled pier foundation and the pile foundation, in that order. The stiffness of the soil supporting the spread footing is generally constant, whereas the soil stiffness generally increases with depth for the drilled pier and pile foundation.

System Sensitivity - The most sensitive system with regard to construction operations is the spread footing. Care must be exercised during construction to ensure a tight, compact surface beneath the footing, or differential settlements will occur due to loose, uncompacted soils. The drilled pier follows the spread footing in sensitivity due to the high water table and fine sands. Techniques of drilling the pier require casing or drilled fluid, tremie-poured concrete, and tight construction supervision. The pile system is least sensitive. It is easily installed and easily inspected.



HELIOSTAT FOUNDATION  
SOLAR DESALINATION PILOT PLANT

Figure 4-9 Heliostat Foundation, Solar Desalination Pilot Plant

Soil Improvement Requirements - Based on the results of the analysis and calculations, the spread footings would require a high degree of soil improvement. A dense sand is required to minimize the potential for elastic settlement. This requirement directly affects the system cost. The drilled pier requires a reduced amount of soil improvement; however, it still requires some amount of improvement. The driven pile, by the nature of its installation, provides soil improvement with vibration and material displacement; the driven pile would not require further soil improvement.

The other foundation systems that were investigated was a 2130 mm x 2130 mm x 610 mm thick (7'x7'x2') spread footing and a 910 mm dia x 6100 mm deep (36" dia x 20' deep) cast-in-place pier. The spread footing of the size evaluated was found to be unsuitable to meet the foundation requirements. This concept was discarded due to the extensive amount of material and soil densification required. The drilled pier did meet the requirements but was not selected due to the relative increase in costs and sensitivity to construction operations. The drilled pier also required considerable soil densification.

#### 4.4.2 Other Design Improvements

No significant design changes have been identified or recommended to the present heliostat design. The minor changes that are recommended and described below are primarily a result of experience from the previous heliostat production and installation experience.

Mirror Assembly Design Improvements - Each Mirror Assembly has 3 mounting pads used to mount the mirror to the heliostat structure. The mounting pads or "doublers" are relatively thick steel sheet bonded to the mirror pan to distribute the mounting loads. The change proposed here is the addition of mechanical fasteners (rivets) to the doubler bond. The rivet-bond will serve two purposes. 1) to reduce the sensitivity of the structural bond during assembly operations and 2) provide additional strength to the primary structural bond.

An additional change being evaluated in the mirror assemblies is to substitute a 2 part catalyst activated curing (RTV) silicone for the present one part RTV. The two part RTV cures rapidly at room temperature and does not require the high humidity to promote curing like the one part RTV. The two part RTV is a relatively new compound that has been under intensive testing on mirror assemblies for approximately 1 year with excellent results. The 2 part RTV allows for rapid cure of the mirror environmental seal to also reduce sensitivity to assembly operations.

Drive Mechanism Design Changes - The single change proposed for the drive mechanism is a slight revision to the tooth profile of the azimuth and elevation output gear sets. Although entirely adequate to meet the operational requirements, the pinion gear has proven to be the "weak link". By utilizing an established industry technique of modifying the addendum/dedendum of the tooth profiles the pinion and gear strengths are equalized for a total net gear train strength increase. The modified addendum/dedendum technique merely reduces the depth of the pinion tooth and increases the depth of the gear tooth.

Limit Switch Mounting/Actuation - In the existing operational heliostat fields, the elevation limit switches occasionally malfunction to inadvertently stop heliostat motion prior to reaching design limits. This has been caused by contamination due to blowing sand causing the mechanism to bind and from a force due to slightly mislocated electrical wire routing. A simple tension spring will be added to the switch mechanism to provide the force necessary to overcome the binding action of the sand and force from the electrical wires.

#### 4.4.3 Heliostat Array Controller

Three vendors were considered for the Heliostat Array Controller (HAC) computer. The first one was MODCOMP, because the system already exists in Spain and only minimal changes had to be made to the software. The other two vendors (Digital Equipment Corp. & Hewlett Packard) were selected because they have representatives in Saudi Arabia which is an important cost saving in the area of spare parts, maintenance, and installation.

Since it was known that the MODCOMP Classic 7860 computer in Spain has a steady state loading of 12% as well as the composition of that 12%, it was easy to determine the lowest priced MODCOMP configuration that would do the job in 50% load or less.

The problem of acquisition was more difficult with the other vendors since no comparative benchmarks were available. Initially, price was used to determine competitive configurations. The results of the comparison are shown in Table 4-3 (Acquisition Trade Off), which also includes the estimated Software cost including conversions from MODCOMP Fortran under the MAX IV executive to Digital Equipment Corporation (DEC) Fortran under the RSX 11M executive, the VMS executive, and to Hewlett Packard (HP) Fortran under the RTE-IV, or the RTE-A executive respectively.

At the hardware level, the DEC PDP 11/24 and HP-100/A600 were the leading contenders. Considering hardware and software combined, the HP-1000/A600 and the VAX 11/730 were leading the competition.

After giving considerations to spare parts, MODCOMP suffered the most because of high sparing requirements. HP lost one model in this part of the trade-off, because their representative in Saudi (Modern Electronic Establishment) would not support the relatively new HP-1000/A600.



Table 4-3 Acquisition Tradeoff

Vendor		Digital Equipment Corp. (DEC)			Hewlett Packard		Modcomp
Model		11/24	11/44	11/730	HP-1000-E Model 60	HP-1000 Model A600	Classic 7825
Cost	H/W(\$)	61K	81K	72K	87K	63K	103K
	System S/w (\$)	7K	7K	6K	9K	7K	0
	MMC S/W(\$)	76K	76K	62K	51K	61K	40K
Training in \$		Free 3 Wks	Free 3 Wks	Free 3 Wks	3K	3K	1.5K
Estimated HAC Cost in \$		144K	164K	140K	150K	134K	145K
Development Risk		High	Medium	Medium	Medium	Medium	Small

Table 4-4 Saudi Installation and Maintenance Tradeoff

Vendor		Digital Equipment Corp. (DEC)			Hewlett Packard (HP)		Modcomp
Model		11/24	11/44	11/730	HP-1000-E Model 60	HP-1000 Model A600	Classic 7825
Estimated HAC Cost in \$		144K	164K	140K	150K	134K	145K
Spares Cost in \$		18K	26K	26K	11K	N/A	57K
U.S. & Saudi Installations (\$)		9K <sup>+</sup>	12K <sup>+</sup>	11K <sup>+</sup>	5K	N/A	3K
Monthly (in \$) Maintenance	U.S.	815	865	839	608	N/A	1363-
	Saudi	3097	3287	3188	2200	N/A	1363*
Total Maint. (10 mo + 6 mo)		27K	28K	28K	19K	N/A	22K*
Support Risk		Low	Low	Medium	Low	Low	High
Control Consoles + Clocks in \$		13K	13K	13K	13K	13K	13K
Overall Costs (\$)		211K	243K	218K	198K	N/A	240K*

\*Plus Travel Expenses from England during Saudi Installation Maintenance  
 +Estimated by Multiplying U.S. Installation x 2

However, the HP-1000-E/60 gained ground because of their low sparing requirement and inexpensive installation charge (no charge for U.S. installation while DEC charges twice). Low monthly maintenance in the U.S. and Saudi put the HP-1000-E/60 further ahead. Table 4-4 shows the maintenance and overall costs for the total maintenance cost and the overall cost.

In parallel to the cost trade-offs, a benchmark program attempting to measure the Spain HAC CPU loading was run on various models which were readily available. For DEC this included the models PDP 11/70, PDP 11/44, and VAX 11/780. For HP this included the HP-1000-F/40. Vendor published data was used to normalize results to the cost-effective models and all models met the criterion of being loaded by 50% or less except the PDP 11/24 as shown in Table 4-5.

Taking into account four items out of the above mentioned Tables; a) acquisition cost including spares, b) maintenance and installation cost, c) development risk and, d) maintenance risk the HP-1000-E/60 was the selected hardware.

Table 4-5 Performance Tradeoff and Summary

Vendor		Digital Equipment Corp. (DEC)			Hewlett Packard (HP)		Modcomp
Model		11/24	11/44	11/730	HP-1000-E Model 60	HP-1000 Model A600	Classic 7825
Performance (ms per second)	Math	55	13	13	196	315	255
	Logic	589	295	304	132	152	109
	I/O	203	102	105	42	35	48
Estimated Steady State HAC Load in %		85	41	42	37	50	41
Conclusion		Load factor too high	Too ex- pensive	Brand new product	Current all around selection	Least expensive optimum per- formance but not supported in Saudi.	Most expensive least S/W risk, most maintenance risk.

NOTE: Additional equipment common to all systems: 2 Color CRTs + 1 Spare = 12K\$  
2 Quartz Clocks + 1 Spare = 1K\$

## 4.5 RECEIVER

The basic function of the receiver is to effectively intercept radiant solar heat flux directed from the collector field and efficiently transfer that thermal energy to the heat transfer fluid for conversion to process steam and electrical power. The receiver for the Desalination Pilot Plant is a north facing aperture cavity type receiver mounted on a 30.17 M (99.0 ft) tower. The receiver cavity was selected over an exposed receiver because of its higher thermal efficiency as shown by extensive thermal analysis conducted during previous programs.

In the absence of specific peak insolation data for the plant site, the maximum possible insolation was assumed to be  $1,100 \text{ w/m}^2$  for the design of the receiver. This value is generally accepted as an upper limit for insolation at solar plant sites throughout the world. This insolation is only used to predict peak metal temperatures on the receiver. An insolation of  $950 \text{ w/m}^2$  was used as an average clear day peak. The receiver design point is defined as: Day 355, 12:00 solar time,  $950 \text{ w/m}^2$  insolation. The receiver and auxiliary equipment are sized to the design point power level. A second parameter requiring specification is the effective angular magnitude of the solar disc (sun disc angle). The angular magnitude of the sun as viewed from space is 32.53 minutes of arc. In order to account for atmospheric effects, mirror imperfections, and tracking inaccuracies, a "degraded" solar disc angle is normally used in the flux calculations, a suitable value being 50 minutes of arc.

### 4.5.1 Cavity Configuration Design

The purpose of this activity was to establish the overall geometry of the receiver cavity, including aperture size, and the dimensions and locations of the active (heat absorbing) walls. The process is an iterative one, and consists of the calculation of flux maps on the aperture plane and on the inside walls of a set of candidate cavity geometries (configured on the basis of previous experience), and selecting the configuration that best meets the criteria for the design. The latter include; (1) Optimizing the aperture size to minimize the sum of re-radiation, convection, and spillage losses; (2) minimizing incident flux levels on non-active cavity surfaces; (3) limiting peak local fluxes to acceptable levels and (4) minimizing the area of the absorption surfaces.

The physical dimensions of the receiver are dependent on the image (solar flux profile) projected onto the receiver from the 75 heliostat field. Each heliostat consists of 12 "facets" or smaller mirrors, each canted towards the center of the aperture. The facets are manufactured with 3 different focal lengths, 77M, 101M, and 132M. The focal length for a given heliostat is selected to obtain the smallest image size on the receiver. The image size projected onto the receiver from a single heliostat is dependent on the length of the facets (3.0M), the focal length of the facets, the slant range (distance from heliostat to receiver), and the angle of incidence of the reflected ray with respect to the aperture plane. Using these parameters with a sun disc angle of 50', the image size can be calculated for a solar beam normal to the receiver aperture. Table 4-6 shows the image diameter at the receiver aperture for each row of the heliostat field.

Table 4-6 Heliostat Image Size at Receiver Aperture

<u>Heliostat Row No.</u>	<u>Slant Range to Aperture (M)</u>	<u>Nominal Mirror Focal Length (M)</u>	<u>Image Diameter at Receiver Aperture (M)</u>
1	43.3	77	1.94
2	49.4	77	1.80
3	55.5	77	1.65
4	61.8	77	1.49
5	70.1	77	1.27
6	78.6	77	1.25
7	89.7	101	1.64
8	101.0	101	1.50
9	115.8	101	2.03
10	130.7	132	1.94
11	150.1	132	2.39

Ideally, the flux distribution at the receiver aperture should be as concentrated as possible without exceeding material temperature limitations. A small flux distribution decreases the aperture area required, thereby reducing thermal losses. The image size projected from Barstow type heliostats cannot be reduced below those values shown in Table 4-6, because the facet length is fixed at 3.0m. The result is a relatively large flux distribution and reduced flux levels from the small (75 heliostat) field. For this reason the efficiency of the pilot plant receiver will not be as high as that of a commercial scale receiver. This, however, should not significantly effect the validity of extrapolating the pilot plant experience to the design and operation of a commercial plant, since all key design parameters are analytically tractable.

The analytical tool used for design of the receiver was the Martin Marietta Thermal Radiation Analysis System (TRASYS) - a computer program originally developed to support thermal analyses of space systems. Over several years, the program was expanded to handle radiation problems associated with heliostat fields by the addition of several subroutines.

The basic element in the heliostat radiation model used by TRASYS is a beam of circular cross section with an area at the origin equal to the effective (cosine-modified) area of the mirror that produced it. In the most general case, the beam is convergent-divergent along its axis; its minimum area occurs at the focal length and is determined by the subtended angle of the sun. The radial distribution of the solar flux within the beam is assumed to be Gaussian. The program accounts for atmospheric attenuation, heliostat reflectivity, and shadowing of the heliostat field by the tower. With insolation, atmospheric attenuation constants, and receiver and heliostat field geometry as inputs, the program calculates the incident radiation flux distribution on the target, which is divided into isothermal nodes. The target type may be exposed or cavity, the latter being distinguished by the inclusion of an "aperture" in the target geometry. The aperture has the unique property of transmitting all radiation impinging inside its boundaries, while blocking all that falls on its plane external to the boundaries. Aim-point coordinates can be specified for each heliostat in the field.

The TRASYS program does not account for shadowing or blocking by adjacent heliostats in the collector field, effects of sun-tracking errors, mirror imperfections, optical aberation due to mirror curvature at large incidence angles, or "sun-shapes" different from the Gaussian. Fortunately, the combined errors in the predicted flux distributions due to these effects are expected to be relatively small during the "high noon" hours, which determine the peak design fluxes on the receiver surfaces.

During the installation of the heliostats, each of the 12 facets of the heliostats will be "canted" or adjusted so that the reflected solar beam from each facet is aimed toward the center of the aperture. Because the pilot plant heliostat field is so small, the heliostat canting has a significant effect on receiver design. The individual adjustment of the heliostats is accounted for by TRASYS model in which each heliostat is broken into 12 facets (or nodes) with each node being canted towards the center of the aperture. This is not necessarily true in the case of larger fields, where each heliostat appears as a single node in the TRASYS model. Figure 4-10 shows the affect on image size at the aperture for the two modeling methods. The 12 node method results in a slightly tighter flux distribution, which agrees more closely to test data from the 93 heliostat field at Almeria, Spain.

#### 4.5.2 Aperture Sizing

The aperture of a cavity receiver has two purposes: (1) capture reflected solar energy from the collector field, and (2) reduce the energy losses from the cavity. The aperture size was optimized by minimizing the sum of the receiver thermal losses and spillage losses (see Figure 4-11). The spillage losses are defined as the reflected radiation that falls outside the aperture. The spillage losses are determined by using the TRASYS program to generate a flux map at the plane of the aperture. The flux map is large enough to intercept all reflected radiation from the heliostat field (see Figure 4-12). The amount of spillage for a given aperture size can be determined by summing the fluxes incident on the nodes external to the aperture.

The receiver thermal losses include reradiation, convection, reflection out of the aperture, and conduction losses through the structure and insulation of the receiver. Calculation of these losses is based on test data from the Alternate Central Receiver (ACR) 5 MWt Molten Salt Receiver recently build by Martin Marietta and tested at th Central Receiver Test Facility (CRTF). The desalination receiver is very similar in configuration to the receiver tested. The loss calculations are based on aperture area, since this is the major parameter that governs thermal losses.

Convection losses -

At design point, the convective losses were found to be 2.18% of the input (through the aperture) energy of 5 MWt. The aperture area for the ACR receiver is 7.81 m<sup>2</sup> (84.1 ft<sup>2</sup>).

$$\begin{aligned} \text{losses per m}^2 \text{ of aperture} &= \frac{(.0218) (5.0) \text{ MW}}{(7.81) \text{ m}^2} \\ &= 13.95 \text{ kW/m}^2 \text{ of aperture} \end{aligned}$$

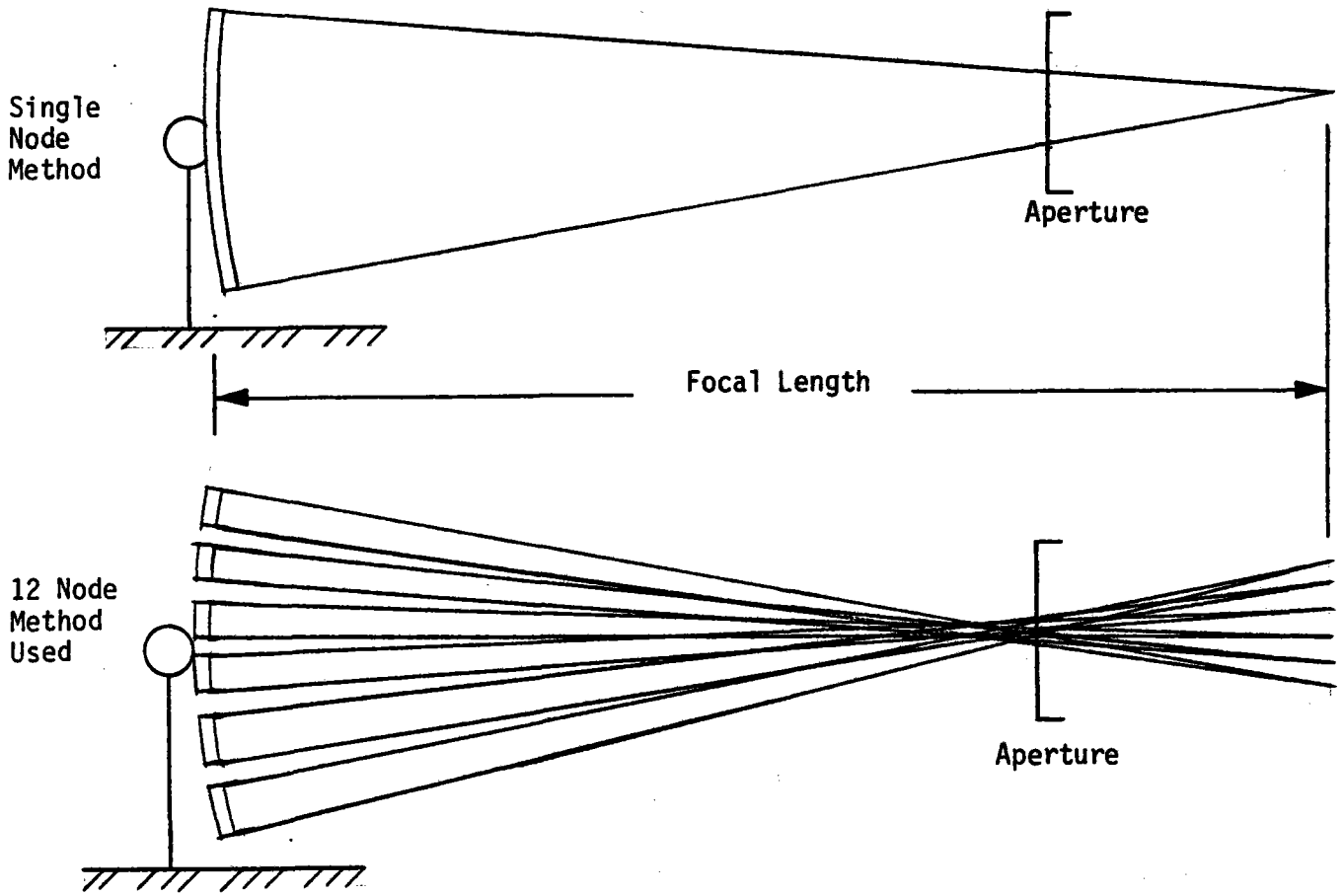


Figure TRASYS Beam Modeling Technique

Figure 4-10 TRASYS Beam Modeling Technique



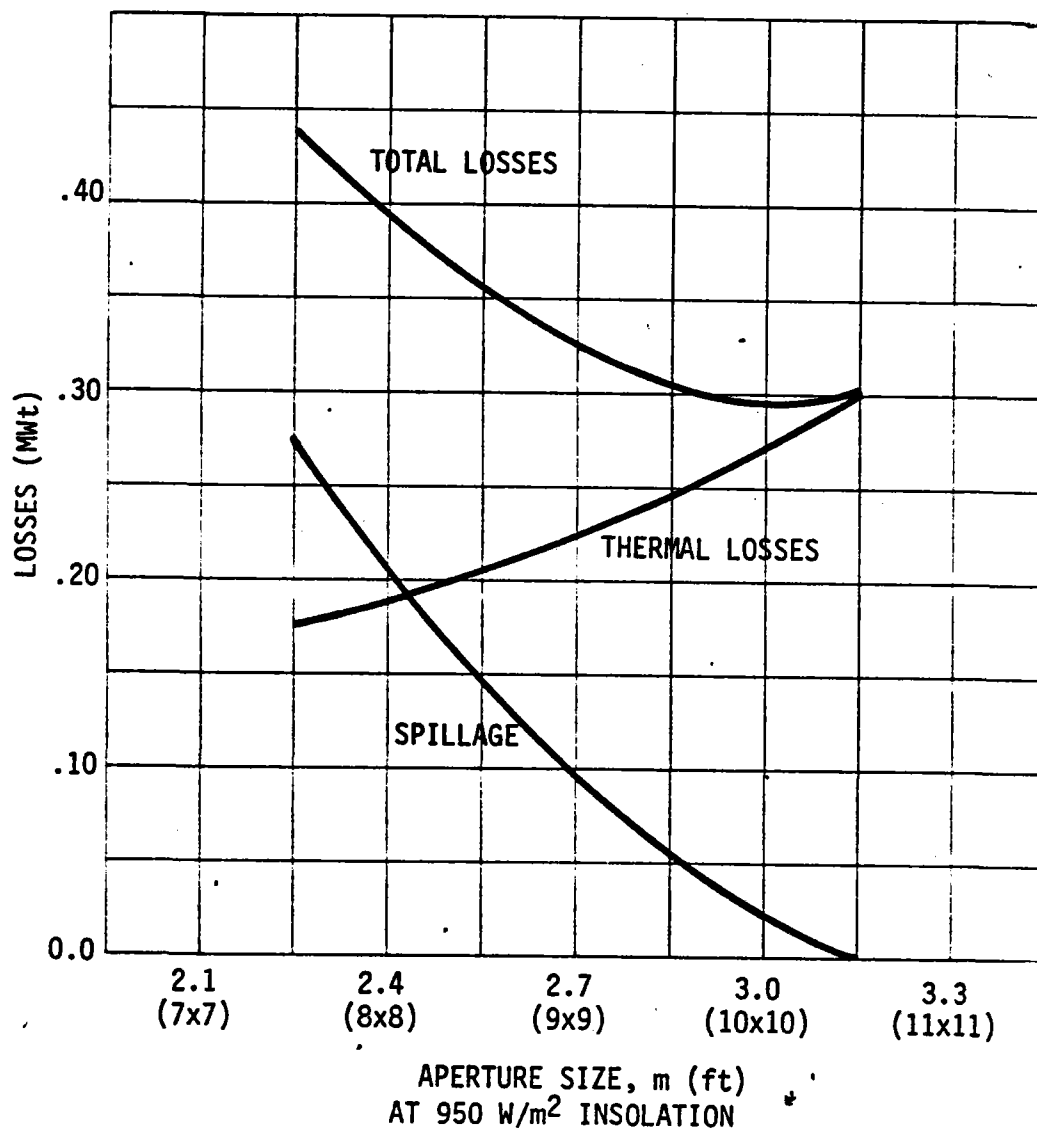
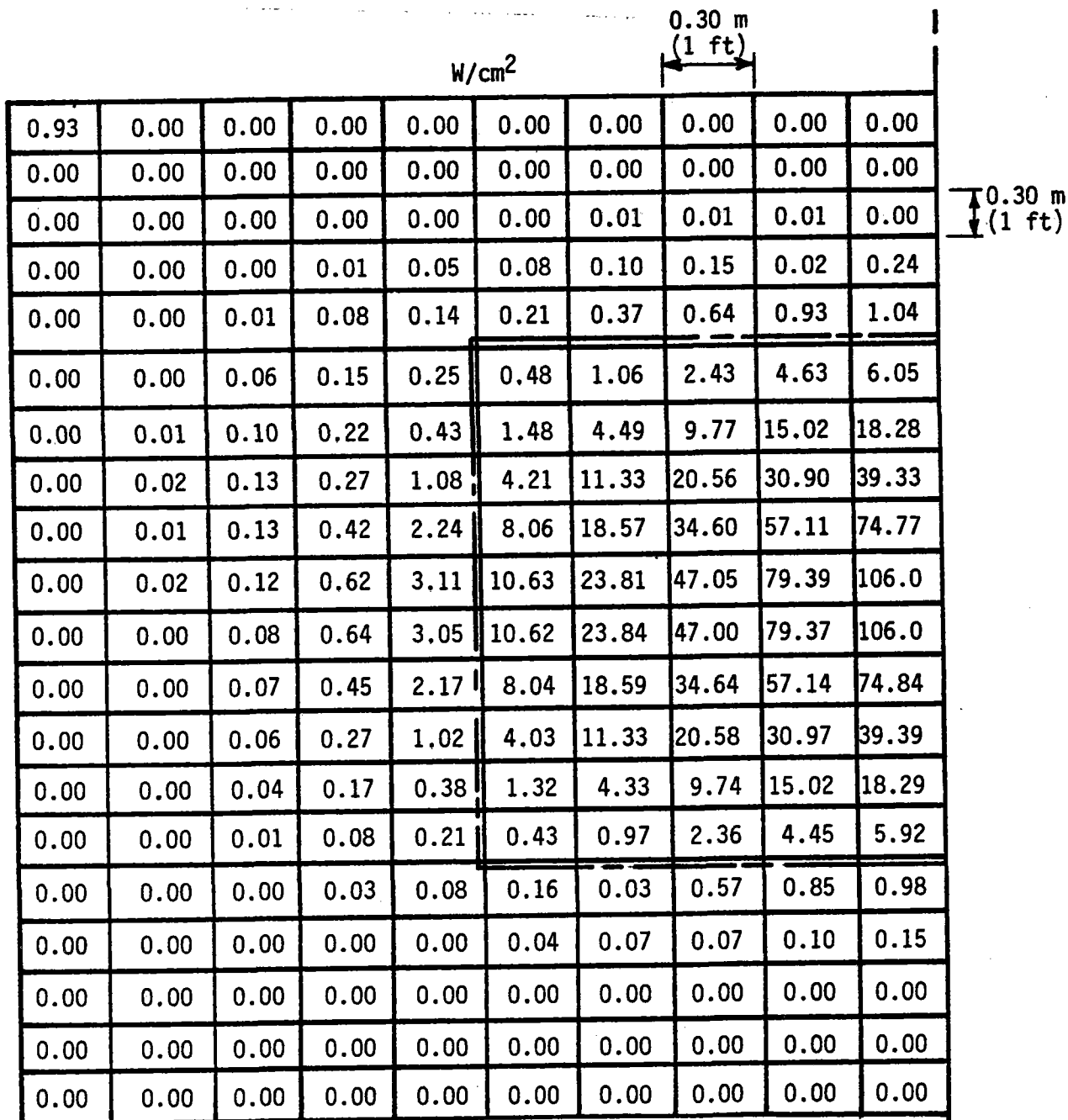


Figure 4-11 75 Heliostat Field Aperture Sizing



INSOLATION 1.1 kW/m<sup>2</sup>  
 DAY 355  
 TIME 12:00

Figure 4-12 Flux Map at Aperture Plane

Emitted losses -

The average receiver cavity temperature is estimated as:

$$T_R = \frac{T_i + T_o}{2} = \frac{(288 + 538)}{2} = 413^\circ\text{C} \\ = 686^\circ\text{K}$$

$$\text{Emitted losses} = Q_R = E A_a (T_R^4 - T_{\text{sky}}^4)$$

E = effective emittance of cavity = .86

$$= .1714 \times 10^{-8} \text{ Btu/hr-ft}^2\text{-}^\circ\text{R}^4$$

$$= 5.669 \times 10^{-8} \text{ w/m}^2\text{-}^\circ\text{K}^4$$

Aa = Aperture area

$$T_{\text{sky}} = -1^\circ\text{C} = 272^\circ\text{K}$$

$$\frac{\text{Emitted losses}}{A_a} = (5.669 \times 10^{-8})(.86)(686^4 - 272^4) = 10.53 \text{ kW/m}^2$$

Conduction losses -

Were found to be .2% of the input power.

$$\frac{(.002)(5) \text{ MWt}}{(7.81) \text{ m}^2} = 1.28 \text{ kW/m}^2$$

Reflection losses -

Reflection losses are effectively .02 or 2% of the incident energy (through aperture).

#### Total losses

Total losses = Convection loss + Reradiation loss + Conduction loss + Reflection loss

$$= (13.95) \text{ kW/m}^2 + (10.53) \text{ kW/m}^2 + (1.28) \text{ kW/m}^2 + (.02) \text{ (incident energy)}$$

$$\text{Total losses} = (25.76) \text{ kW/m}^2 \text{ aperture} + (.02) \text{ (incident energy)}$$

The optimized aperture size was found to be 3.05m x 3.05m (10 ft x 10 ft). This is a fairly large aperture for the small number of heliostats, because of the reasons stated earlier concerning the image size projected from the Barstow heliostats. In fact, for any collector field of 125 heliostats or less, the optimum aperture size is about the same (3.0m x 3.0m). The receiver will produce 1.76 MWt of power at the design point with this configuration.

#### 4.5.3 Receiver Cavity Design Tradeoffs

**Tilted Aperture vs. Vertical Aperture** - The area of the aperture was minimized by tilting it down towards the heliostat field by  $15^\circ$  so that the reflected radiation is more normal to the aperture. The design of the aperture door is somewhat more difficult with a tilted aperture compared to a vertical aperture, but the increase in receiver efficiency is worthwhile.

**Tilted Receiver Panel vs. Vertical Receiver Panel** - The area of the active receiver panel can also be minimized by tilting it down towards the heliostat field. To evaluate this option, TRASYS was used to generate a flux map on the receiver panel for both the tilted and vertical case. The flux distribution on the panel determines the height and width of the panel. The panel is sized large enough to intercept almost all of the radiation entering the aperture, with the radiation on the non-active surfaces being below acceptable limits. It was found that the height of the panel could be reduced by .305m (1.0 ft) by tilting it towards the heliostat field by  $15^\circ$ . However, a tilted panel causes problems in the design and fabrication of the panel support structure. Suspending the receiver to allow for thermal growth becomes more difficult and downward bowing of the receiver tubes during operation becomes a problem. To avoid these problems a vertical absorber panel was used in the design of the receiver.

**Single Wall Receiver Panel vs. Triple Wall Receiver Panel** - An alternate to the single absorber panel at the back of the receiver cavity is to break the panel into three sections. One panel is on the east wall of the cavity one on the west wall, and one on the back (south) wall of the cavity. This method results in a more compact receiver with the total width of the panels less than that of the single wall configuration. The triple wall configuration results in increased cost, however, resulting from a more complex panel support structure and header piping system. Therefore, the single wall receiver panel configuration was used.

**Cavity Depth and Heliostat Aim Point Strategy** - The highest solar flux intensity occurs at the center of the aperture where the heliostats are aimed. The flux intensity decreases as the radiation passes through the cavity. The cavity depth (distance from the center of the aperture to the receiver panel) is usually set at a distance sufficient to maintain peak fluxes on the panel below acceptable limits. Because of the relatively large flux distribution with low intensity flux in the case of the pilot plant receiver, the panel could be placed only .914m (3 ft) behind the aperture and still maintain acceptable flux levels. However, convection losses from the cavity would be unacceptable with such a short cavity depth. The solution to this problem was to move the aim point of the heliostats .914m (3 ft) into the cavity (.914m behind the center of the aperture). This allowed the cavity depth to be increased to 1.83m (6 ft) while keeping the size of the panel reasonably small.

The final cavity configuration is shown on Figure 4-13. The 3.05m x 3.05m (10 ft x 10 ft) aperture is tilted by 15°. The 3.05m (10 ft) high x 3.66m (12 ft) wide vertical absorber panel sits .914m (6 ft) behind the center of the aperture. The peak point and design point flux incident on the panel is shown on Figures 4-14 and 4-15.

#### 4.5.4 Thermal and Hydraulic Design

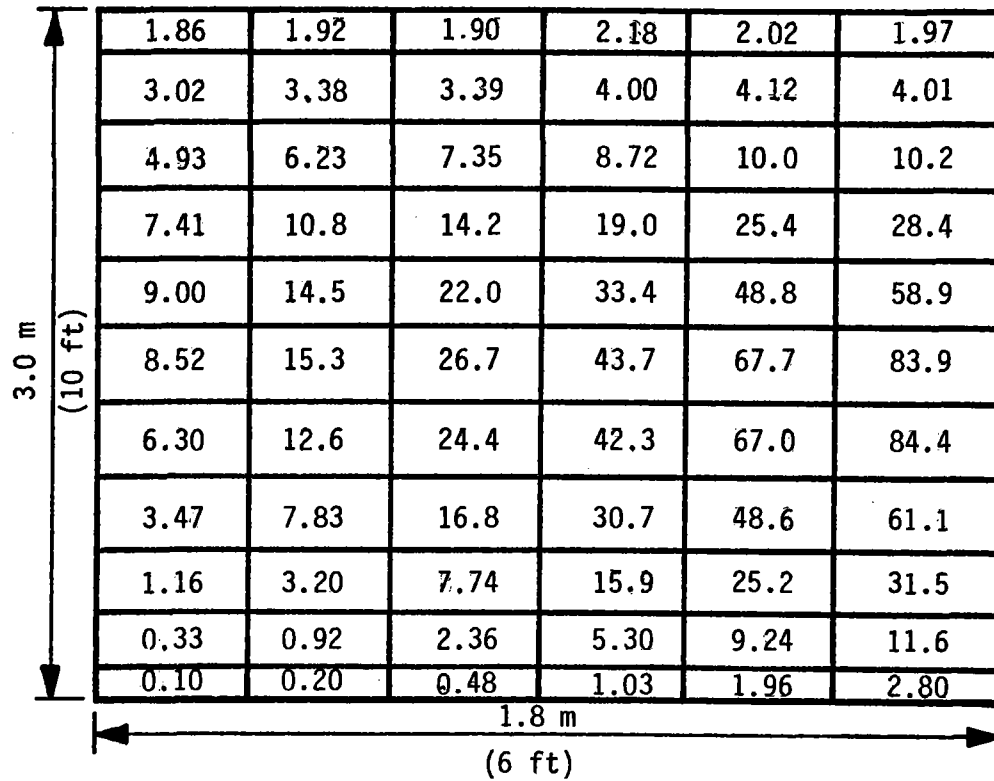
A flow schematic of the receiver is shown in Figure 4-16. Molten salt (60% NaNO<sub>3</sub>, 40% KNO<sub>3</sub> by wt.), nominally at 288°C (550°F), is pumped from a cold storage tank at ground level to the cold surge tank located on the top of the receiver. During normal operation, the liquid level and the ullage pressure in the surge tank are maintained constant. The principal function of the surge tank is to temporarily maintain salt flow through the receiver following a pump failure. It also decouples the receiver control system from pump transients during normal operation by providing a salt supply at essentially constant upstream pressure. The salt flows through 14 serpentine tube bundle passes of the receiver where it is heated to 538°C (1,000°F). The hot salt is discharged through a hot surge tank into the downcomer. The function of the hot surge tank is to maintain the receiver outlet pipe submerged at all times, and in conjunction with the controlled level of the cold tank, to maintain a constant static head across the receiver. The hot salt is then returned to the hot storage tank. The headers, valves, tanks and interconnecting piping will be heat-traced to prevent freezing of the salt during startup or standby.

With the heat flux levels and distribution inside the cavity established, the tubing panels comprising the active (heat absorbing) wall of the cavity can be sized to provide proper heat transfer coefficients at acceptable pressure drops through the receiver. The thermo-hydraulic design criteria are as follows: 1) the local peak metal temperature on the outside of the tubes should not exceed 649°C (1,200°F), 2) the local peak metal temperature on inside of the tubes should not exceed 600°C (1,112°F), 3) The Reynolds number inside the tubes should not be less than 4,000 at the minimum operational flowrate to avoid laminar flow. Laminar flow would significantly reduce the heat transfer from the metal to the salt and cause damage to the tubes from overheating. The minimum operational flowrate is defined as 30% of the design point flowrate, 4) The peak thermal stress in the tubes should not exceed twice the yield strength of the Incoloy 800, 5) The pressure drop through the receiver should be minimized to reduce the molten salt pump work.

The principal elements of the physical layout of the absorbing panels that need to be defined are: 1) number of control zones, 2) tube diameter, 3) number of passes, 4) salt flowpath arrangement. A receiver control zone is that portion of the receiver associated with a single inlet and a single outlet. The pilot plant receiver will have a single control zone, mainly because of its small size. The tube size chosen is 13mm (.50 in) OD with a 1.65mm (.065 in) wall. The small tubes are required to decrease the cross-sectional flow area, thereby increasing fluid velocities and heat transfer coefficients. The number of passes in a receiver is determined by the required fluid velocity in the

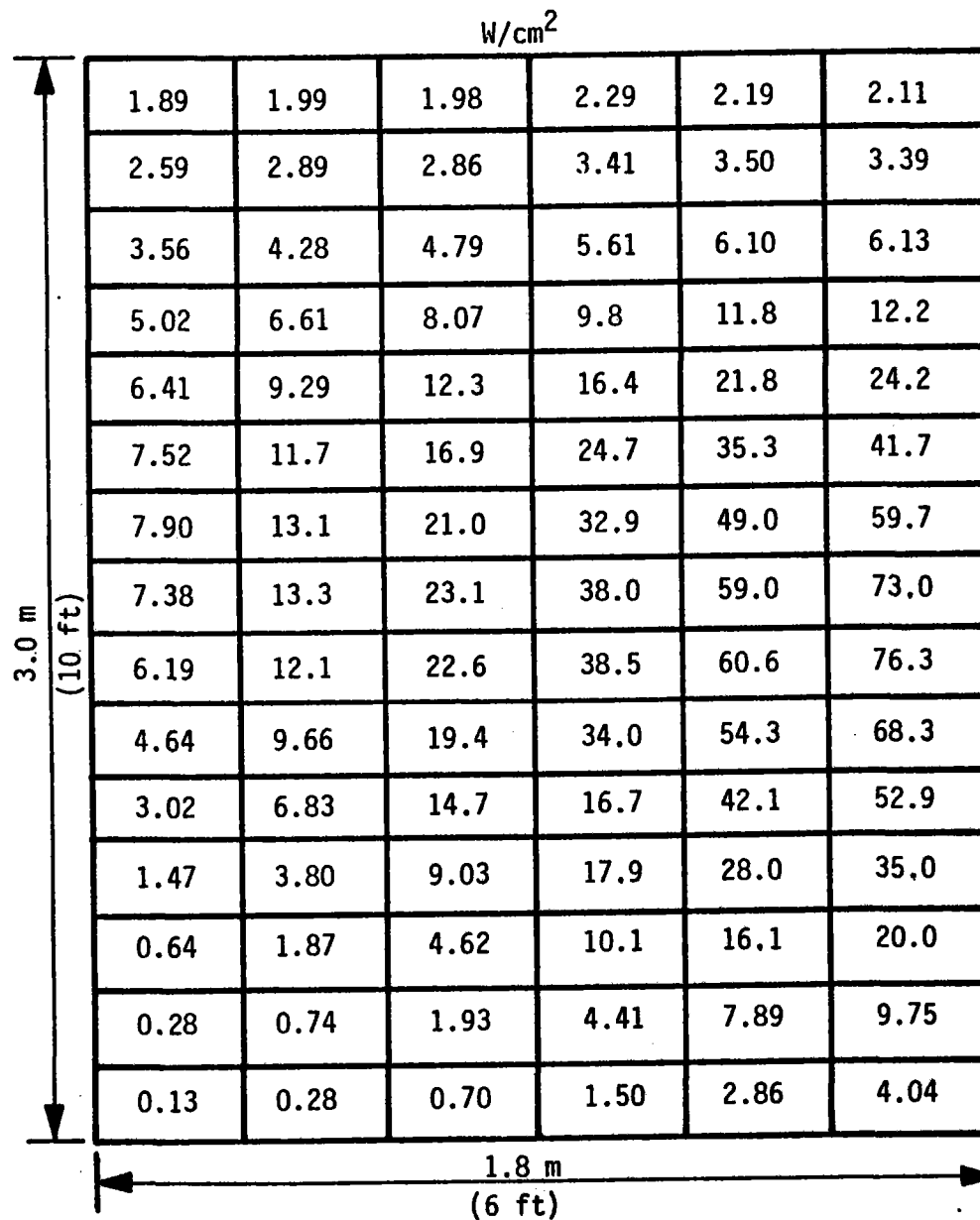


Receiver Incident Flux Map ( $W/cm^2$ ) - Peak Point



Day 355  
 12:00  
 1100  $W/m^2$  Insolation

Figure 4-14 Incident Flux at Peak Point



950  $W/m^2$  Insolation

Time: 12:00

Day: 355

Figure 4-15 Receiver Incident Flux Map - Design Point



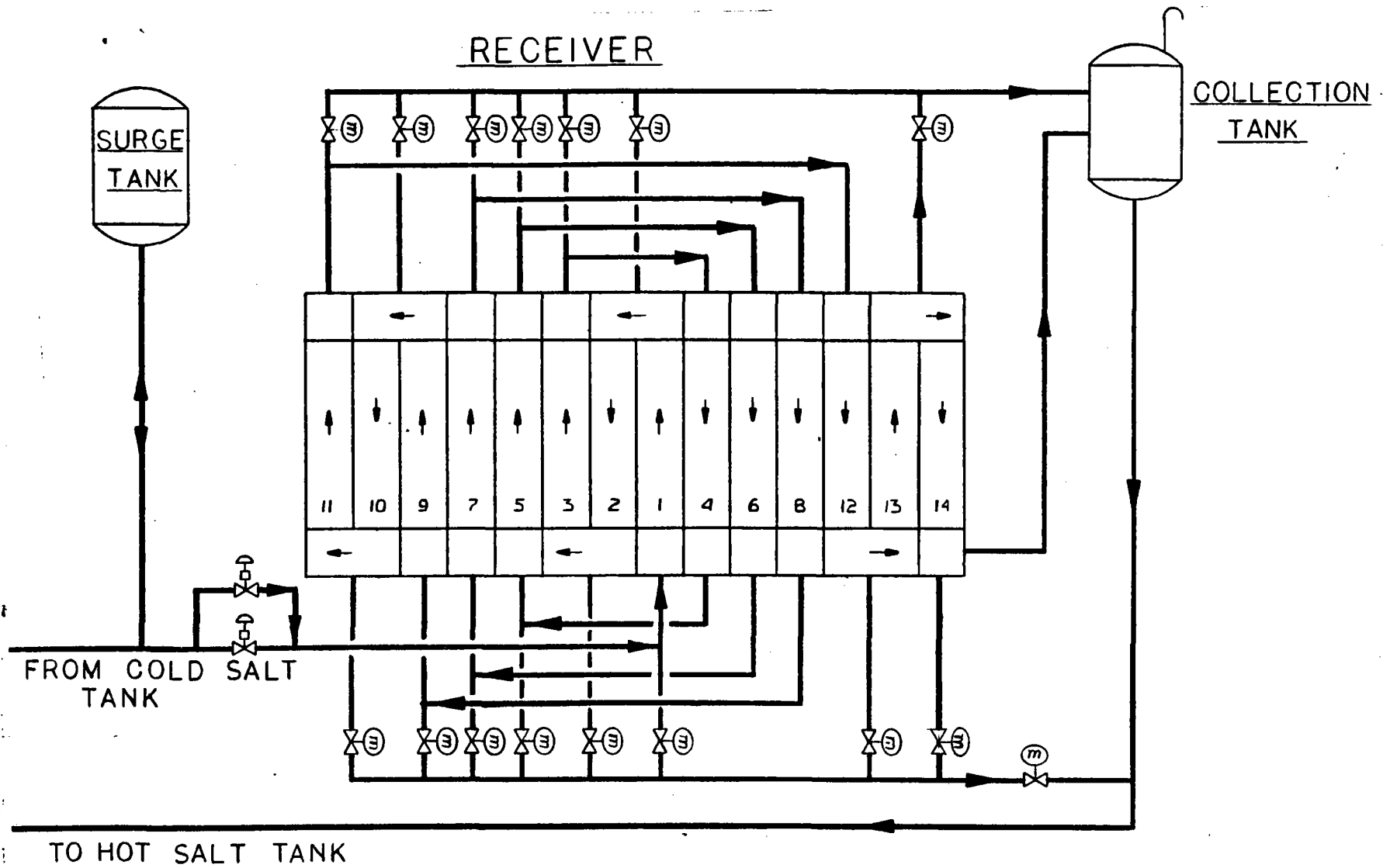


Figure 4-16 Receiver Schematic

tubes. The greater the number of passes, the fewer the number of tubes per pass, therefore, higher fluid velocities are achieved. The pilot plant receiver consists of 14 passes. The cold salt first enters through the center pass of the receiver, then works out to the passes on the edge of the panel (see Figure 4-16). This arrangement keeps the coldest salt in the high flux areas of the receiver. There are 15 tubes per pass in the high flux areas of the active walls (passes 1 and 2), 18 tubes per pass in the medium flux regions (passes 3 through 6), and 23 tubes in the low flux regions (passes 7 through 14). The pressure drop through the receiver with this arrangement is 634 kPa (92 psi) at the design point flowrate of 16,556 kg/hr (36,500 lb/hr).

The selection of the size and number of passes was based on an iterative thermo-hydraulic analysis which breaks each pass into 10 nodes for subsequent calculation of flow velocities, Reynolds, Prandtl, and Nusselt numbers, heat transfer coefficients, fluid temperatures, metal temperatures, and pressure drop for each heated node. Table 4-7 summarizes the salt and metal temperatures for the peak flux node of each pass. The maximum metal temperature of 627°C (1,161°F) in pass no. 8 compares favorably with the 650°C (1,202°F) peak temperature determined for the ACR molten salt receiver experiment.

Table 4-7. Peak Temperature Summary (1,100 w/m<sup>2</sup> Insolation)

Pass No.	No. of Tubes	Salt Temperature (°C)	Heat Transfer Coefficient (kw/m <sup>2</sup> -°C)	I.D. Metal Temperature (°C)	O.D. Metal Temperature (°C)
1	15	301	5.85	490	564
2	15	327	6.19	506	579
3	18	354	5.76	535	605
4	18	383	6.19	551	621
5	18	409	6.47	544	603
6	18	433	6.81	562	620
7	23	457	5.79	566	608
8	23	478	5.91	585	627
9	23	494	6.02	562	588
10	23	504	6.13	547	565
11	23	510	6.19	533	543
12	23	526	6.25	591	618
13	23	530	6.25	573	590
14	23	536	6.25	558	568

#### 4.5.5 Receiver Emergency Protection

Both the heliostat field and the control system will be connected to an Uninterruptable Power Source (UPS) to enable the heliostats to defocus (move beam away from receiver) in the event of a power failure or pump malfunction. As indicated previously, the principle function of the cold surge tank is to maintain temporary salt flow through the receiver following a power (or pump) failure. Accordingly, its size is directly proportional to the time required to remove the heliostats from their targets (25 seconds).

The cold surge tank configuration selected eliminates the requirement for level control and is based on the "blow-down" process often used in rocket propellant feed systems. This operational mode requires that the surge tank is trace-heated to salt inlet temperature  $288^{\circ}\text{C}$  ( $550^{\circ}\text{F}$ ), and it may be assumed to be initially filled with either air or residual gases from a previous run. After the pump is started and the operating pressure at the receiver inlet is established, molten salt flows into the tank compressing the ullage gasses from atmospheric to receiver inlet pressure. After thermal equilibrium is reached, the ullage-to-tank volume ratio will correspond to that of an isothermal compression of the gases in the empty tank. Following a power failure, the salt in the tank is pushed through the receiver by the expanding ullage gases. This blow-down process is associated with a decaying salt flow rate and ullage pressure, as shown in Figure 4-17. For design purposes, the polytropic expansion of the ullage gasses is bracketed by adiabatic and isothermal processes. The adiabatic assumption represents worst-case conditions for tank sizing. The blow-down curve shown in this figure, as well as a series of similar curves for different initial conditions were calculated by the use of a small computer program (FAIL) by step-wise integration of the set of equations representing polytropic expansion of the ullage gases, and the pressure drop vs. flow characteristics of the receiver and control valve. The program allows for a time-dependent opening or closing of the control valve as input. (The time required for valve travel from fully open to fully closed was approximately 20 seconds in the case of the ACR receiver).

The solar flux level on the receiver is constant for 5 seconds following a pump failure. At that time the control signal reaches the heliostats and they begin defocusing. The heliostats rotate at a rate of  $0.2^{\circ}/\text{sec}$  until the beam is completely off the receiver. This results in the flux distribution shown in Figure 4-17.

The required capacity of the cold surge tank was determined to be  $.121\text{m}^3$  ( $4.28\text{ft}^3$ ). The ullage volume is  $.045\text{m}^3$  ( $1.62\text{ft}^3$ ) and the salt volume is  $.075\text{m}^3$  ( $2.65\text{ft}^3$ ). These volumes include a 30% increase over the volume required to produce the flow profile shown on the figure. The 30% increase is a safety factor intended to offset any errors in analytical predictions. The hot surge tank is sized to accept 30 seconds of full flow from the receiver in case a downstream valve fails closed. This would allow time for the heliostats to defocus. Under normal operation, the level in the hot surge tank is controlled by the flow control valve located at the inlet of the hot storage tank.

#### 4.5.6 Operating Modes

At the design point, the receiver will deliver molten salt at a controlled temperature of  $538^{\circ}\text{C}$  ( $1,000^{\circ}\text{F}$ ), at a flow rate consistent with available insolation. The diurnal operational sequence associated with this function consists of: (1) normal operation, (2) normal shutdown and (3) startup. These sequences will be performed routinely during day to day operation. Other operating modes include: (4) emergency shutdown and (5) cloud passage.

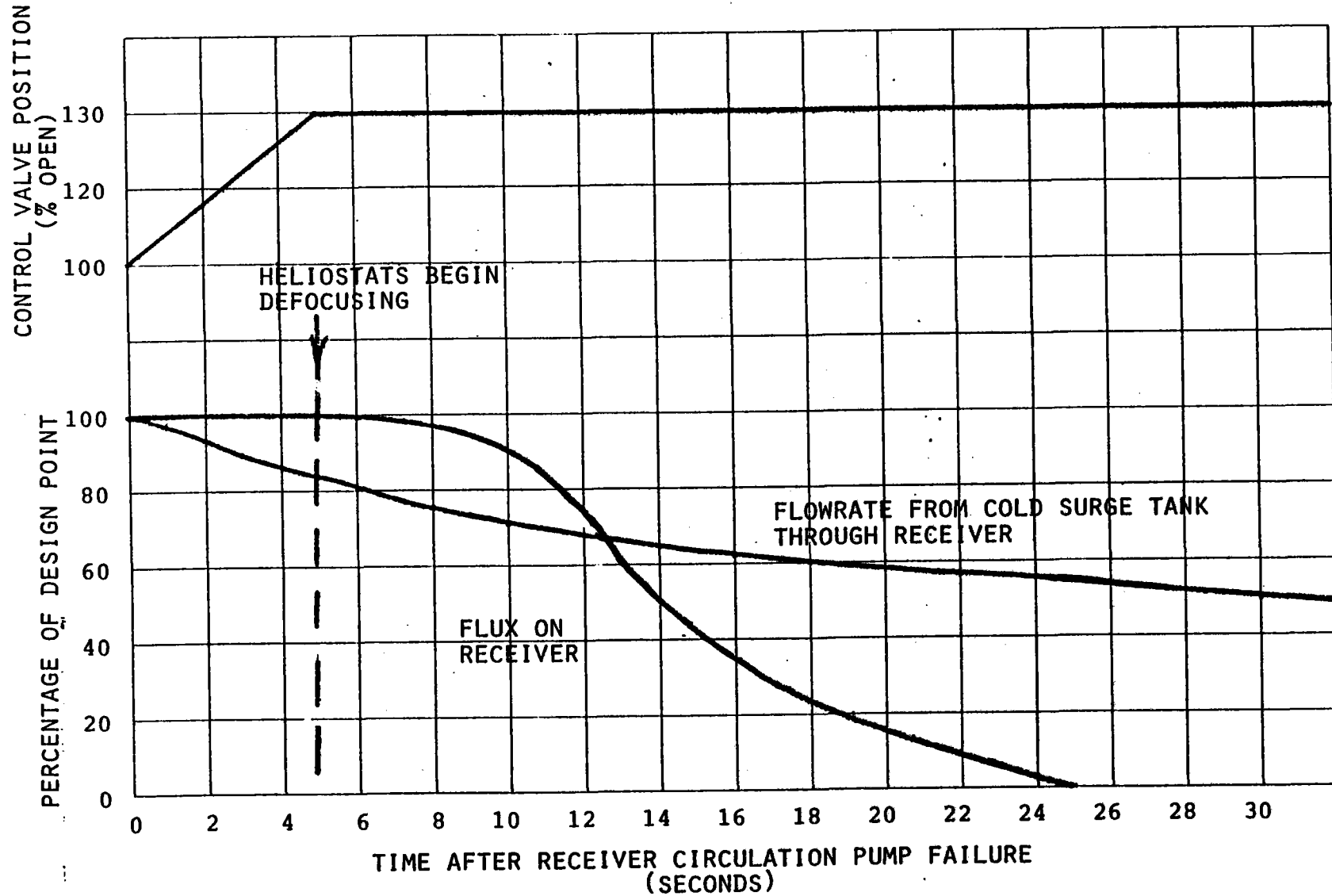


Figure 4-17 Receiver Salt Flowrate Following a Pump Failure

- 1) Normal Operation - The receiver control system will regulate the salt flow rate to maintain the receiver exit temperature constant at the set point. The heliostats operate in the tracking mode.
- 2) Normal Shutdown - The heliostats are removed from the target, put into the stow position, and the cavity door is closed. The drain and purge valves are opened and the receiver is drained.
- 3) Diurnal Startup from Cold Conditions - The receiver is warmed up to above melting temperature by the use of "warmup heliostats" with the cavity door open. The warmup heliostats are selected so as to provide a relatively uniform low level flux distribution over the receiver tubes, and to avoid exceeding maximum allowable metal temperatures. The parallel flow control valves are closed, the drain and vent valves are open and the pump is started. The level and pressure in the surge tank is established. The drain and vent valves are closed, the flow control valves are opened, flow through the receiver is established. The heliostat field is "ramped up" from "warmup" to full power with the flow control valves fully open. The flow control valves are throttled back to establish the desired receiver outlet temperature, and the system is set on automatic control.
- 4) Emergency Shutdown - The critical failure mode of the system is loss of salt flow to the receiver. This can be caused by pump failure, valve failure, or total loss of power. As discussed previously, the recovery from this emergency relies on the use of the UPS to defocus the heliostats, and on the cold surge tank to provide temporary salt flow throughout the defocus process. Following removal of the heliostats, the receiver is drained.
- 5) Cloud Passage - A minimum flow rate of 30% of design point will be maintained (by the control system) to prevent overheating of the receiver tubes during sudden recovery of insolation after cloud passage. This procedure assumes that the heliostats will remain on the receiver throughout this operating mode.

#### 4.5.7 Receiver Control

The function of the receiver control is to maintain the receiver exit salt temperature at the desired level. The system is operated in an insolation-following mode by matching the salt flow rate to the amount of absorbed solar energy. The collector field will be controlled to maximize the amount of energy reflected into the receiver cavity and the receiver will be controlled to absorb the incident energy safely and to maintain the outlet salt temperature at the setpoint.

The receiver can be either manually or automatically controlled. The receiver will be operated manually during startups and shutdowns. Automatic control of the receiver will be activated after the receiver has reached a normal operating mode and will be capable of maintaining the outlet salt temperature at the setpoint under most operating

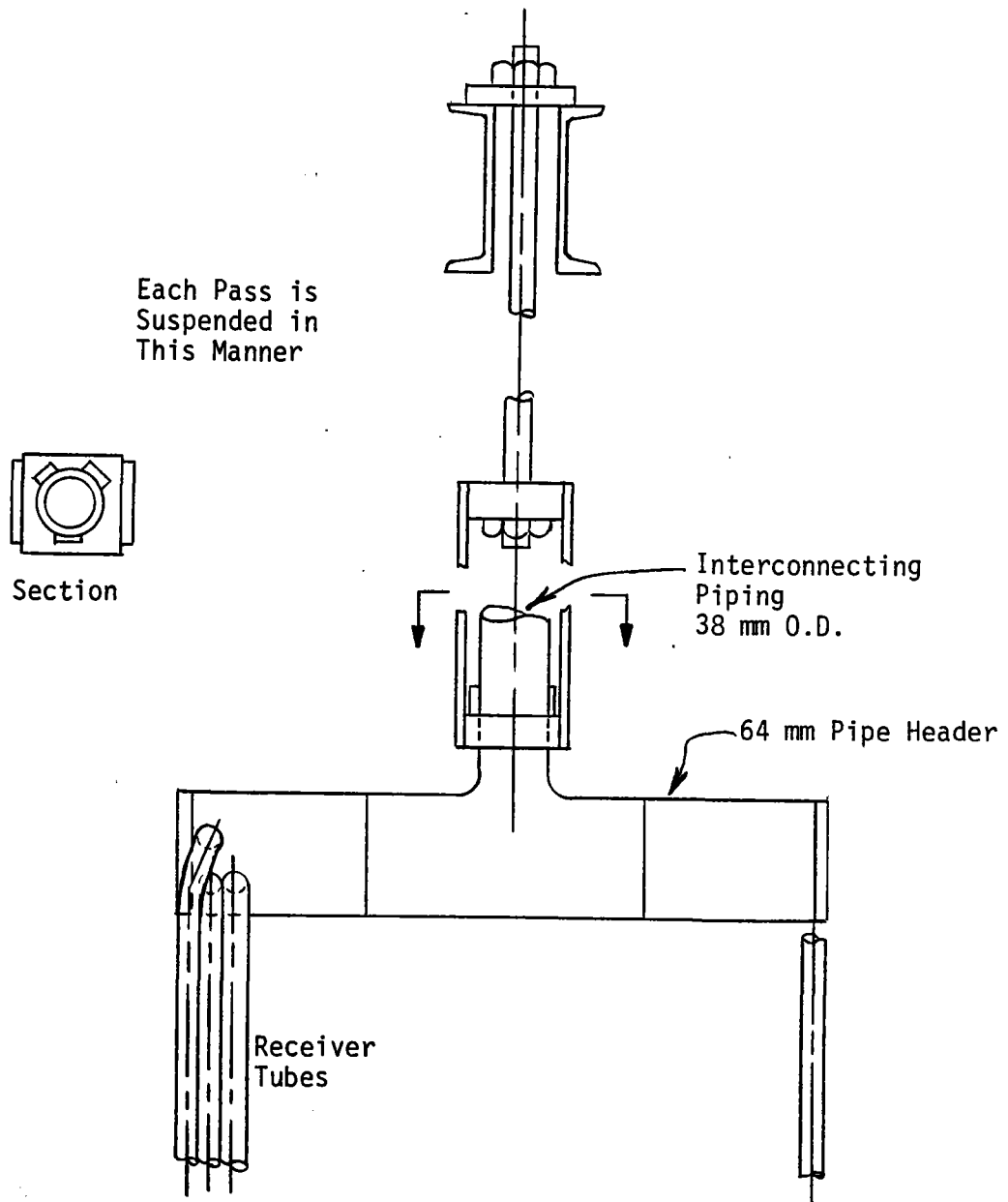
conditions. Severe transients may require manual operator control to minimize the production of low temperature salt. The control system is designed such that the safety of the receiver is of the highest priority, and will signal an alarm and execute predetermined emergency procedures in the event of receiver overtemperature or other system failure. The automatic operation of the receiver is coordinated through the Heliostat Array Controller (HAC). Any receiver emergency will immediately result in a defocus of the heliostat beam from the receiver cavity.

The domain of the receiver control system starts with the supply of cold salt to the receiver at constant pressure and ends with the return of hot salt to the downcomer. A cold surge tank is provided in the receiver as previously discussed, which decouples the supply of cold salt from the use of salt in the receiver. Two flow control valves are provided in parallel. Both are capable of independent control should one valve fail. The hot salt exits the receiver into a small collection tank which then drains via the downcomer at atmospheric pressure. As the cold surge tank is charged to 876 kPa (127 psia) and the hot salt surge tank is allowed to stabilize at atmospheric pressure, a relatively constant pressure difference has been established for control of salt flow through the receiver.

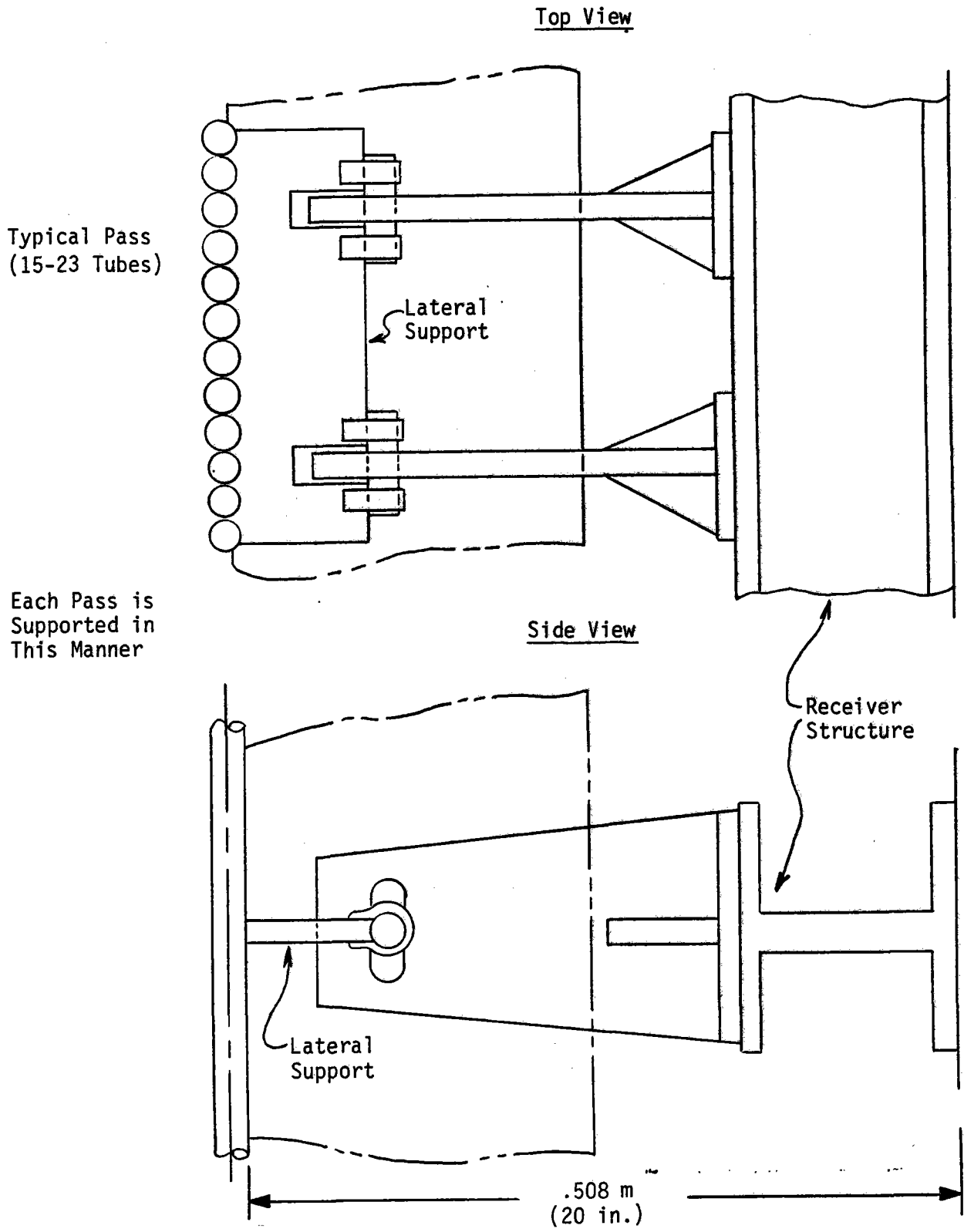
Investigations into the dynamic aspects of receiver control have resulted in the development of specialized digital control algorithms. The algorithm is based on a hybrid combination of feed back and feed forward control. The control algorithm requires intermediate header temperatures and the exit salt temperature as inputs to adjust the salt mass flow rate in order to maintain the outlet salt temperature at the desired value. From the levels and the rate of change of these temperatures, and the existing flow rate, the algorithm calculates the flow rate required to maintain the exit temperature at the setpoint. This value is, then, input to the receiver control system. The receiver control system will also be discussed in section 4.11 Master Control System.

#### 4.5.8 Receiver Fabrication

Provision must be made for thermal expansion of the receiver panel tubes when the receiver is in operation. This is accomplished by suspending the panel from above in a manner that allows for both downward and lateral growth. Each pass of the panel is suspended from its associated inter-connecting piping as shown in Figure 4-18. The header is free to move horizontally but is restrained in the vertical direction. Each pass of the receiver is braced with two lateral supports, one near the top and one near the bottom. (see Figure 4-19). The lateral supports for each pass are individually constructed and are hinged so that each pass is free to move independently. The bottom edge of the receiver is not restrained so that the receiver panel can bow outward without restriction (bowing minimized the thermal stress in the tubes). Figures 4-20 a and b are a comparison of two techniques of panel support. The conventional method shown in figure a holds the headers in place in the



*Figure 4-18 Receiver Suspension Method*



Typical Pass  
(15-23 Tubes)

Each Pass is  
Supported in  
This Manner

Top View

Side View

Receiver  
Structure

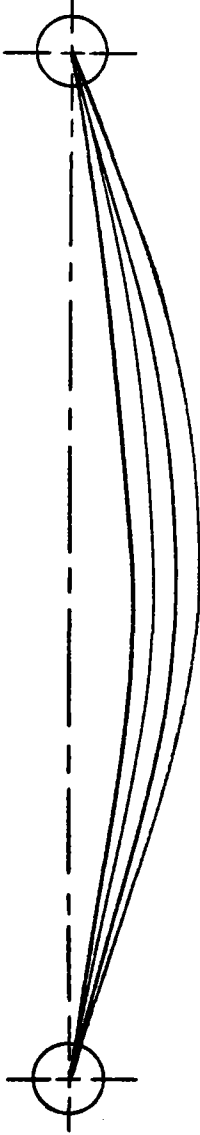
Lateral  
Support

.508 m  
(20 in.)

Figure 4-19 Receiver Panel Lateral Support

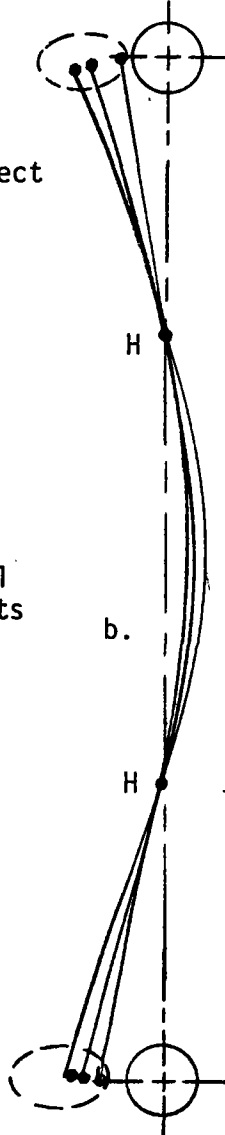


Free Thermal Bowing  
From Headers



Thermal Bowing  
From Ties

Headers  
Allowed  
to Deflect



Method  
Used

Lateral  
Supports

Figure 4-20 Receiver Tube Thermal Expansion

horizontal direction and allows all the bowing due to thermal expansion to occur at the center of the passes. Figure b shows the method used where the headers are free to move and the passes are held in place by the lateral supports. This method reduces "shine through" (solar flux not intercepted) between passes in the high flux areas at the center of the panel. Using this method the maximum midspan displacement of tubes between passes was calculated to be 13mm (.5 in), as shown in Figure 4-21.

A preliminary estimate of tube thermal stresses is shown on Figure 4-22. A detailed stress analysis of the receiver will be conducted during phase II of the program. The full restraint stress shown refers to a stress calculated by a finite element computer program for a tube not allowed to bow. The bowed stress (30% reduction) refers to an estimate of the reduced circular membrane stress when the tube is allowed to bow. The 30% reduction in stress is a conservative estimate based on studies done under the 2nd Molten Salt Receiver contract conducted by Martin Marietta Corporation. The circular gradient stress is used to predict creep while the total stress shown is used to predict low cycle fatigue damage over the life of the receiver. The receiver design is within acceptable limits in both of these areas.

The Incoloy 800 heat absorbing tubes will be coated with high temperature black paint (Pyromark 2400 or equivalent) having the following properties: absorptivity = .96, emissivity = .90. Hot salt piping will be Type 316 stainless steel. Cold salt piping will be ASTM A106 Grade B carbon steel.

#### 4.5.9 Receiver Structural Design

The structural framework of the receiver module is designed to provide unobstructed entry for solar flux, and protection from the environment for the absorber tube panels. The structure is symmetrical about the north-south axis, incorporating one aperture 3.05m x 3.05m (10 ft x 10 ft).

The main structural framing offers no lateral or vertical restraint inhibiting thermal expansion and contraction of the tube panels. The steel roof sections were designed to accommodate hoists at the door. The door is insulated to minimize heat leak during standby conditions. Provisions have been made for rigging and supporting temporary hoists that can be used for component removal and replacement. The receiver structure is shown in Figure 4-23.

All structural elements of the receiver are made from standard ASTM A36 steel sections selected in accordance with AISC specifications. The roof and siding is made of corrugated 14 gauge steel. The exterior wall siding is carried by angle joist (and vertical columns). Open-web joists are used to carry the floor deck.

The heat absorption panels and supports are designed to sustain dead weight, wind loading, and applicable seismic loading conditions. Lateral supports are applied as necessary to restrict lateral deflection of the panels. The design of the interconnecting piping allows for differential expansion loads (mechanical and thermal).

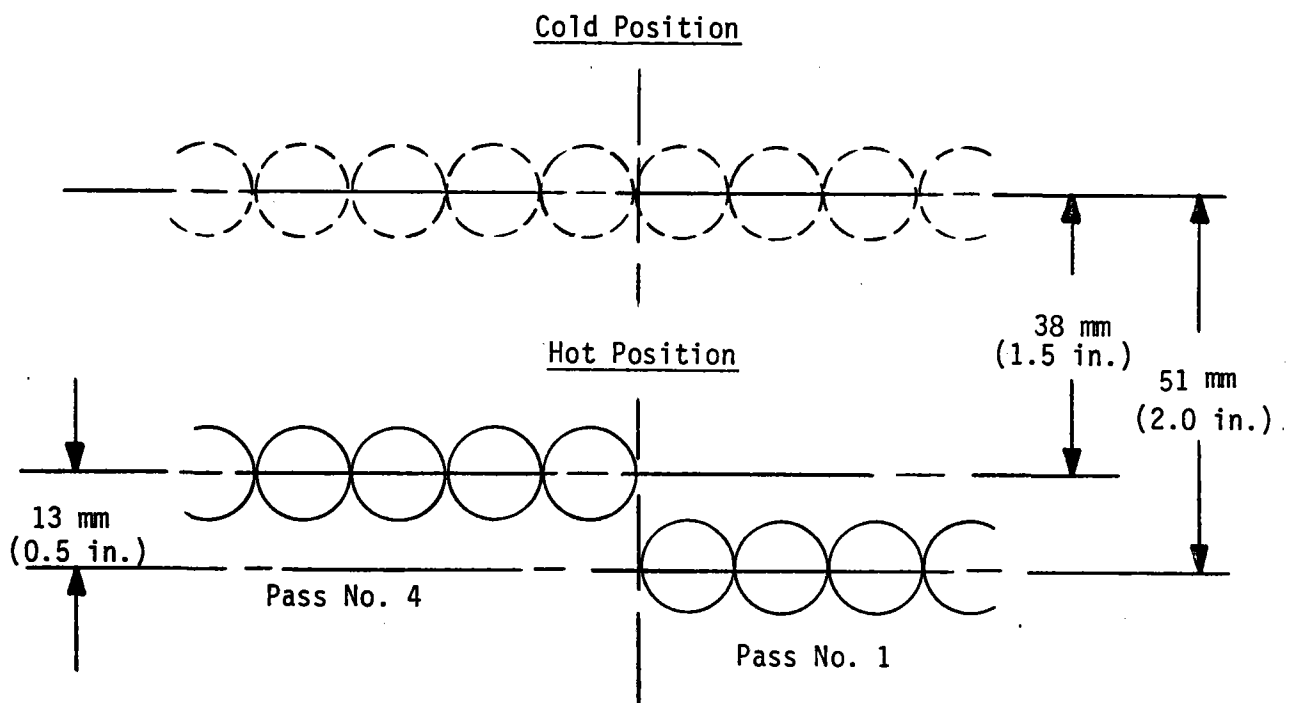
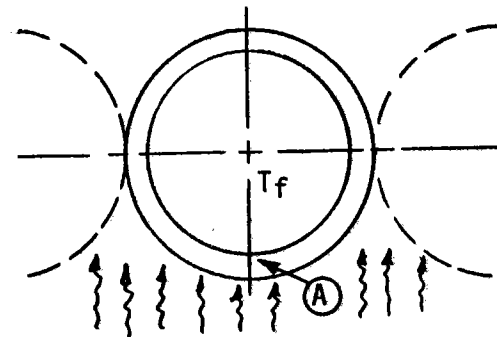


Figure 4-21 Midspan Displacement of Tubes Between Passes



Tube - 13 mm (0.5") O.D. x  
1.7 mm (0.067") Wall

Design Point Max Flux - 76.2 W/cm<sup>2</sup>

Location	Radial ΔT, °C (°F)	Radial Grad. Stress, MPa (ksi)	T <sub>f</sub> °C (°F)	T <sub>m</sub> °C (°F)	Full Restraint Stress		Bowed Stress (30% Reduction)	
					σ <sub>Total</sub> MPa (ksi)	σ <sub>Circ.Grad.</sub> MPa (ksi)	σ <sub>Total</sub> MPa (ksi)	σ <sub>Circ.Grad.</sub> MPa (ksi)
A Outside	68 (122)	-115.8 (-16.8)	314 (597)	551 (1023)	-419.9 (-60.9)	-304.1 (-44.1)	-328.9 (-47.7)	-213.0 (-30.9)
A Inside	68 (122)	115.8 (16.8)		483 (901)	-188.2 (-27.3)	-304.1 (-44.1)	97.2 (14.1)	-213.0 (-30.9)

Summary

Circular Gradient Stress

-213.0 MPa (-30.9 ksi) < 2x Yield Strength  
of 219.9 MPa (31.9 ksi)

Elevated Temperature Evaluation

Creep Ratcheting < 0.1% Vs. 1.5% Allowable

Creep-Fatigue Damage  $\frac{n}{N} + \frac{t}{T} = .672$  Vs. Allowable of 1.0

(Based on 7300 cycles and 60,000 hours)

Figure 4-22 Tube Thermal Stress



An aperture door is provided to protect the absorption panels when not in use. The door is raised and lowered from above and has the ability to close within 10 seconds. The door is designed to withstand maximum seismic and wind loads, and to protect heat absorption panels from high wind loads.

#### 4.5.10 Receiver Tower

The receiver tower supports the solar receiver which weighs a maximum of 15,422kg (34,000 pounds) and measures approximately 3.7m x 2.1m (12' by 7') plan and has an overall height of 6.9 m (22'-6") (see Figure 4-24). The solar receiver is supported 30.2m (99'-0") above grade on the receiver tower.

The receiver tower is constructed of structural tube sections for the columns, beams, and bracing. The tubes are fabricated and shipped to the site for field erection. The tubes are field bolted as required for field erection. The connection of the members is by gusset plate and field welding.

Access to the solar receiver is by a stair from grade to the platform at the base of the solar receiver. A vertical lift access area is also provided.

The tower is supported on spread footing foundations located at grade. These footings are approximately 3.1m (10') square and are located at the center of each of the four tower support columns.

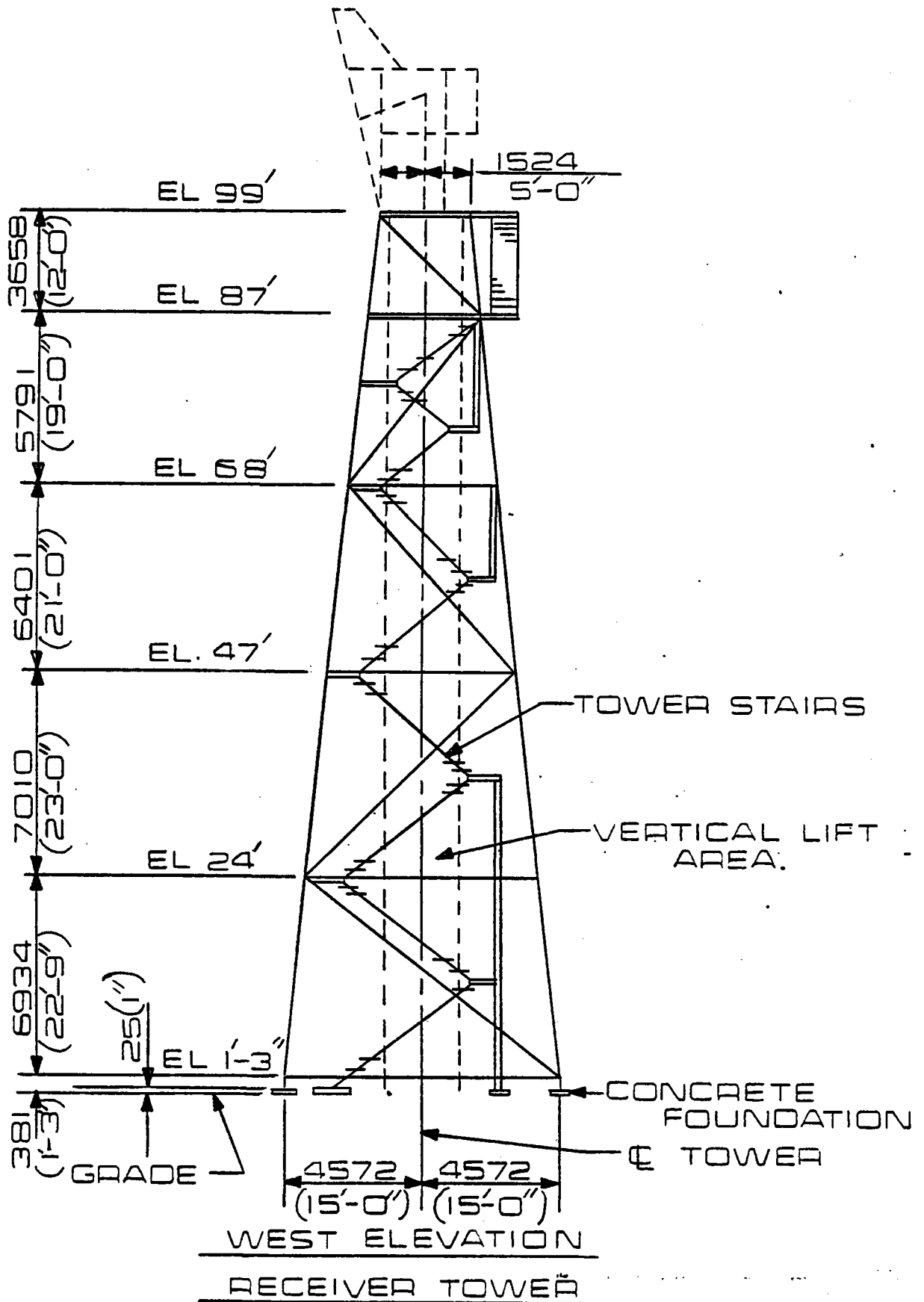


Figure 4-24 Tower Structural Design

#### 4.6 STEAM GENERATING EQUIPMENT

The steam generating equipment (SGE) is the interface between the molten salt and the turbine feedwater. The SGE transfers the thermal energy stored in the molten salt to the feedwater, thus providing steam for the cycle in a safe and reliable method.

The SGE is required to provide the steam turbine with 427°C (800°F)/5.516 MPa (800 psia) superheated steam with a flow rate of 579 Kg/hr (1276 lbm/hr), and the MED with saturated steam for the steam ejector. The turbine exhaust is used to evaporate the distillate in the MED.

During startup operations, the heat exchangers must be warmed up before going to nominal operation. Therefore, the SGE is required to provide some form of heat to the heat exchangers.

In addition to nominal steam requirements, the SGE must be capable of providing steam at flow rates from 10 to 110% of the nominal flow rate.

The SGE has a required life of 20 years and is designed to ASME Section I, Section II, Section V, and Section VIII Boiler and Pressure Vessel Code, and must be designed to allow for thermal stress and expansion. The SGE must be on a rigid, skid mounted subbase and designed for overseas shipment.

The heat transfer fluid shall be molten salt consisting of 60% NaNO<sub>3</sub> and 40% KNO<sub>3</sub> by weight, with thermophysical properties as shown in Table 4-8. Provisions must be made for the detection and elimination of salt freezing. Furthermore, the heat exchangers must be completely drainable on both the salt and water/steam sides. Solidification first occurs when the salt is lowered to 245°C (473°F). The solidification continues until the temperature is lowered to 221°C (429°F), where the mixture is solid (Figure 4-25).

The materials for the manufacture of the SGE components are required to meet the strength requirements of ASME Section VIII Division 1 as well as offering the corrosion resistance necessary in the operating environment.

Departure from nucleate boiling (DNB) must be prevented to avoid failure of tubes from thermal cycling and to prevent rapid deposit buildup and overheating in an extremely short time. Figure 4-26 shows available boiling data for a horizontal surface at atmospheric pressure. The graph shows the heat flux vs. the temperature of the heating surface in excess of the saturation temperature. It is seen that if the fluid being heated "jumps" from the nucleate regime to the film regime (along the horizontal dashed lines) the temperature of the heating surface increases dramatically while the heat flux remains constant. Such a transition must be prevented.



Table 4-5 Properties of 60/40 Salt Vs. Temperature

Temperature		Density		Viscosity		Specific Heat		Thermal Conductivity	
°C	(°F)	KG M <sup>3</sup>	lb ft <sup>3</sup>	Ns M <sup>2</sup>	x10 <sup>-3</sup> lb ft hr	J KG°K	x10 <sup>-3</sup> Btu lb°F	W M°K	Btu ft hr°F
232	450	1948	121.6	28.06	11.60	1.531	0.366	0.519	0.30
260	500	1929	120.4	23.42	9.68	1.531	0.366	0.519	0.30
288	550	1911	119.3	19.57	8.09	1.531	0.366	0.519	0.30
316	600	1892	118.1	16.47	6.81	1.531	0.366	0.519	0.30
343	650	1873	116.9	14.01	5.79	1.531	0.366	0.519	0.30
371	700	1855	115.8	12.07	4.99	1.531	0.366	0.519	0.30
399	750	1836	114.6	10.62	4.39	1.531	0.366	0.519	0.30
427	800	1818	113.5	9.53	3.94	1.531	0.366	0.519	0.30
454	850	1799	112.3	8.73	3.61	1.531	0.366	0.519	0.30
482	900	1780	111.1	8.15	3.37	1.531	0.366	0.519	0.30
510	950	1762	110.0	7.67	3.17	1.531	0.366	0.519	0.30
538	1000	1743	108.8	7.23	2.99	1.531	0.366	0.519	0.30
566	1050	1725	107.7	6.72	2.78	1.531	0.366	0.519	0.30
593	1100	1706	106.5	6.07	2.51	1.531	0.366	0.519	0.30

Melt Temperature = 221°C (429°F) (onset) - 245°C (473°F) (complete)

Heat of Fusion =  $1.09 \times 10^5$  J/KG (46.8 Btu/lb)

4.6.1 Configuration - The basic SGE cycle is presented on a temperature-entropy (Ts) diagram in Figure 4-27a. The area under the curve of the Ts diagram represents liquid and vapor. Saturated liquid is on the left side, saturated steam is on the right. Two constant pressure lines are shown as P<sub>1</sub> and P<sub>2</sub>.

Starting with saturated liquid, the feedwater pumps increase the pressure from P<sub>1</sub> to P<sub>2</sub>, resulting in a subcooled liquid at state 2. The preheater heats the feedwater from state 2 to state 2' where it is saturated liquid. The evaporator provided saturated steam by heating the feedwater at constant temperature to state 3'. Superheated steam is produced by the superheater and results in state 3.

The superheated steam now leaves the SGE and is expanded to pressure P<sub>1</sub> through the turbine. This results in the lower temperature, pressure state 4. Note that the steam is slightly superheated and contains a large amount of thermal energy for use by the distillation process (MED).

This basic SGE cycle can be accomplished in three configurations: Once-through, Sulzer and Recirculating. These are presented schematically in Figures 4-27b through 4-27d.

- I. Initial Melting - As-received salt is made up of solid particles of  $\text{NaNO}_3$  and separate solid particles of  $\text{KNO}_3$ . Theoretically the initial melting of the salt would begin at point A (the melting temperature of pure  $\text{NaNO}_3$ ) and continue isothermally until all the  $\text{NaNO}_3$  is melted. Then the temperature would rise to point B (the melting temperature of pure  $\text{KNO}_3$ ) and the process would continue isothermally until all the  $\text{KNO}_3$  was melted. Observations of the initial melting process have shown that the salt melts at much lower temperatures than those consistent with the theoretical process described above. This is the case since the solid particles of  $\text{NaNO}_3$  and  $\text{KNO}_3$  are in intimate contact, especially the fine dust like particles, and the melting of this pseudo mixture is similar to the melting of an actual mixture of the salt compounds. Also once melting begins the solid phases readily dissolve into the liquid. These actual processes cause the initial melting to take place at roughly  $450^\circ\text{F}$  with complete melting accomplished at about  $473^\circ\text{F}$ .
- II. Solidification - Solidification first occurs when the temperature of the mixture is lowered to C at the 60/40 by weight composition point. Solidification takes place while the temperature is lowered from C to D where the mixture is completely solid.
- III. Subsequent Operational Melting - Melting first occurs at D and continues until the temperature is raised to C where the mixture is completely liquid.

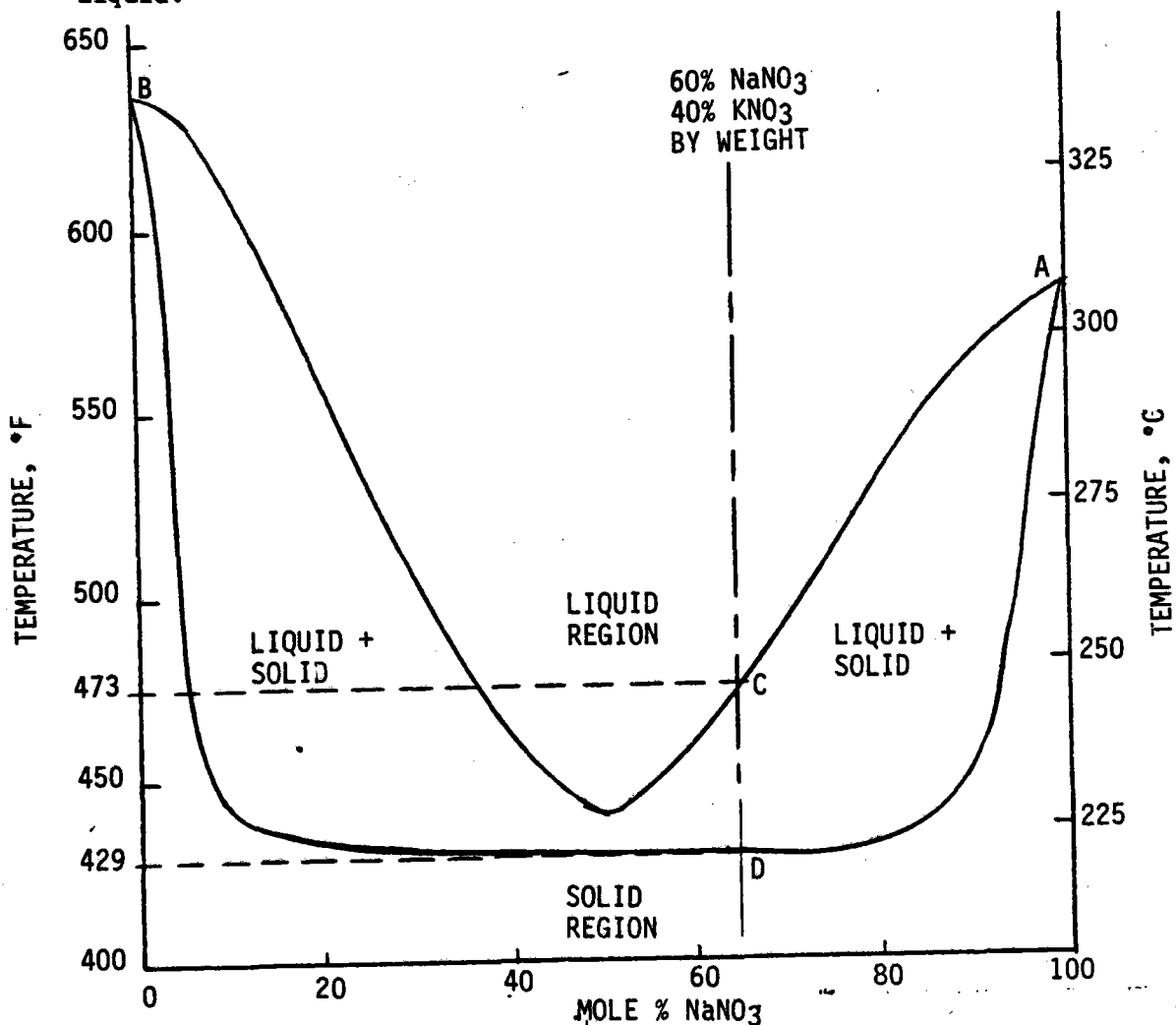


Figure 4-25 Temperature - Composition Phase Diagram for  $\text{NaNO}_3$ - $\text{KNO}_3$

The Once-Through cycle produces dry saturated steam in the preheater/evaporator, and superheated steam in the superheater. Such a configuration can lead to DNB and requires high purity feedwater.

The Sulzer Cycle produces low quality steam in the preheater/evaporator which is fed to the steam drum for dry steam separation before entering the superheater. Depending on water mass flow, mass heat flux and heat exchanger tube geometry, DNB may or may not be present in the evaporator. The low quality steam in the evaporator is known to preclude DNB. However, the condensate in the drum must be drained and purified before reentry into the cycle. This is a large percentage of the flow and requires a large purifying system. Otherwise the liquid is dumped and the heat is lost.

The Recirculating cycle also produces low quality steam in the preheater/evaporator which is separated in the steam drum. However, the feedwater is recirculated through the evaporator for further evaporation. DNB can be avoided with low quality steam in the evaporator, a high recirculation ratio (the rate of the mass flow through the evaporator to the mass flow of the feedwater and the proper tube geometry).

While all three cycles could be used, the Once-Through and Sulzer cycle present significant disadvantages. They both require sensitive control, extensive feedwater cleaning and require longer time for startup. In addition, the Sulzer cycle has a low efficiency due to difficulty in recovering let-down heat. Therefore, it is recommended that the recirculating cycle be used for this project. A comparison of the steam cycles is presented in Table 4-9.

Once the Recirculating cycle is chosen, the number of heat exchangers and sizes can be determined. The choice of turbine sizes for a plant this small is limited and only a single stage turbine can be procured. This eliminates the need for a reheater.

To design the SGE a cycle energy balance is performed to determine flow ratios and temperatures. The selected configuration is shown in Figure 4-28 and the results of the energy balance are shown in Table 4-10. The configuration consists of superheater, evaporator and preheater salt-to-water/steam heat exchangers. The feedwater heater heats the water from 158°C (316°F) to 238°C (460°F). This is necessary to keep the salt exit temperature above 260°C (500°F).

The heat transferred in the heat exchangers is shown in Figure 4-29, along with the inlet and exit temperatures. The salt, shown at the top, decreases from 510°C (950°F) to 260°C (460°F) while the feedwater is heated from 238°C (460°F) to 427°C (800°F). The feedwater remains constant at 285°C (545°F) since the evaporation is isothermal. The heat transferred in the preheater is 54.7 kWt, while the heat transferred in the evaporator is 348.9 kWt. Note the temperature approach between the preheater and evaporator is 9°C (17°F).

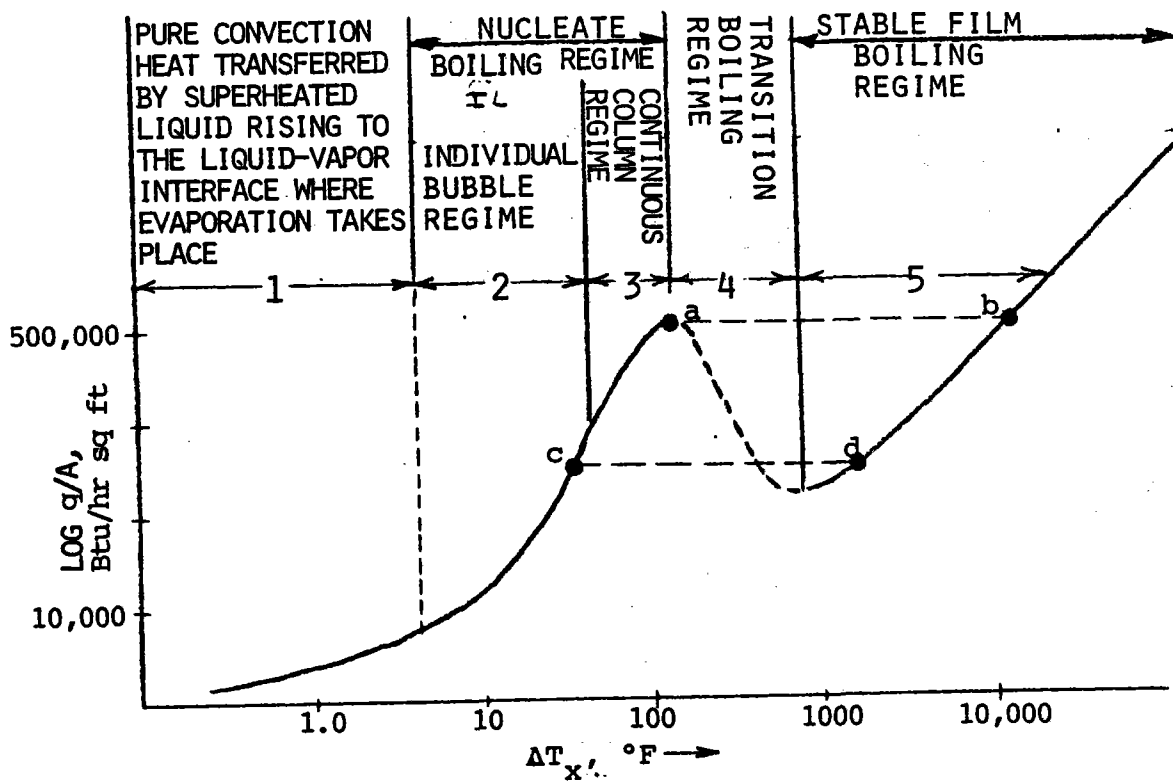


Figure 4-26 DNB, Horizontal Surface at Atmospheric Pressure

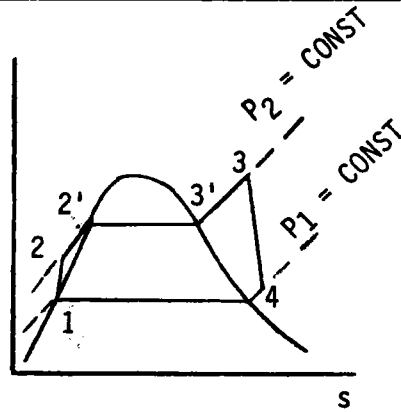


Figure 4-27a Basic Cycle      Figure 4a Basic Cycle

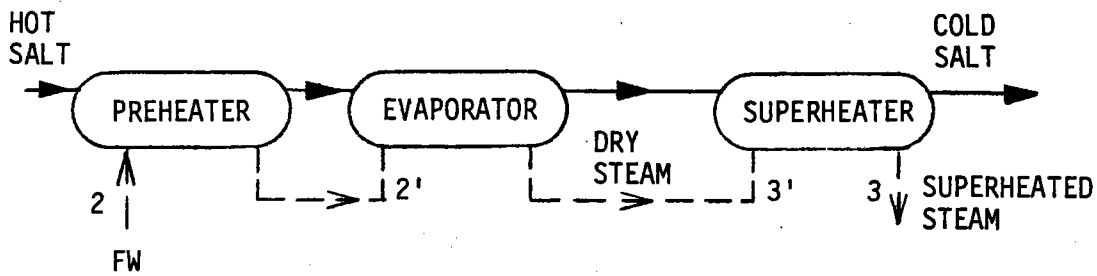


Figure 4-27b Once-Through Cycle

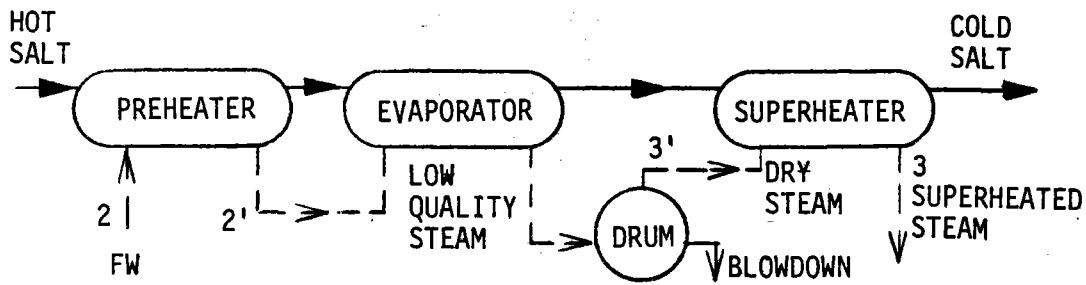


Figure 4-27c Sulzer Cycle

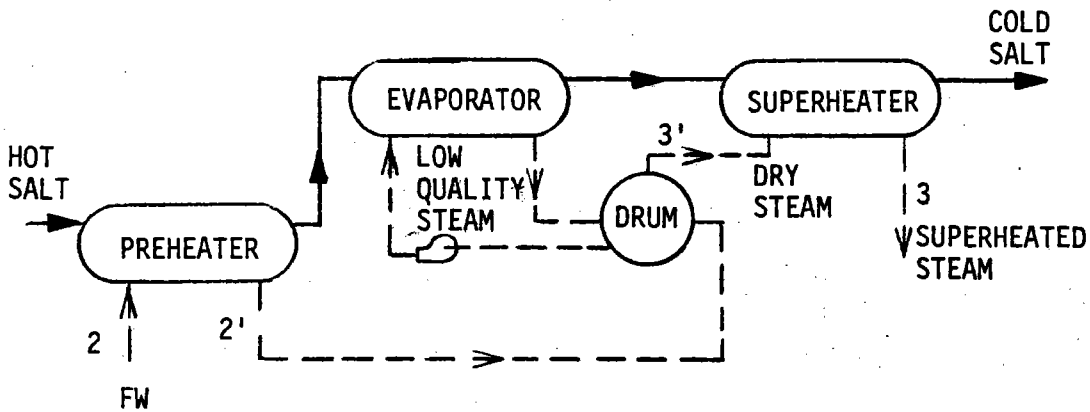


Figure 4-27d Recirculating Cycle

Table 4-9

## Comparison of Steam Cycles

	<u>ONCE-THROUGH</u>	<u>SULZER</u>	<u>RECIRCULATING</u>
Cycle Efficiency	High	Lower due to difficulty of recovering let-down heat	Lower than once-through if power required for pumps is high
Plant Cost	Low	Slightly higher than once-through due to letdown line costs and drum, and feedwater purifier size	Slightly higher than once-through due to pumps, piping, and drum
Control	May require more sensitive control than recirc. but within current technology.	Similar to once-through but additional problems due to controls on letdown lines	A more forgiving cycle due to steam drum water inventory
Feedwater Chemistry	Requires state-of-art once-through chemistry and stainless steel feed heaters	Similar to once-through	Can be relaxed from once-through requirements - more relaxation on balance of plant systems & materials
Evaporator Size	Smallest heat transfer surface	Slightly greater once-through	Evaporator Size greater due to higher quantity of water being recirculated
Operation	Takes longer time to start up due to clean up of feed-water	Same as once-through	Quick start up to facilitate diurnal starts

This preliminary configuration presented some major concerns: the control scheme must keep the salt above 260°C (500°F) by controlling the feedwater temperature before the preheater to 238°C (460°F); the low temperature approach and the low amount of heat transferred in the preheater.

Therefore the preheater is combined with the evaporator with only a small increase in size and cost. To avoid the control of the exiting salt and evaporator inlet temperatures, the salt is raised by 27.8°C (50°F); 538°C (1000°F) entering and 288°C (550°F) exiting the SGE.

The final configuration is shown schematically in Figure 4-30 along with the results of the energy balance. Note the addition of the deaerator and the auxiliary boiler. The deaerator also acts as a feedwater heater. The auxiliary boiler is necessary for start-up and can also be used to supply superheated steam to the turbine and saturated steam to the deaerator and MED for use during nonsolar periods. The addition of an attemperator provides the ability to control the temperature of the steam to the turbine.

To preclude DNB, the evaporator has a recirculation ratio of 14 and an exiting quality of 7%.

The SGE consists of the following major components:

1. Evaporator;
2. Superheater;
3. Steam Drum;
4. Feedwater Recirculation Pumps;
5. Main Feedwater Pumps;
6. Main Steam Attemperator;
7. Piping and Valves;
8. Trace Heating;
9. Insulation;
10. Instrumentation;
11. Deaerator;
12. Skid Assembly.

4.6.2 Design - The SGE components have 25% excess surface margin at the nominal flowrate. This allows operation up to 110% of rated load with a 15% allowance for uncertainties.

The specified salt flow of 1.261 kg/s (10,006 lbm/hr) enters the superheater at 538°C (1000°F) and leaves at 498°C (929°F) having heated dry steam from 278°C (532°F) to at least 431°C (807°F). The salt then passes through the evaporator and is cooled to 288°C (550°F) while generating 0.191 kg/s (1516 lbm/hr) of dry steam.

The SGE is supplied with 0.180 kg/s (1430 lbm/hr) of water at 125°C (257.5°F) which flows through the deaerator and is pressurized to 6.2 MPa (900 psia). The deaerator draws 0.01 kg/s (85.71 lbm/hr) of dry steam which heats the feedwater from 125°C (257.7°F) to 159°C (318°F). In the steam drum, the feed water is mixed with water from

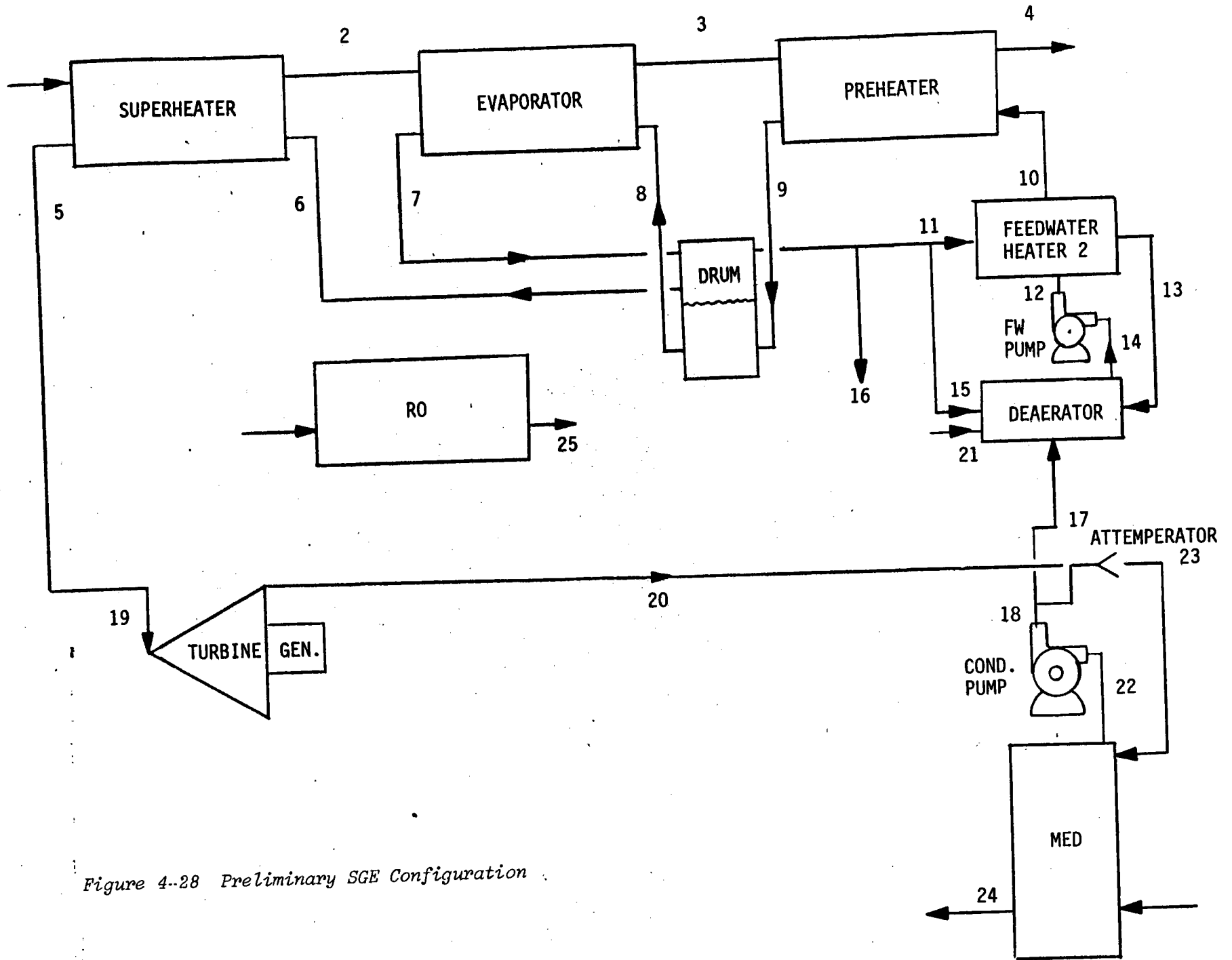


Figure 4-28 Preliminary SGE Configuration



Table 4-10 PRELIMINARY CONFIGURATION STATE POINTS

Flow Diagram Point	Fluid	Pressure		Temperature		Flow	
		MPA (psia)		(°C) (°F)		kg/HR (LBm/HR)	
1	SALT	-	-	510	(950)	4539	(10006)
2	SALT	-	-	469	(876)		
3	SALT	-	-	288	(551)		
4	SALT	-	-	260	(500)		
5	SH STEAM	6.03	(875)	429	(805)	570	(1257)
6	SAT STEAM	6.90	(1000)	285	(545)	570	(1257)
7	SAT STEAM/FW	6.90	(1000)	285	(545)	1808	(3985)
8	SAT/FW	6.96	(1010)	285	(545)	1808	(3985)
9	FW	6.90	(1000)	279	(534)	904	(1993)
10	FW	6.96	(1010)	238	(460)	904	(1993)
11	STEAM	3.38	(490)	241	(465)	156	(345)
12	FW	6.96	(1010)	158	(316)	904	(1993)
13	FW	3.38	(490)	163	(326)	156	(345)
14	FW	0.59	(85)	158	(316)	904	(1993)
15	STEAM	0.59	(85)	158	(316)	108	(237)
16	STEAM	1.03	(150)	285	(545)	70	(154)
17	CONDENSATE	0.69	(100)	78	(173)	570	(1257)
18	CONDENSATE	0.69	(100)	78	(173)	630	(1388)
19	SH STEAM	5.52	(800)	427	(800)	570	(1257)
20	SH STEAM	0.06	(8.5)	224	(435)	570	(1257)
21	MAKE-UP	-	-	27	(80)	70	(154)
22	CONDENSATE	0.04	(6.5)	78	(173)	630	(1388)
23	SH STEAM			88	(190)	630	(1388)
24	MED PRODUCT					182*	
25	RD PRODUCT					90*	
26	SH STEAM	0.04	(6.5)			630	(1388)

\*M<sup>3</sup>/day

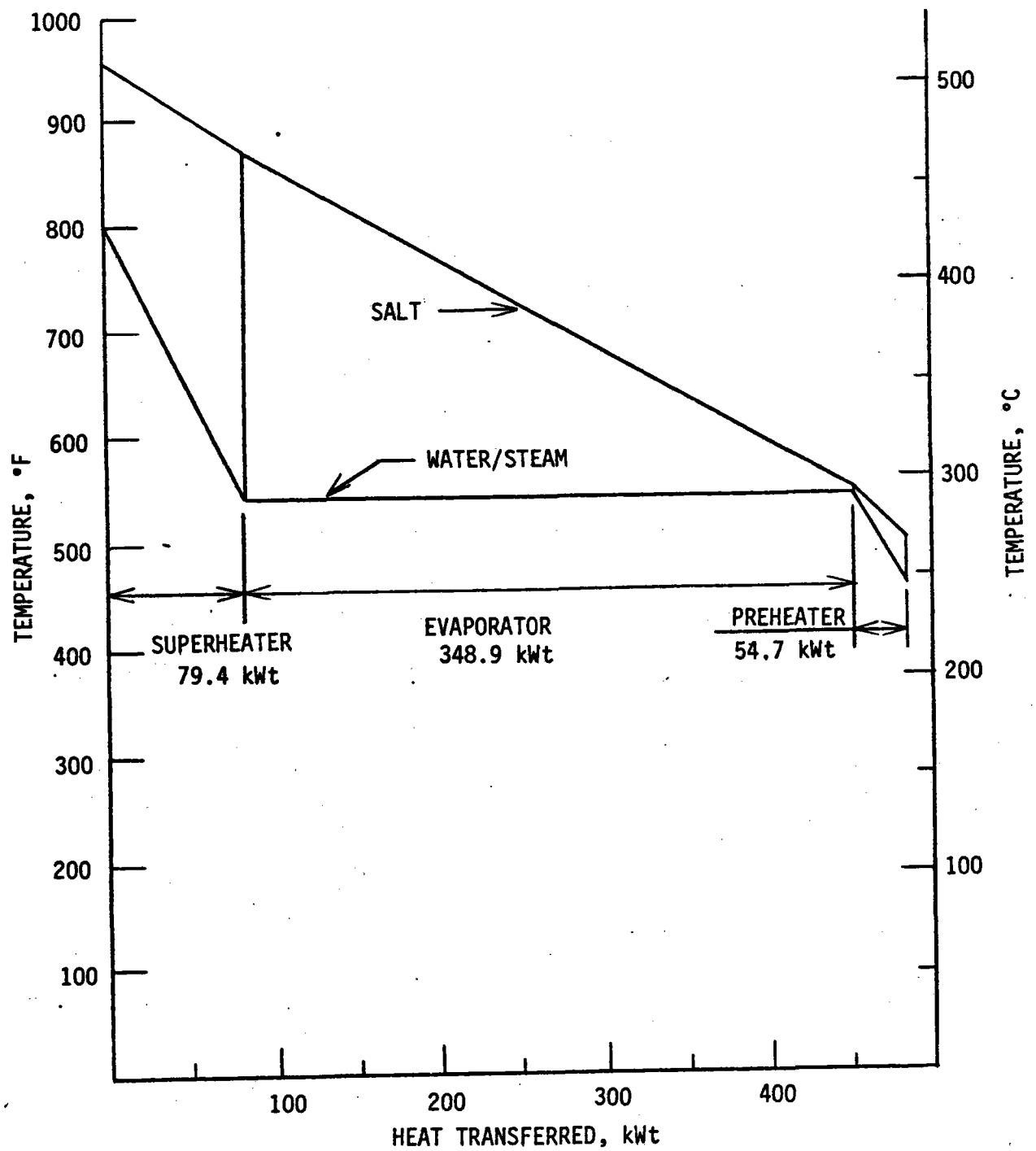


Figure 4-29 Preliminary Configuration Energy Balance



the evaporator yielding a drum water temperature at or above 270°C (518°F). Dry steam, being separated from evaporator water in the drum, leaves the drum and is heated in the superheater to 431°C (807°F) or above. Any excess temperature generated by the superheater is attemperated by bypass steam from the superheater inlet. As a result, dry steam at 427°C (800°F) and 6.1 MPa (890 psia) leaves the SGE skid.

The proposed superheater concept shown in Figure 4-31 is a U-tube counterflow heat exchanger employing state-of-the-art design and manufacturing methods. Four tubes are supported inside the shell by seven support plates. The design affords the following:

- optimal sizing as a result of being a pure-counterflow-unit;
- elimination of tube vibration;
- accommodation of differential expansion;
- simplicity of internal design.

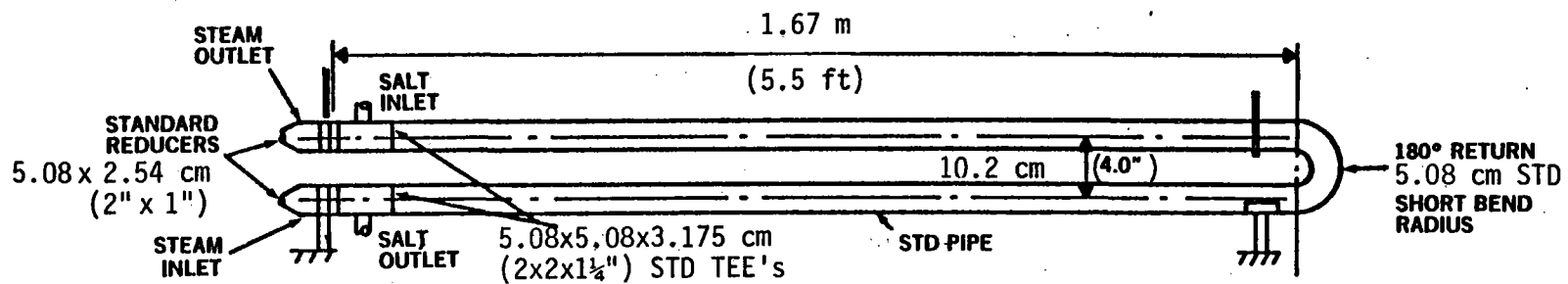
The selection of the evaporator configuration was obtained by a trade-off study, weighting the advantages against the disadvantages. A summary of this trade study results is shown in Table 4-11. The tube-in-tube configuration is a single tube within a tube. The salt flows in the annulus and the steam/water in the inner tube. Horizontal and vertical configurations were studied. The helical configuration is a tube spiraled in a helical fashion in an annulus formed by two concentric shells. The vertical, tube-in-tube and helical configurations have major disadvantages with respect to the project, therefore, the horizontal tube-in-tube configuration was chosen for this project. The proposed evaporator concept shown in Figure 4-32 is a ribbed tube within a ribbed tube single pass counterflow heat exchanger. This design affords the following features:

- preclusion of DNB under all conditions, transient and low power;
- utilization of all standard components;
- low salt pressure drop;
- low water pressure drop.

Figure 4-33 shows the relative sizes and locations of the components. It can be seen that the complete SGE is within the space envelope for shipment on a standard flat bed truck. All that is necessary for on-site preparation is connection of salt inlet and exit, water inlet, steam outlet, auxiliary boiler, blowdown tank and instrumentation.

A shell and tube heat exchanger was selected over a spray type Main Steam Attemperator due to the increased steam cycle efficiency that can be achieved with the shell and tube configuration.

The remaining components of the SGE are conventional power plant equipment and are selected to be compatible with the SGE.



TUBESHEET THICKNESS = 1.27 cm (.500")

NO. OF TUBES = 4 1.27 cm (.500") O.D. x 1.24 mm (.049") WALL

TUBESHEET THERMAL SHIELD @ 2.54 cm (1.000") FROM SURFACE

AVG. TUBE LENGTH (INCL. TUBESHEETS) = 3.563 m (140.283")

Figure 4-31 Superheater

Table 4-11 Evaporator Trade-off

Tube-in-tube: Horizontal

Advantages

- o Precludes DNB (with availability of 316 SS ribbed tube)
- o Less material
- o Less analysis

Disadvantages

- o Thermal Expansion
- o Concentricity
- o Long

Tube-in-tube: Vertical

Advantages

- o Precludes DNB (smooth tube)
- o Less analysis

Disadvantages

- o Thermal expansion
- o Very long (100 ft; 10 ft high; 10 vertical sections)
- o Structural support

Helical

Advantages

- o Compact

Disadvantages

- o DNB
- o Extensive analysis

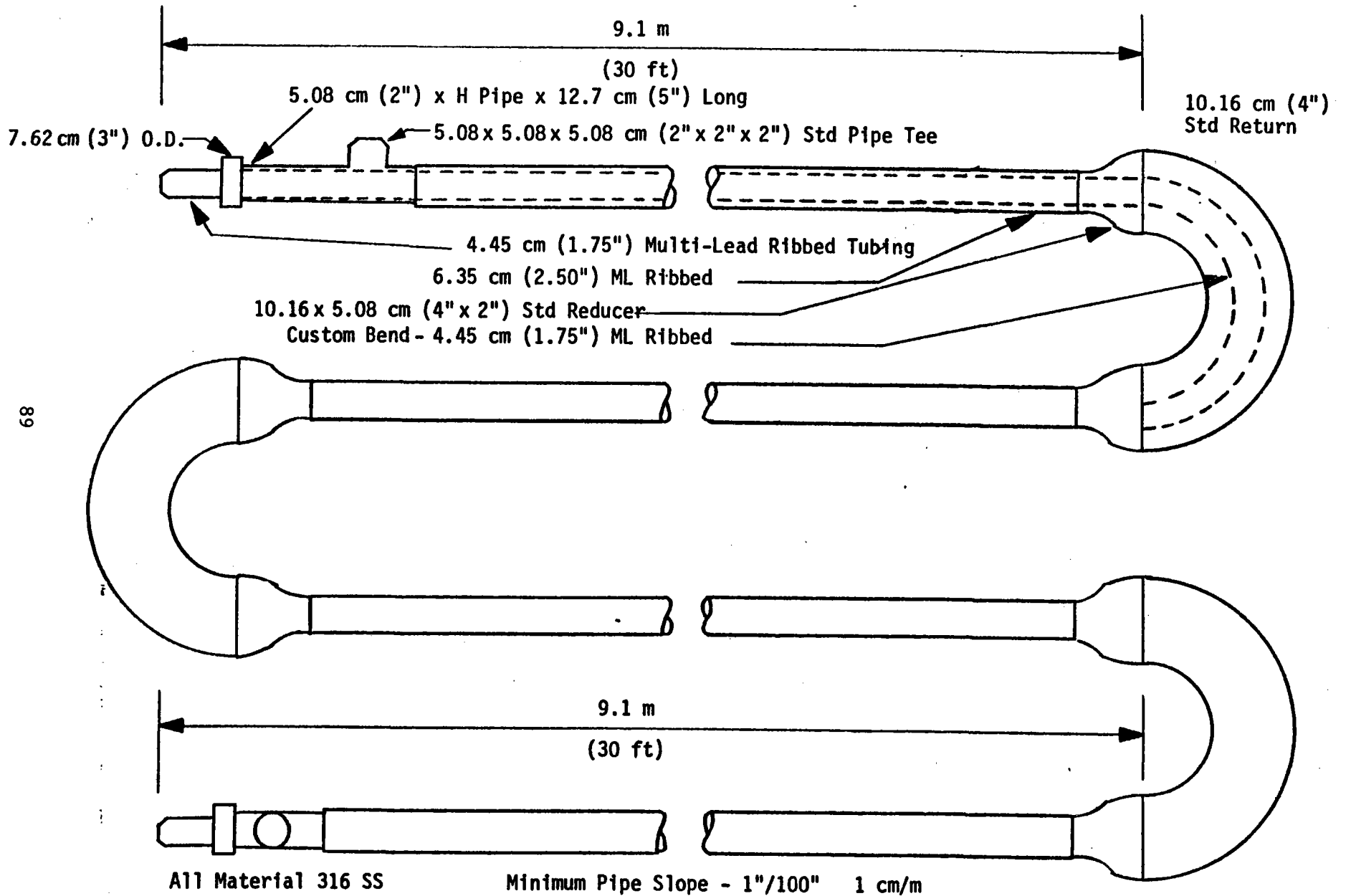


Figure 4-32 Evaporator

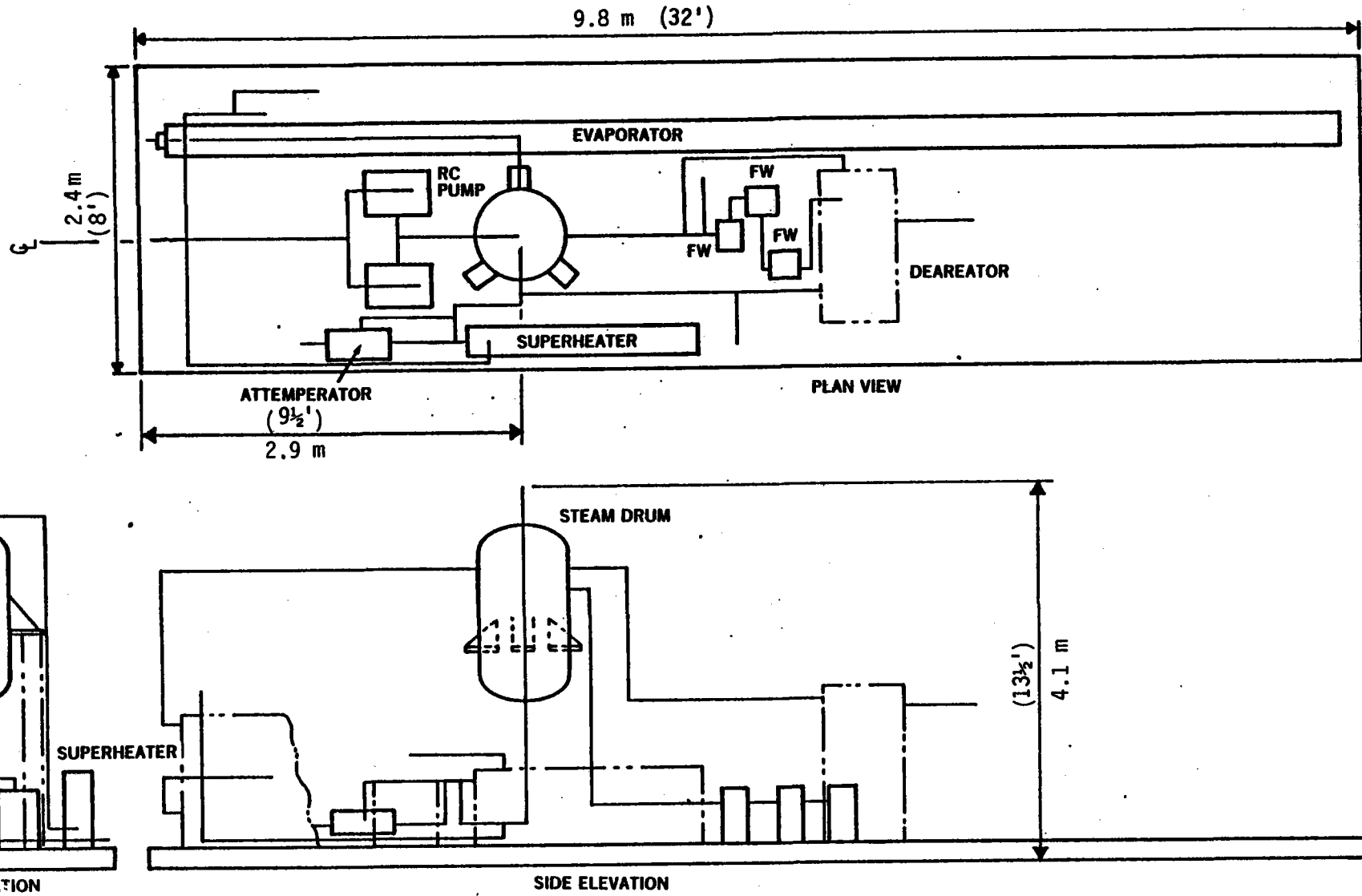


Figure 4-33 Skid Assembly Layout for the Solar Desalination Pilot Plant Steam Generator Subsystem.



#### 4.7 ENERGY STORAGE

The energy storage system is necessary to store thermal energy collected during periods of good insolation for nighttime use and for use during cloudy periods. Two storage tanks are used, one to store the hot 538°C (1,000°F) molten salt from the receiver and one to store the cold 288°C (550°F) molten salt returned from the steam generator equipment. The energy storage system is the interface between the receiver and the steam generator equipment. Its function is to not only store thermal energy, but also to decouple the receiver and steam generator. That is, storage acts also as surge capacity which allows the steam generator to operate independently from the receiver. This prevents daily insolation variations from affecting the electricity and process steam output.

##### 4.7.1 Configuration

The storage is sized to supply energy to the process for 28 hours of operation. This corresponds to a thermal energy storage capacity of 13.52 MWh<sub>t</sub>. The storage is designed to accommodate the energy being collected that is in excess of the energy requirement of the steam generator subsystem. A primary factor that effects storage size is the percentage of the total thermal power available from the heliostat field that is stored for later use. At the design point (Day 355, 12:00 solar noon, 950 w/m<sup>2</sup> insolation) 73% of the energy collected is stored for later use, and 27% is delivered to the steam generator. This ratio will change with the varying insolation levels and times of year, but defining the fractional use of the available energy at the design point is useful for comparing various plant configurations and storage sizes.

The insolation at the site and the economic scenario used also affect storage size optimization. All these factors can be taken into account by selecting the storage size that minimizes the annual cost/unit of energy (\$/MWh<sub>t</sub>) from the Solar Thermal Central Receiver system (see Figure 4-34). This is achieved as follows:

- (1) Determine the capital cost of three plants with three different storage sizes (22, 26, 30 hours);
- (2) Calculate the amount of money expended annually for each plant;

Assumptions = 20 year plant life  
10% cost of capital  
Annual operation and maintenance = 3% capital cost  
8% escalation on operation and maintenance

- (3) Use STEAEC system simulation program with the Solar Irradiance Model (SIM) insolation data to determine the annual energy (MWh<sub>t</sub>/yr) delivered to the process for each plant:

22 hr. storage -- 3797 MWh<sub>t</sub>/yr  
26 hr. storage -- 3859 MWh<sub>t</sub>/yr  
30 hr. storage -- 3876 MWh<sub>t</sub>/yr

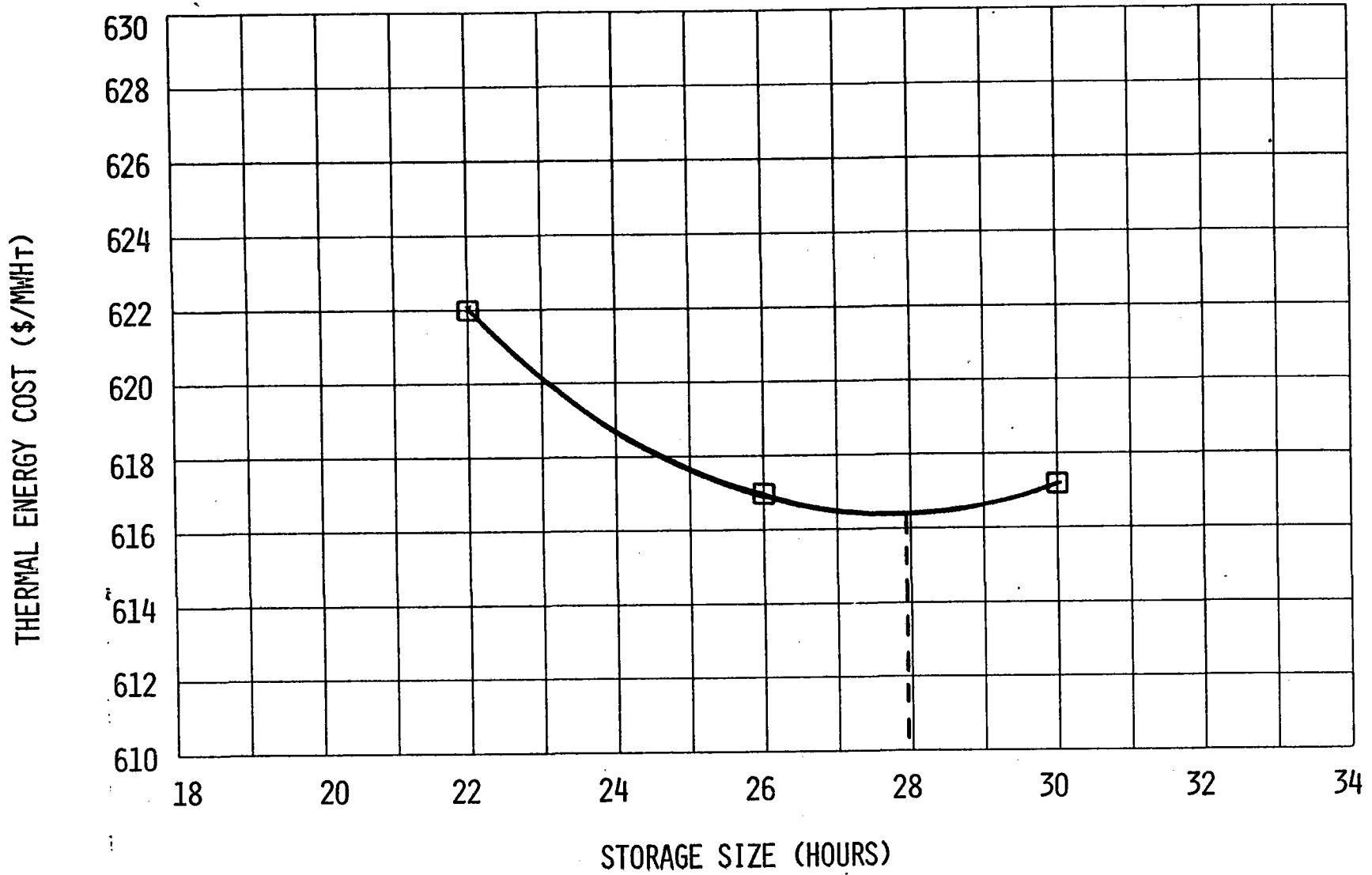


Figure 4-34 Storage Size Vs. Thermal Energy Cost

There are periods of the year when very high insolation causes the operator to turn down heliostats because the hot salt storage is fully charged. As the storage size is increased, less energy is dumped as a result of a fully charged storage.

- (4) Divide the annual cost of each plant by the amount of energy delivered to the process for each plant. This results in the values on the y-axis of Figure 4-34.

The point at which the curve optimizes (28 hours) represents the lowest cost of energy from the system. This method of optimizing storage size will result in a small amount of energy being dumped on a few peak insolation days out of the year. This is because the value of the small amount of energy dumped is less than the cost of the additional storage that would be required to accommodate it. With a 28-hour storage size, about 3% of the annual energy available is dumped because of a fully charged storage.

These calculations are based on the SIM program insolation data described earlier. To check the need for 28 hours of storage, six consecutive days were selected from the actual Yanbu data, and the storage charge/discharge history was plotted (see Figure 4-35) the six days consist of four clear days, one partly cloudy day, and one overcast day. The power output of the receiver vs. time of day is plotted on the lower graph, along with the process energy consumption rate. The difference between the receiver power output and the process energy consumption rate is used to charge storage, which is shown on the upper curve. The storage capacity of 28 hours is shown as a dotted line. The graph indicates that the storage is nearly charged at the end of the fourth day, and one more clear day would have fully charged the storage. However, the fifth day (Day 3) is a partly cloudy day and there is almost no useable insolation on the sixth day (Day 4). Therefore, the storage is exhausted in the afternoon of the sixth day. At that point, the auxiliary boiler can be used to continue the desalination process, or the plant can be shut down.

#### 4.7.2 Design

The energy storage equipment includes the hot and cold salt tanks, hot and cold salt pumps, hot and cold salt sumps, and the associated valves, piping and trace heating. The flow of hot salt from the hot storage tank is regulated by the level in the hot salt sump which, in turn, depends upon the salt demand from the steam generator. The flow of cold salt from the cold storage tank is dependent on the demand from the receiver (see Figure 4-36).

The hot and cold salt storage tanks are horizontal, 89.7 m<sup>3</sup> (3167 ft<sup>3</sup>) storage tanks measuring 3.66 m (12.0 ft) in diameter and 8.53 m (28 ft) long. Of the storage volume in each tank, approximately five percent is unrecoverable storage. This results in approximately 84.9 m<sup>3</sup> (3000 ft<sup>3</sup>) of useable storage capacity for each tank. The cold salt tank is constructed of 13mm (.5 in) thick carbon steel and the hot salt tank is constructed of 13 mm (.5 in) thick stainless steel.

6-DAY STORAGE CHARGE/DISCHARGE HISTORY  
 (ACTUAL YANBU DATA USED)

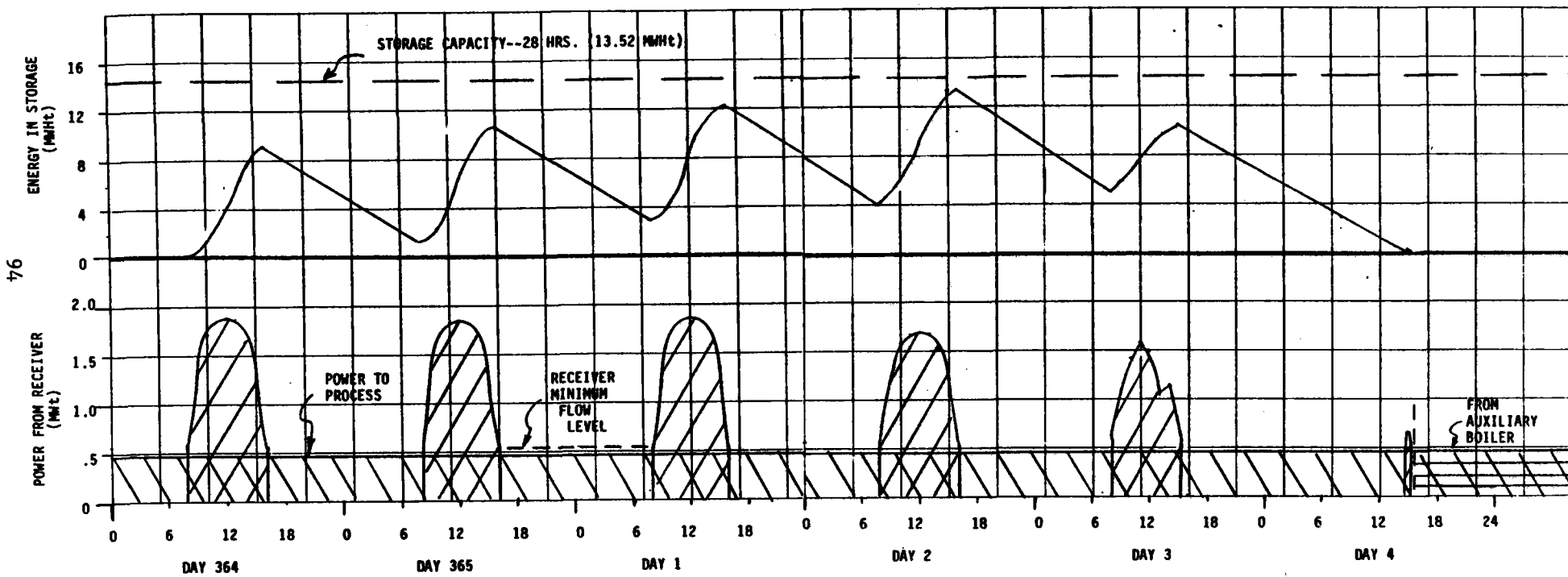


Figure 4-35 6-Day Storage Charge/Discharge History (Actual Yanbu Data Used)



The salt tank wall thickness was selected to minimize tank wall stresses caused by storing the high density salt in horizontal tanks. The thickness was based on Black and Veatch's past experience with horizontal tanks. This experience has indicated that horizontal tanks must be of rigid construction to ensure that the tank walls do not deflect as a result of load and that the load is transferred to the two or three supports being utilized.

The tanks will be furnished with support saddles for mounting on fire brick supports. Insulation studs for mounting mineral fiber block and board type insulation will be attached to the tank. The hot salt tank will be insulated with 279 mm (11 in) of Flexwhite insulation and will have a calculate average heat loss of .143 MWhT/day. The cold tank will be insulated with 152 mm (6 in) of Fléxwhite insulation and will have a calculated average heat loss of .135 MWhT/day.

Two vertical salt tanks are used as sumps, one to be designated the hot salt sump and the other cold salt sump. Both sumps will be 2.44 m (8.0 ft) in diameter by 1.83 m (6.0 ft) tall and will be furnished with a flat bottom and top. The bottom will be suitable for mounting on insulating fire brick. The top will have provisions for mounting of a vertical, cantilever pump and a mixer. The initial melting of the salt will be done in the cold salt sump. The cold salt sump will have provisions for inserting immersion heaters through access openings in the top; each opening will have a cover and will be about 0.762 m (2.5 ft) in diameter to accommodate four resistance heaters.

The tanks and sumps are atmospheric storage vessels designed and constructed in accordance with the ASME Pressure Vessel Code. Vents on the vessels are provided with carbon dioxide and moisture scrubbers to prevent contamination of the salt. A salt regeneration system may be provided to allow regeneration of the salt in the event contamination occurs; the decision on whether or not to implement the salt regeneration system will be made in Phase 2 after more design and cost information is obtained.

The material selected for subsystem piping is based on results of material compatibility tests and thus depends upon the salt temperatures. Stainless steel pipe is used for all salt piping with temperatures in excess of 371°C (700°F). Carbon steel is utilized for all salt piping with temperatures less than 371°C (700°F).

One hot salt pump and one cold salt pump are used in the system. The hot salt pump is used for circulating the hot salt from the hot storage tank through the steam generator subsystem and back to the cold storage tank. The cold salt pump is used for circulating salt from the cold storage tank through the receiver and back to the hot storage tank. The pumps are suitable for pumping high temperature salt and are constructed of 316 Stainless steel. Pump capacities will be as indicated below:

Cold Salt Pump - 3.15 1/5 (50 gpm) @ 99.1 m (325 ft) head  
Hot Salt Pump - .95 1/5 (15 gpm) @ 19.8 m (65 ft) head

We estimate that 158,000 kg (350,000 lb) of nitrate salt (60% NaNO<sub>3</sub>, 40% NKO<sub>3</sub> by wt.) will be required for initial fill of the thermal storage system.

#### 4.8 REVERSE OSMOSIS UNIT

The RO system is designed to produce 90 m<sup>3</sup>/day of 840 ppm total dissolved solids produce water from seawater. This design includes sufficient equipment to allow operation at up to 180 m<sup>3</sup>/day. The majority of the components selected for this design are based on BVI power plant experience. This includes the sizing criteria for the roughing and polishing filters, design of the chemical feed equipment, and piping sizing and materials of construction. Items unique to the RO system, and the basis for their selection, are as follows.

1. Energy Recovery Turbine - The energy recover turbine receives high pressure reject brine from the permeators, and converts this residual energy to rotational motion to aid in driving the permeator high pressure supply pump. Without the energy recovery turbine the RO system would consume approximately 34.1 kWh electricity for each 1,000 gallons of water produced (34.5 kW used at 90 m<sup>3</sup>/day treatment rate). With the energy recovery turbine, the energy consumption would be reduced to about 20.9 kWh electricity for each 1,000 gallons of water produced (21.2 kW used at 90 m<sup>3</sup>/day treatment rate).
2. Membranes - Dupont B-10 membranes were specified for this application since Dupont has the most experience with the treatment of seawater by reverse osmosis, and their B-10 membrane provides the best combination of cost, performance, and durability. The B-10 membranes are of the hollow fiber configuration and are constructed of non-corrosive polymers to provide resistance to bacterial and chemical attack.
3. Location of Degasifier - The degasifier is provided to remove CO<sub>2</sub> and other noncondensables from the water and could be located either upstream or downstream of the permeators. However, the advantages of downstream location include the following.
  - a. With downstream location, the degasifier is smaller, since it must be sized to handle the RO product water flow only; this amounts to 30 percent of the upstream feedwater flow.
  - b. Carbon dioxide present in the feedwater reduces the required amount of acid feed for feedwater pH adjustment. Therefore, removing CO<sub>2</sub> after the permeators results in H<sub>2</sub>SO<sub>4</sub> feed savings.
  - c. The presence of CO<sub>2</sub> in the feedwater has no detrimental effect on the permeators or upstream piping. The upstream piping consists of corrosion resistant PVC or Type 316 stainless steel. The permeators pass the CO<sub>2</sub> with no detrimental effect.

#### 4.9 MULTIPLE-EFFECT DISTILLATION UNIT

The MED system is a sixteen effect, low temperature, horizontal tube, thin film type and is designed to produce 182 m<sup>3</sup>/day of 5 ppm total dissolved solids product water from seawater. This design was selected in order to maximize both the amount of electrical energy produced by the turbine, and the quantity of product water from the MED system.

Because of the low temperature design, the MED can operate from low cost "waste heat." In this case exhaust steam from the turbine, at a design condition of 44.8kPa (6.5 psia) and 88°C (190°F), is supplied to the MED. This low temperature operation also serves to minimize scale and corrosion within the unit as compared to the more conventional high temperature MED's.

The sixteen effect design results in an excellent overall efficiency. The economy rating for this system is 5.4kg (12 pounds) of distillate produced for each 1,000 Btu input to the MED in the form of turbine exhaust steam.

#### 4.10 TURBINE GENERATOR

Selection of the turbine-generator size was influenced by two key factors. The plant size tradeoff study comparing the plants utilizing the 111, 75 and 50 heliostats in the collector field showed an economic advantage to the smallest plant configuration. However, the steam throttle conditions were established at 5,516kPa (800 psia) and 427°C (800°F), and the smallest available turbine-generator designed for these steam conditions is a nominal 50kW machine and corresponds to a plant with 75 heliostats.

The final turbine generator configuration has a turbine cycle efficiency of 11.8% with the output of 54kW electric. Of this total 37kW electric is used for the essential desalination processes (RO and MED) and the remainder is used for powering auxiliary systems. The turbine exhaust steam contains .426Mwt of usable energy which is used to distill 182m<sup>3</sup>/day of product water in the MED.

The turbine generator will be designed in accordance with the following conditions:

<u>Turbine</u>	<u>Design Condition</u>
Steam flow, maximum kg/s (lb/hr) steam inlet	0.174 (1,380)
Pressure, MPa (psia)	5.5 (800)
Steam inlet temperature, °C (F)	427 (800)
Steam exhaust pressure, kPa (psia)	58.6 (8.5)
Rotative speed, rpm	3,600
Horsepower rating	1.15 times required horsepower at rated generator output



GeneratorDesign Condition

Generator rating at 0.80 power factor	Maximum available with the steam conditions listed above - 50 kW minimum
Voltage at generator terminal, volts	277/480 wye
Time for voltage to stabilize following full load change to <u>+ 5 per cent</u>	1 second or less
Maximum telephone influence factor (for this size unit, 100 is best obtainable and acceptable for normal operation)	100
Electrical output characteristics	4 wire, 3 phase, 60 hertz
Temperature rise by resistance methods over 40 C (104°F) ambient	80 C (144°F)
Generator speed, rpm	3600
Motor starting capability with voltage dip not to exceed 25 percent, kW, NEMA Code F motor	30
Overload capacity for 2 hours	123 percent
Short circuit current, 3 phase symmetrical, in percent of rated generator current for 10 seconds	250
Maximum wave form rms harmonic content, percent, total	5
Maximum voltage excursion from rated voltage upon application of rated kVa, percent	<u>+15</u>
Voltage regulation, no-load to rated kVa, percent	<u>+1</u>

#### 4.11 MASTER CONTROL

Displays and control equipment are provided in the control room for operation of the desalination plant during startup, routine operation, and normal and emergency shutdowns. Individual control panels are provided for the RO and MED subsystems. The heliostat field is controlled and monitored from a CRT terminal that is part of the Heliostat Array Controller. The Master Control Subsystem (MCS) controls the receiver, steam generator, thermal storage and electrical power generation subsystems. The MCS also performs the data acquisition function for all of those subsystems and for the RO and MED subsystems.

The MCS is made up of digital controllers; I/O (input/output) units for interfacing with the plant; operator I/O equipment including CRT terminals, printers and manual control stations; data storage equipment; and interconnecting data buses and wiring. The MCS interfaces with transducers (thermocouples, pressure sensors, level sensors, etc.) and control valves that are included in the controlled subsystems. In the automatic mode, the MCS uses the sensor inputs to generate control signals to operate control valves and to perform on-off functions in the proper sequence. In the manual control mode, the operator uses operating manuals and data displayed on the CRT terminals to initiate on-off functions and change set points; capability is also provided for the operator to control critical valves directly from manual control stations.

The requirements for the MCS are established by the number and types of automatic control loops, on-off functions, interlock logic functions, and data acquisition points required by the controlled and monitored subsystems. The following paragraphs describe the control of the subsystems and present a summary of the data acquisition requirement and a description of the baseline and other candidate Master Control Subsystem.

##### 4.11.1 Receiver Control

The function of the receiver control is to maintain the receiver exit salt temperature at the desired level. The system is operated in an insolation following mode by matching the salt flow rate to the amount of absorbed solar energy. The collector field will be controlled to maximize the amount of energy reflected into the receiver cavity and the receiver will be controlled to absorb the incident energy safely and to maintain the outlet salt temperature at the setpoint.

The receiver can be either manually or automatically controlled. The receiver will be operated manually during startups and shutdowns. Automatic control of the receiver will be activated after the receiver has reached a normal operating mode and will be capable of maintaining the outlet salt temperature at the setpoint under most operating conditions. Severe transients may require manual operator control to minimize the production of low temperature salt. The control system will be designed such that the safety of the receiver is of the highest

priority, and will signal an alarm and execute predetermined emergency procedures in the event of receiver overtemperature or other system failures. Any system emergency will immediately result in an automatic defocus of the heliostat beam from the receiver aperture.

A schematic which illustrates the receiver control system which starts with the supply of cold salt to the receiver and ends with the return of hot salt to the downcomer is shown in Figure 4-37. A cold surge tank is provided in the receiver, to ensure the supply of cold salt through the flow control valves (FCV). The hot salt exits via the hot surge tank and downcomer. As the cold surge tank is charged to 662 kPa (96 psig) and the hot salt is at atmospheric pressure, a relatively constant pressure difference is established for control of salt flow through the receiver.

Operating Modes - At the design point, the receiver will deliver molten salt at a controlled temperature of 538°C (1000°F), at a flow rate consistent with available insolation. The diurnal operational sequence associated with this function consists of: (1) startup from drained condition; (2) normal operation; and (3) normal shutdown. These sequences will be performed routinely during day-to-day operation. Other operating modes include: (4) emergency shutdown; and (5) cloud passage. The diagram notation for the Control interlock diagram is shown in Table 4-12. Control Function Diagrams is given in Table 4-13.

- a. Startup from drained condition (initial startup). The sequence of events associated with the warmup and startup procedure is shown in Figures 4-38 and 4-39. The receiver is warmed up to above salt freezing temperature by the use of the selected heliostats. When the receiver temperature is stable, the operator can initiate cold salt flow to fill the receiver and pressurize the surge tank. As soon as the MCS pressure display has confirmed the ullage pressure, the trace heating will be terminated. The operator can then focus the remaining heliostats onto the receiver. After the salt-exit temperature has stabilized the operator will then switch to auto-control to enable the MCS to modulate the salt-flow in accordance with insolation.
- b. Normal operation will consist of the MCS continually modulating salt-flow to maintain a constant outlet temperature, and continually monitoring the receiver for trip conditions (as shown in Figure 4-39).
- c. Normal shut-down - the heliostats are removed from the target and put into the stow position. The cavity door is closed, the pump turned off and the receiver drained of salt.
- d. Emergency shutdown is defined by the trip conditions shown in Figure 4-39. A trip automatically produces a defocusing of the heliostats and a consequent setting of the trip flag.
- e. Cloud Passage - A minimum flow rate of 1.36 kg/sec (10,800 lbs/hr) will be maintained (by the control system) to prevent overheating of the receiver tubes during sudden recovery of insolation after the cloud passage. This procedure assumes that the heliostats will remain "on target" throughout this operating mode.

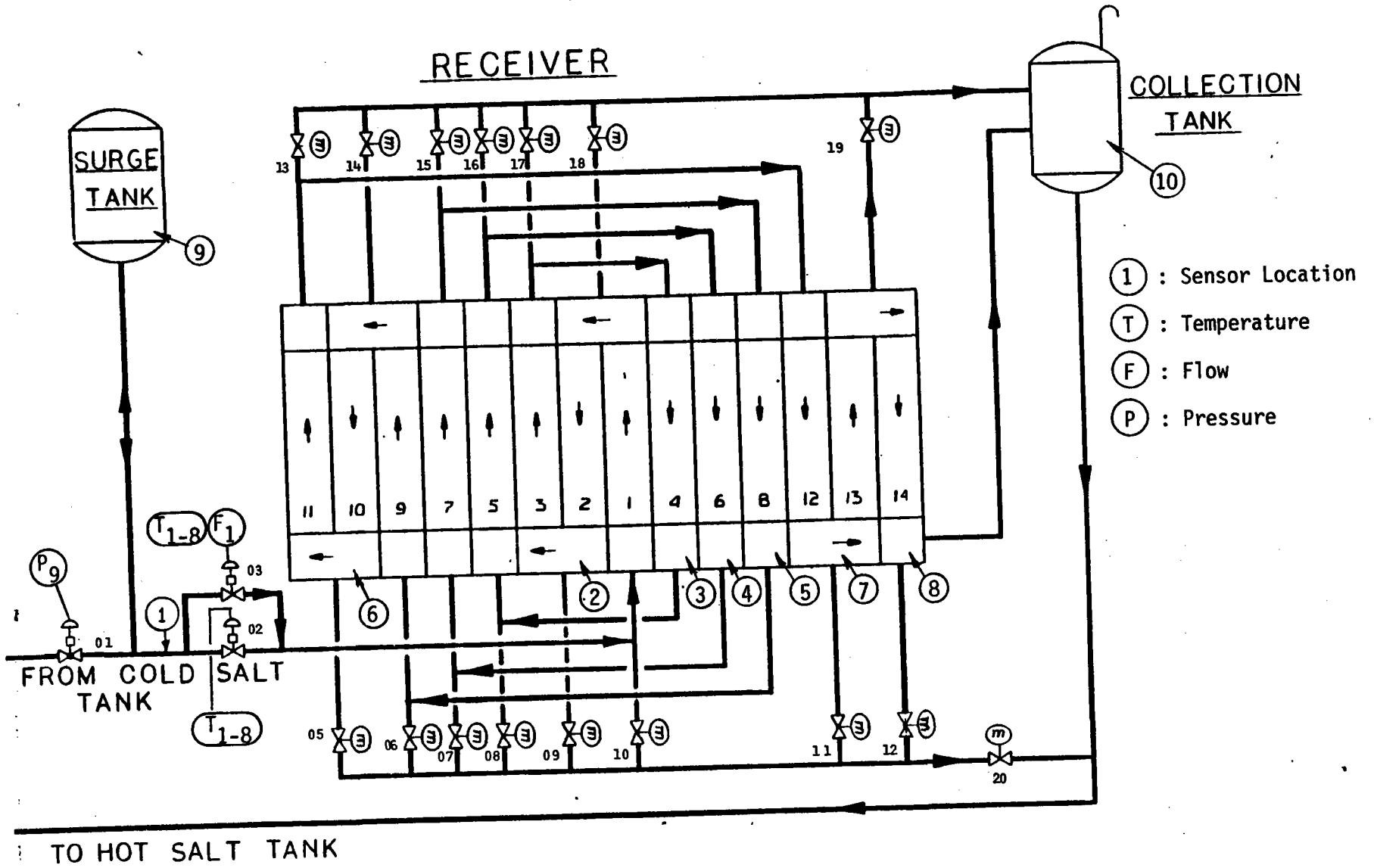
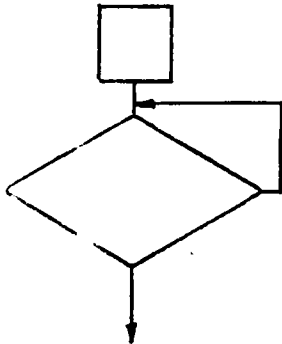


Figure 4-37 Receiver Control Schematic

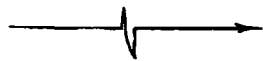
Table 4-12 Procedure Diagram Notation



Information to Display



Flow Diagram, describing  
Process Control Logic




















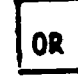






Communication



Operator Action

Table 4-13 Control Function Diagram Notation

	Flag, A through Z		Proportional Control
	Pressure Transmitter		Integral Control
	Flow Transmitter		Derivative Control
	Temperature Transmitter		Difference
	Operator Set Point		Track (Initializes Integrator)
	Analogue to Digital Conversion		Summer
	Function Generator		Square Root Extractor
	Digital to Analogue Conversion		Signal Check
	High, Low Signal Monitor		Current to Pneumatic Conversion
	Indicator		OR Gate
	Alarm		High, Low Limiter
	Transfer		Low Signal Selector

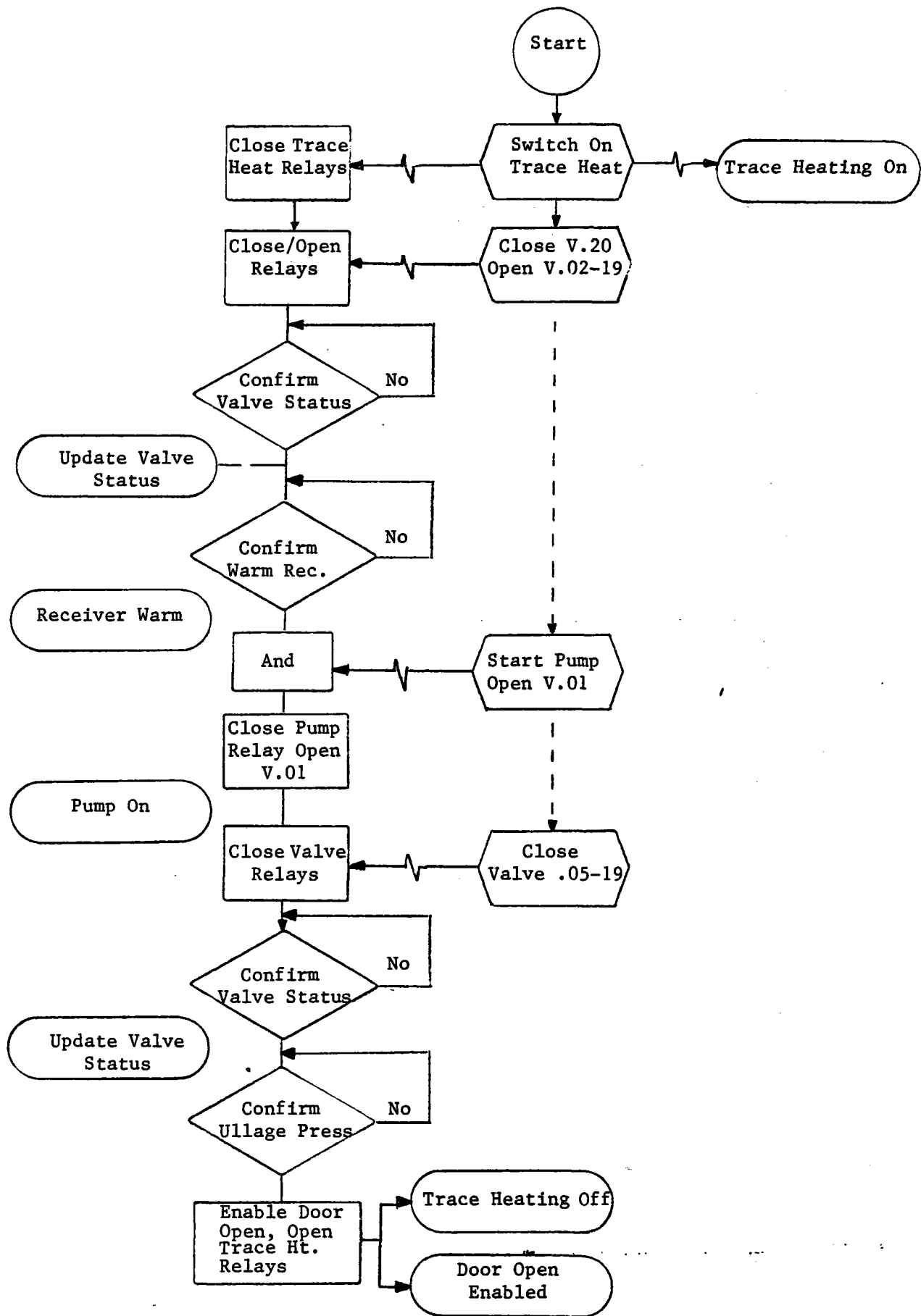


Figure 4-38 Receiver Warm-up Procedure

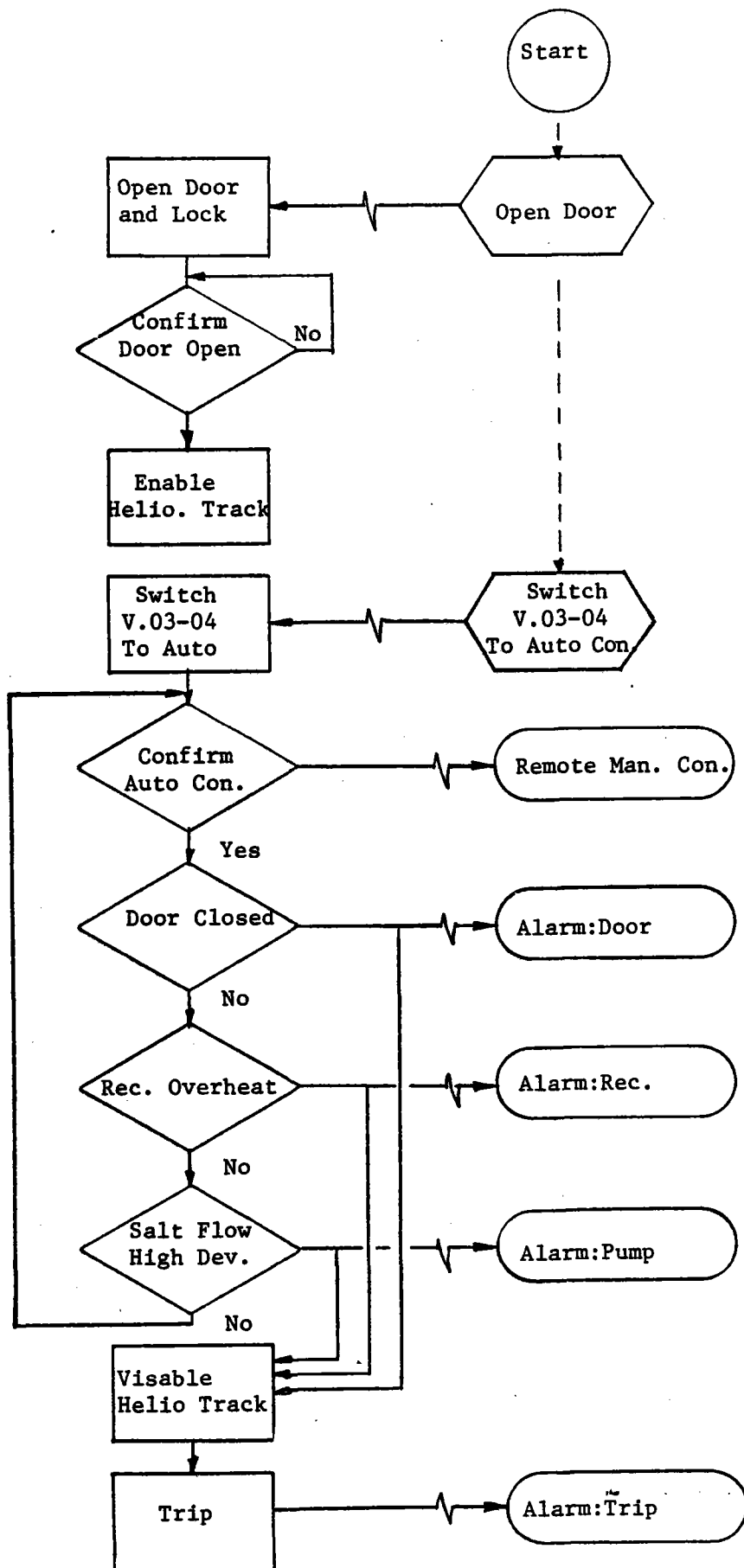


Figure 4-39 Receiver Start-up and Trip Conditions



Automatic Control - The control algorithm used to set the salt flowrate of the receiver is shown in Figure 4-40. The algorithm estimates the absorbed flux in order to calculate the required salt-flow rate.

The salt flow is modulated by two valves in parallel (#03, #04 in Figure 4-37). This is to safeguard against the case of increasing flux damaging a receiver when a valve has stuck. Figure 4-41 shows the method used to control the valves. Valve #04 is controlled open loop and carries most of the load. Valve #03 is controlled such that it is always partly open but only moves to correct error in the salt flow rate.

The two remaining automatic control loops are shown in Figures 4-42 and 4-43. The control on the ullage pressure is to avoid any oscillatory motion in the riser. The level control on the hot surge tank is to guard from two phase flow.

Control and Instrumentation Requirements - The requirements for control are given in Tables 4-14 and 4-15. Table 4-14 lists those relating to the automatic control and remote supervision of valves and Table 4-15 relates to the control interlock logic for startup, trip monitor and fail safe. The instrumentation requirements are given in Table 4-16.

#### 4.11.2 Steam Generation Control

Figure 4-44 shows the layout of the steam generation plant complete with control scheme. The purpose of the control scheme is twofold. It is to enable startup of the plant and supply a steady flow of steam as demanded by the steam turbine.

Startup is enabled via the auxiliary boiler fired up to produce the necessary steam for warming the water side of the plant. This steam is then condensed and cooled before returning to the condensate hold up drum. The salt side of the plant can be warmed by mixing salt from the hot and cold salt stores. Once this is complete, the salt flow can be automatically modulated, via valve #01, and the plant pressurized, at which point the auxiliary boiler can be closed down.

During steady-state running, the plant is driven according to the steam turbine flow rate. The steam supplied by the plant is first used to drive the turbine/generator set and the electrical power used to drive the RO system and remainder of the plant. Any imbalance in electrical power will be accommodated via the power grid which can be used either to make up deficiencies or absorb excess.

The steam from the turbine is cooled to near saturation point before entering the MED unit which it exits as saturated water. The MED unit also bleeds off a small amount of steam from the steam drum which acts to pull a vacuum before being dumped as waste. To maintain the water inventory in the condensate drum, product water from the MED is used.

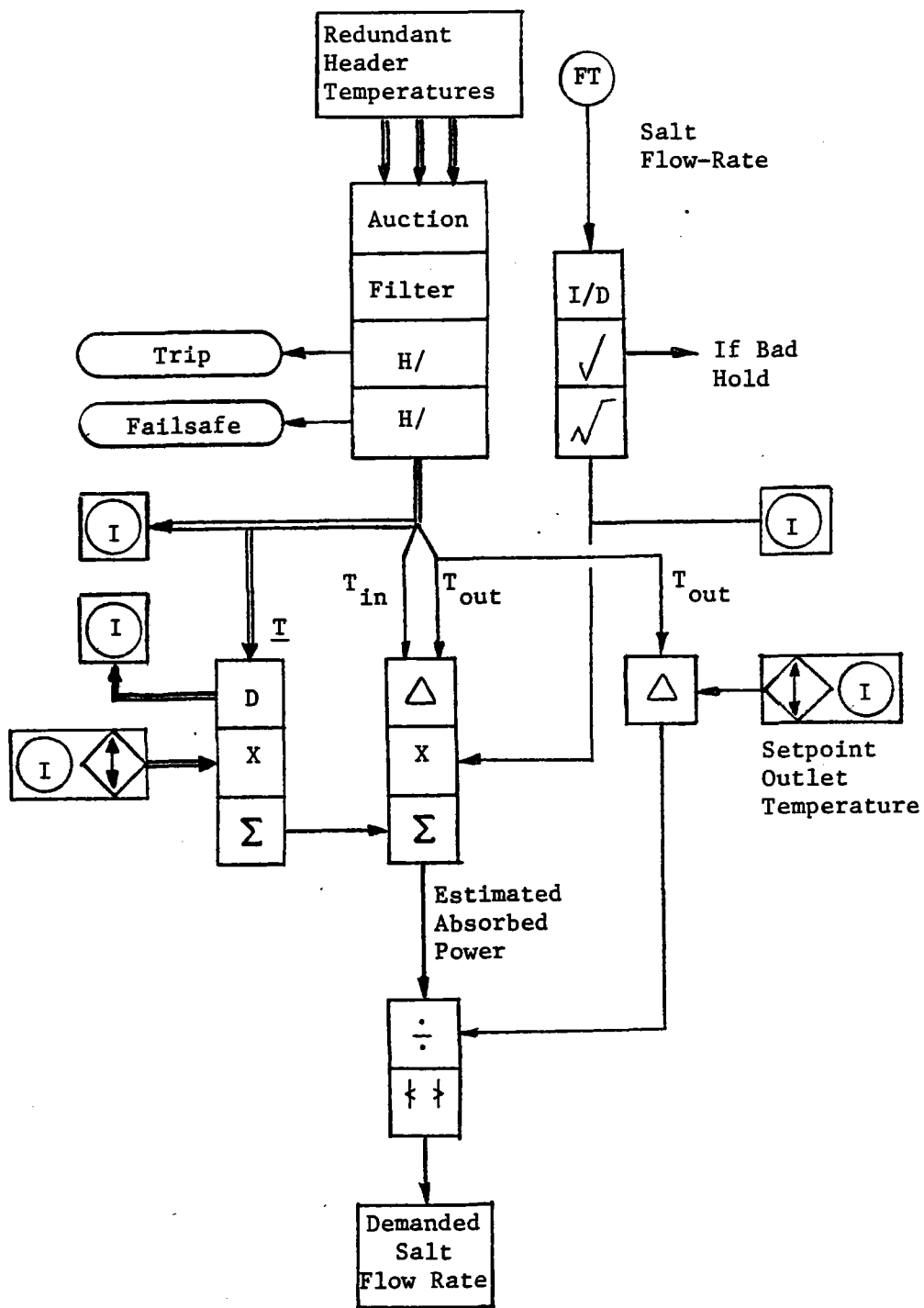


Figure 4-40 Receiver Control Algorithm



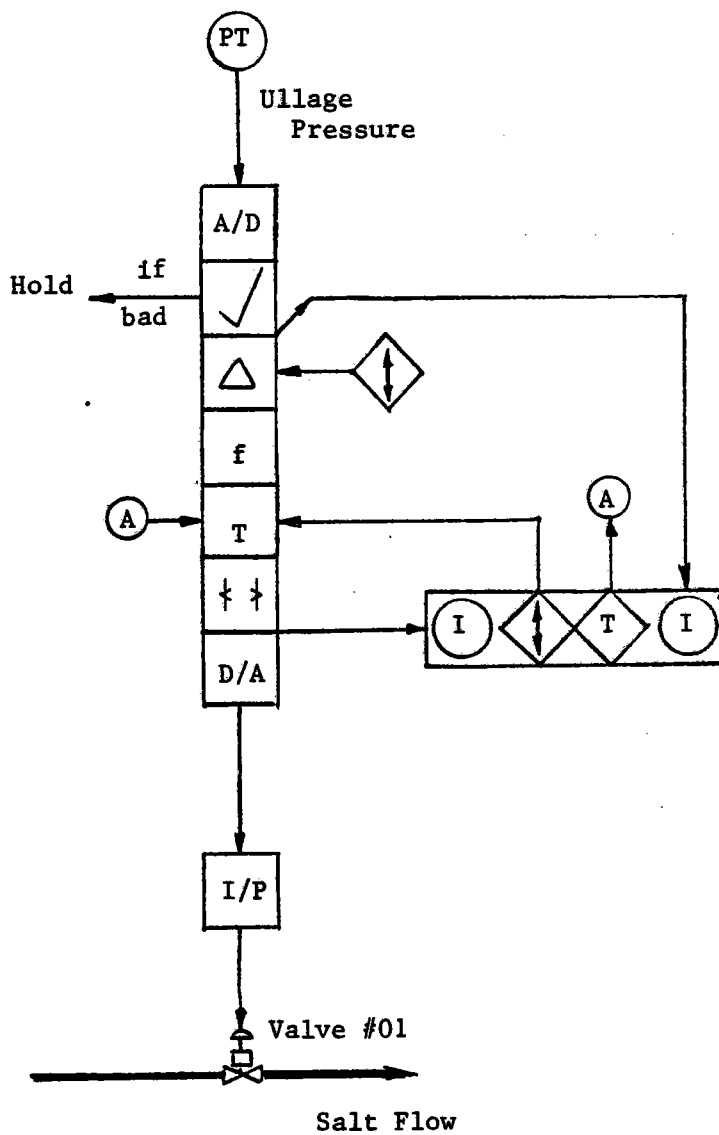


Figure 4-42 Control Functional Diagram: Ullage Pressure Damping

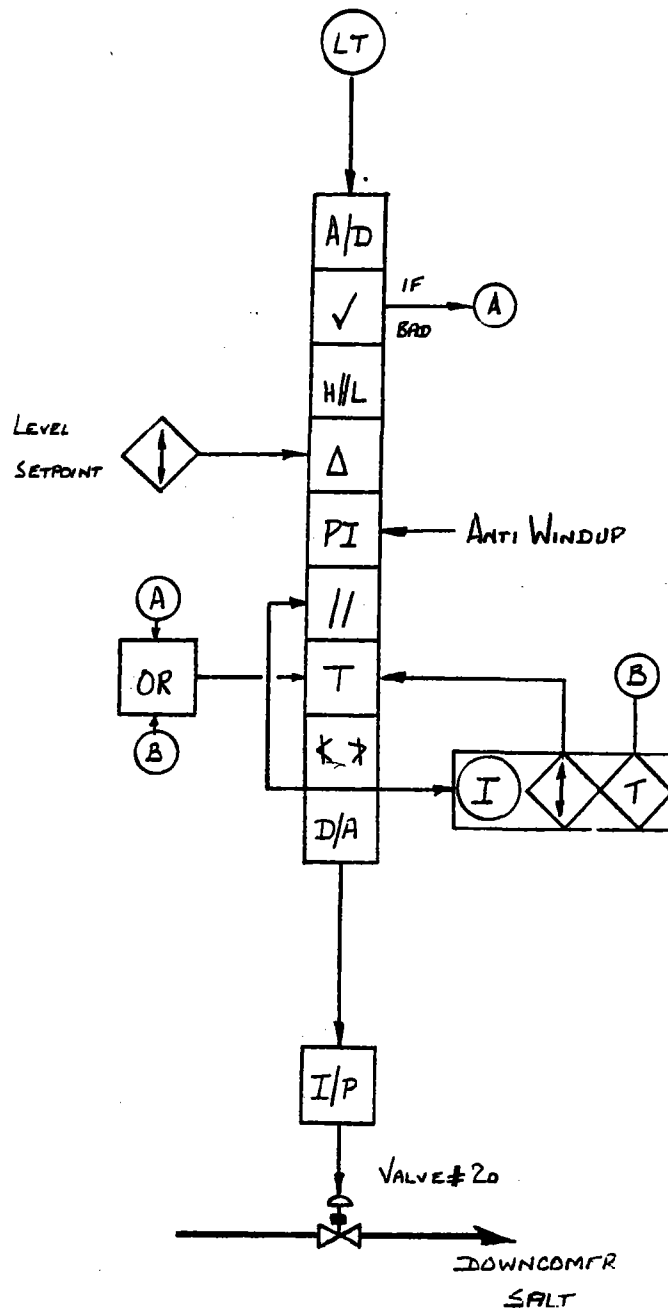


Figure 4-43 Control Functional Diagram: Downcomer Salt Valve

CONTROL REQUIREMENTS

SYSTEM DESIGNATION: Receiver Figure 4-37

FUNCTION	TYPE	CONTROL	PROCESS VARIABLES	CONTROL FUNC. DIAGRAM	REMARKS
Valve #01	Position	Ullage Pressure Regulation	Ullage Pressure	4-37	
Valve #02	Isolation	Remote supervision	--	--	
Valve #03	Position	Flow set point defined in Fig 4.5 PI control	i) Header Temps ii) Salt Flow to receiver	4-37	Manual override required using flow set-point and position.
Valve #04	Position	Position set point defined by Fig. 4.5 using function generator	Header Temps	4-37	Manual override required for position set-point.
Valves #05-11	Isolation	Remote Supervision	--	--	Ganged for single relay operation.
Valves #12-17	Isolation	Remote Supervision	--	--	Ganged for single relay operation.
Valves #18-20	Isolation	Remote Supervision	--	--	Seperate relays to operate each valve.
Door	Motor	Remote Supervision	--	--	
Trace Heaters	Relay	Remote Supervision	--	--	
Door Lock	Electro-mechanical	Interlock Logic	--	--	Manual override required.

Table 4-14 Receiver Control Requirements for Automatic and Remote Supervision of Valves

INSTRUMENTATION REQUIREMENTS

SYSTEM DESIGNATION: Receiver Figure 4-37

113

NAME	TYPE	RANGE OF MEASUREMENT	ACCURACY	SAMPLE RATE	TRANSDUCER/ CONDITION. REQUIRED	SCS DISPL.	PRINT TABLE	ARCHIVE	REMARKS
Salt Outlet (3 each)	Temp.	200-800°F	+ 2°F	2 sec	LIN	Yes		Yes	
Salt Inlet (3 each)	Temp.	50-400°F	+ 2°F	2 sec	LIN	Yes		Yes	
5 Headers (3 each)	Temp.	200-800°F	+ 2°F	2 sec	LIN	Yes		Yes	
Trace Heaters	Temp.	0-400°F	+ 3°F	1 min	LIN	15		45	
Trace Heater Relay	Contact	Opened/Closed	N/A	2 sec		Yes			
Tube Metal - Back side	Temp.	200-1100°F	+ 3°F	2 sec	LIN	15		45	
Heliostat Track Enable	Contact	Opened/Closed	N/A	2 sec		Yes			
Trip	Contact	Opened/Closed	N/A	2 sec					
Displacement Transducers (12 each)	LVDT.	TBD		1 min				Yes	

Table 4-15 Receiver Control Requirements for Control Interlock

INSTRUMENTATION REQUIREMENTS

SYSTEM DESIGNATION: Receiver Figure 4-37

NAME	TYPE	RANGE OF MEASUREMENT	ACCURACY	SAMPLE RATE	TRANSDUCER/ CONDITION. REQUIRED	SCS DISPL.	PRINT TABLE	ARCHIVE	REMARKS
Surge Tank	Pressure	0-100 psi	<u>+ 3</u> psi	2 sec		Yes		Yes	
Valve Positions	Analog	0-100%	<u>+ 1%</u>	2 sec				Yes	#01, 03, 04
Valve Positions (16 each)	Contact	Opened/ Closed	N/A	2 sec		Yes			#02, 05-19 display status on SCS console
Cavity Door Position	Contact	Opened/ Closed	N/A	2 sec		Yes		Yes	
Salt Flow Rate	Flow	0-TBD	<u>+ 2%</u>	2 sec		Yes		Yes	
Insolation	Epply or Equiv.	0-1.1 KW/m <sup>2</sup>	TBD	2 sec	N/A	Yes	Yes	Yes	
Wind Speed and Direction	Anemo-meter	TBD	TBD	2 sec	N/A	Yes	Yes	Yes	
Ambient Air	Temp.	TBD	TBD	2 sec	N/A	Yes	Yes	Yes	

Table 4-16 Receiver Instrumentation Requirements

114



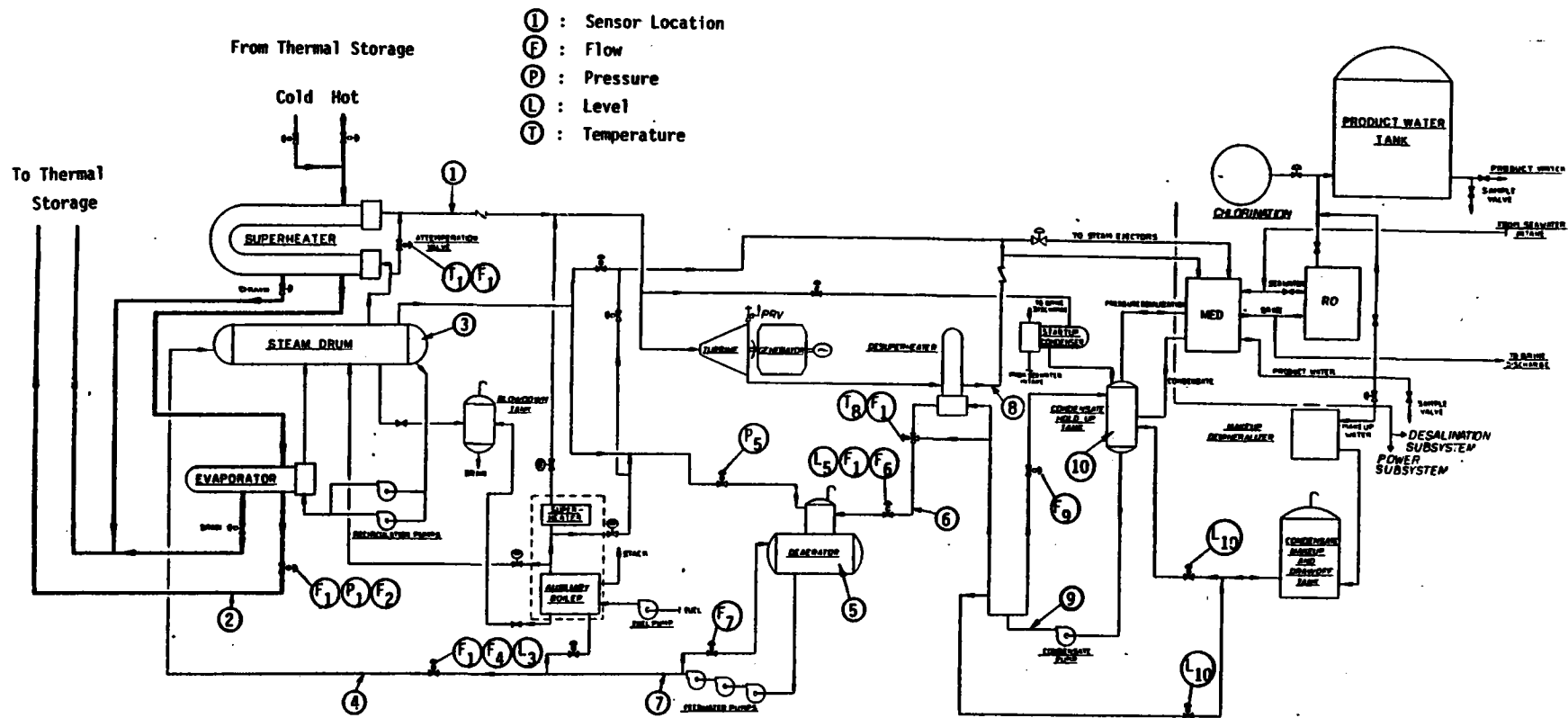


Figure 4-44 . Steam Generation Control Schematic

The control scheme reacts to demanded steam by automatically increasing the salt flow through valve #01. This is a load following term (servocontrol) which adjusts salt flow so as to thermally balance the plant. An additional term is included to control steam pressure. By modulating the salt flow, the pressure of the steam at the throttle can be maintained constant (regulatory). Figure 4-45 is a control functional diagram for this loop.

Any fluctuations in steam temperature are damped and controlled by mixing with cooler steam from the drum, valve #05. The control functional diagram is shown in Figure 4-46.

The feedwater is supplied through valve #02. This valve is controlled to maintain fluid level in the drum using level feedback (regulatory) and steam supply rate (servocontrol) as shown in the control functional diagrams of Figures 4-47 and 4-48. An identical control is applied to the Deareator, to maintain its level. Of the remaining controlled valves: 10 and 13 maintain adequate flow through their related pumps and 07 and 08 maintain condensate hold-up drum level.

#### a. Control and Instrumentation Requirements

These requirements are listed in Tables 4-17 and 4-18.

### 4.11.3 Thermal Storage Control

The thermal storage subsystem, Figure 4-49, is organized to control the flow of salt to and from the remainder of the plant without degrading the temperature of the salt in the hot storage tank.

During steady state operation, salt is supplied to the receiver from the cold salt sump (valve #08) and to the steam generation subsystem from the hot salt sump (valve #07). Salt returning from the tower is steered into either the hot or cold salt tanks depending on its temperature. These valves are also used to maintain the salt level in the hot surge tank.

The salt level in each sump is controlled using valves #03, #05 for hot salt and valves #04, #06 for cold salt. In each case, valves #03, #04 rely on gravity head to feed each sump and valves #05, #06 are used to avoid flooding of either sump. Valves #05, #06 are also used to ensure minimum flow through each pump.

#### Control and Instrumentation Requirements

The control requirements are given in Table 4-19. The instrumentation requirements have not been formulated but Table 4-20 summarizes an estimate.

### 4.11.4 Turbine Generator, RO and MED Control

The MCS provides the capability for the operator to monitor the EPGS and send commands to the turbine-generator to control the load set point.

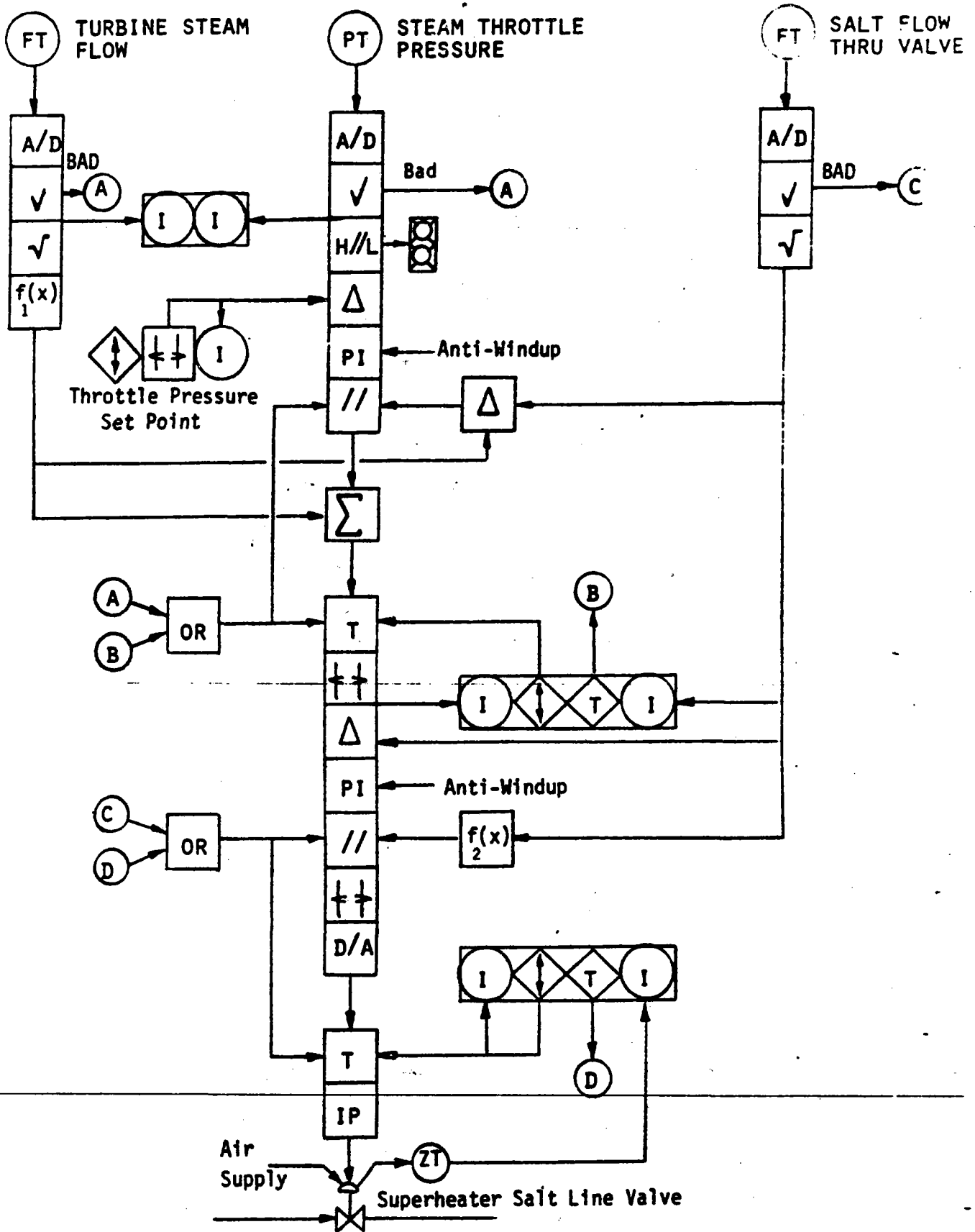


Figure 4-45 Control Functional Diagram - Salt Line Valve #01

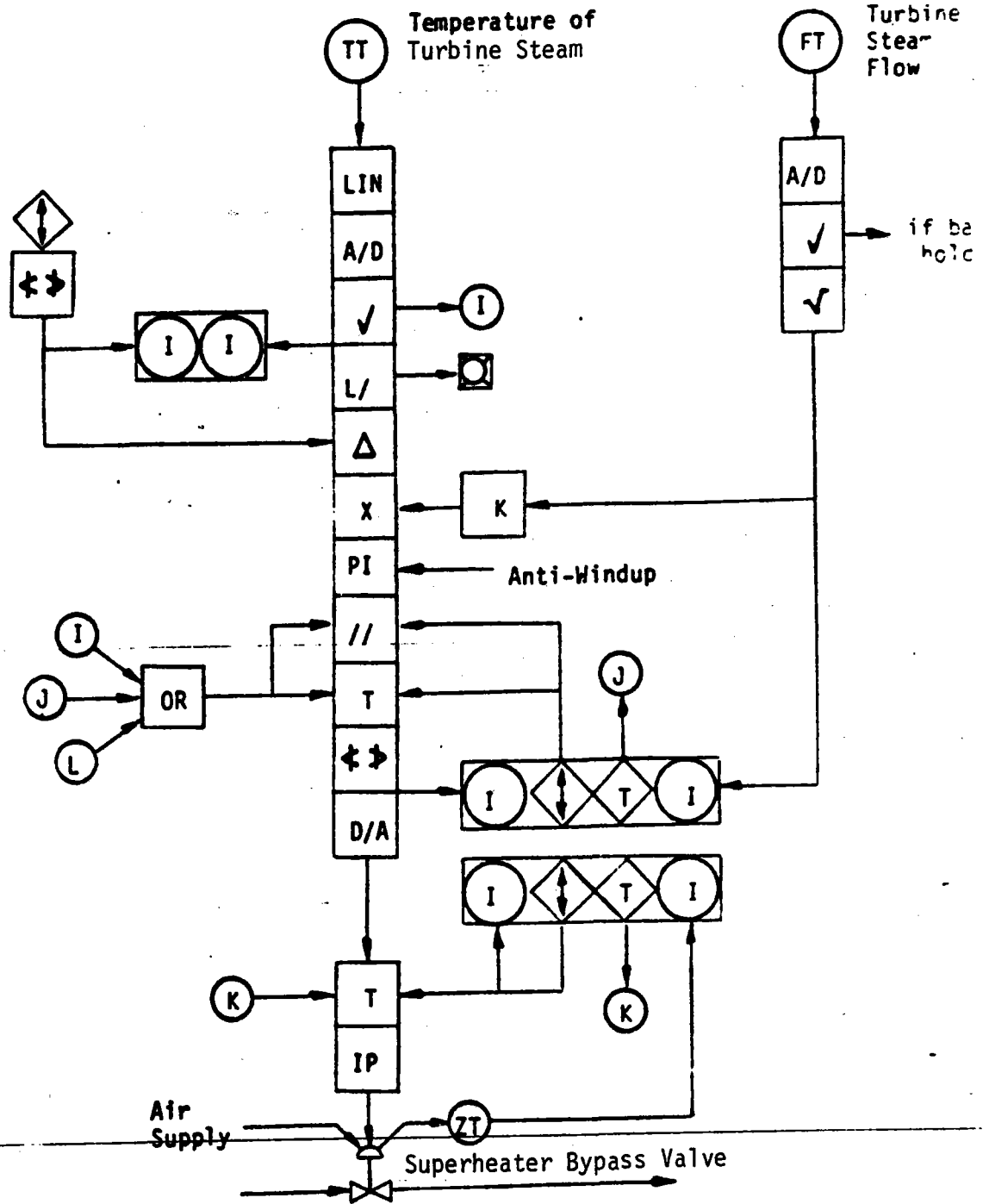


Figure 4-46 Control Functional Diagram - Turbine Steam Attemp #05

Three Independant Drum Level Measurements

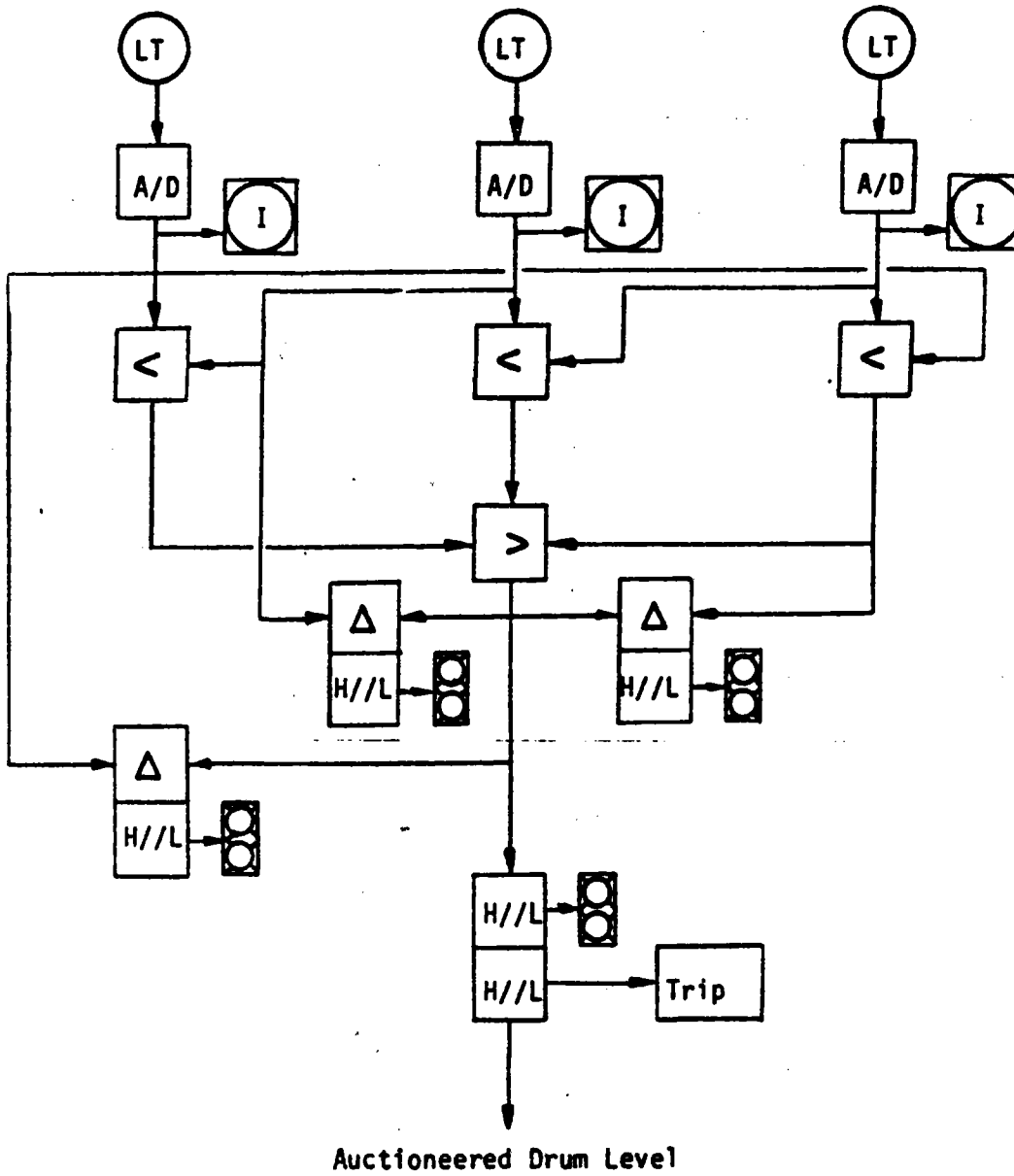


Figure 4-47 Control Functional Diagram - Steam Drum Level Auctioneer

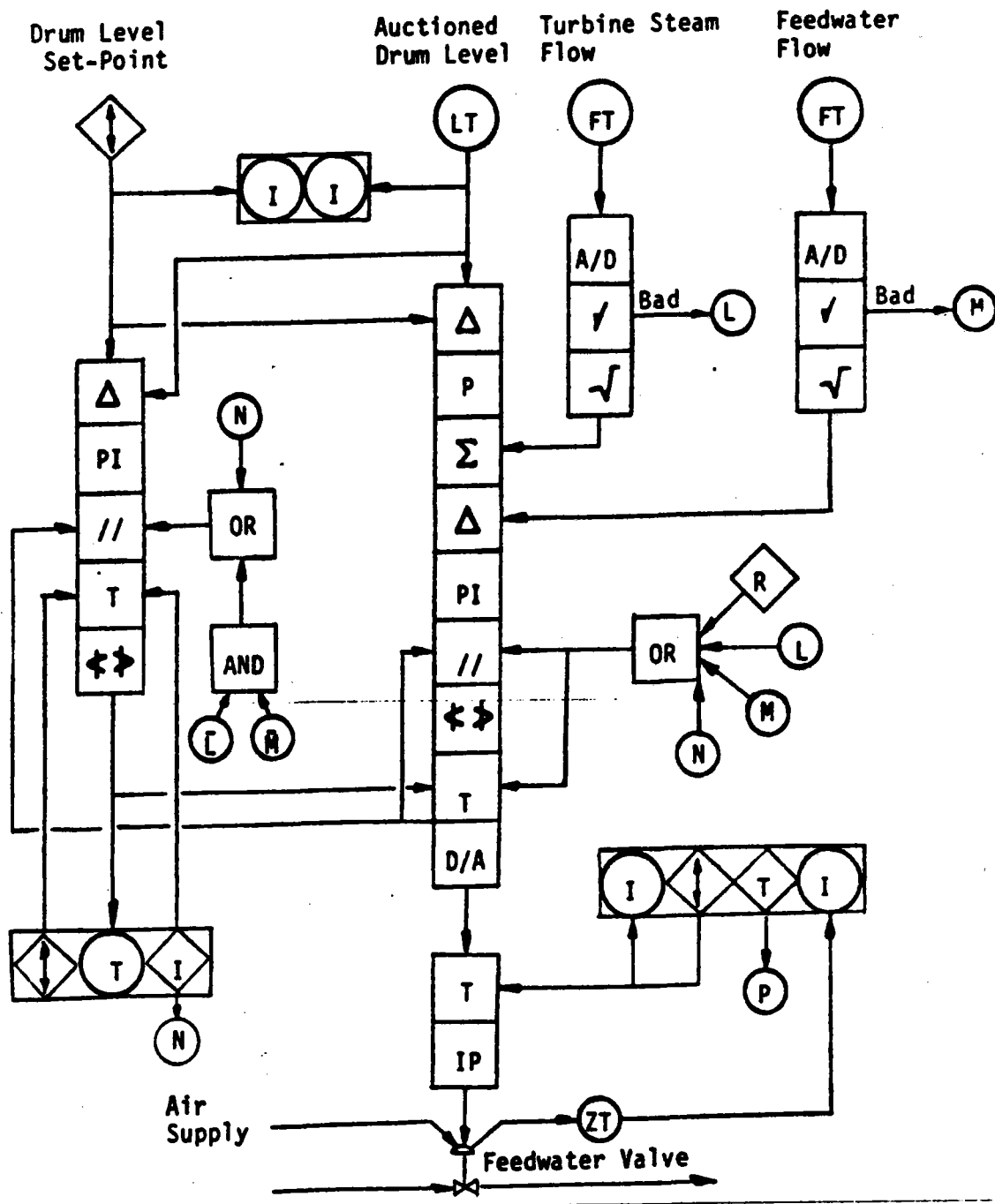


Figure 4-48 Control Functional Diagram-Feedwater Valve Control #02

CONTROL REQUIREMENTS

SYSTEM DESIGNATION: Steam Generation Figure 4-44

Table 4-17 Control Requirements for Steam Generation

FUNCTION	TYPE	CONTROL	PROCESS VARIABLES	CONTROL FUNC. DIAGRAM	REMARKS
Valve #01	i) Servo, and ii) Regulatory	Cascaded, using computed salt flow to control valve position.	i) Steam flow rate ii) Throttle pressure iii) Salt flow rate	Figure 4-45	This valve controls salt flow rate. It follows the steam flow (servo) and maintains throttle pressure (regulatory).
Valve #02	i) Servo, and/or ii) Regulatory	Cascaded, using computed feed-water flow to control valve position.	i) Steam flow rate ii) Drum level iii) Feedwater flow rate	Figure 4-47, 4-48	This valve controls feedwater flow to load follow the steam flow (servo) and maintain constant drum level (regulatory). At low loads, the control is regulatory only.
Valve #03	i) Servo, and/or ii) Regulatory	Cascaded, using computed feed-water flow to control valve position.	i) Steam flow rate ii) Deareator level iii) Feedwater flow rate	Similar to Figures 4-47, 4-48	This valve functions in a similar manner to #02.
Valve #04	i) Regulatory	Single loop, pressure feedback	i) Deareator Pressure	-	Maintains deareator pressure.

CONTROL REQUIREMENTS

SYSTEM DESIGNATION: Steam Generation Figure 4-44

Table 4-17 Control Requirements for Steam Generation (continued)

FUNCTION	TYPE	CONTROL	PROCESS VARIABLES	CONTROL FUNC. DIAGRAM	REMARKS
Valve #05	Regulatory	Adaptive Gain	i) Steam flow rate ii) Steem Temp.	Figure 4-45	This valve controls the temperature of the steam supplied to the turbine such that it never exceeds 427°C (800°F)
Valve #06	Regulatory	Adaptive Gain	i) Steam flow rate ii) Steem Temp.	-	This valve diverts part of the water supply to the desuperheater
Valves #07, 08	Regulatory	-	Condensate Hold-up drum level	-	These valves are controlled together.
Valve #09	Isolation	Remote Supervision			
Valve #10	Regatory	Single loop, flow feedback	Feed water flow rate		
Valve #11	Isolation	Remote Supervision			
Valve #12	Isolation	Remote Supervision			



CONTROL REQUIREMENTS

SYSTEM DESIGNATION: Steam Generation Table 4-14

Table 4-17 Control Requirements for Steam Generation (continued)

FUNCTION	TYPE	CONTROL	PROCESS VARIABLES	CONTROL FUNC. DIAGRAM	REMARKS
Valve #13	Regulatory	Single loop, flow feedback	Condensate Pump rate		
Valve #14, 15	Isolation	Remote Supervision			Used during start-up
Valve #16-18	Position	Remote Supervision			Used during start-up
Pump; RC1, RC2	-	On-Off	N/A	-	-
Pump; CP1 CP2	-	On-Off	N/A	-	-
Feedwater Pump, FWP	-	On-Off	N/A	-	-

123

INSTRUMENTATION REQUIREMENTS

SYSTEM DESIGNATION: Steam Generation Table 4-15

Table 4-18 Instrumentation Requirements for Steam Generation

NAME	TYPE	RANGE OF MEASUREMENT	ACCURACY	SAMPLE RATE	TRANSDUCER/CONDITION REQUIRED	SCS DISPL.	PRINT TABLE	ARCHIVE	REMARKS
Salt thro' #01	Flow				N/A			Yes	Input for Control
Salt thro' #01	Temp				Yes			Yes	
Feedwater, #02	Flow				N/A			Yes	Input for Control
Deareator	Level				No			Yes	Input for Control
Deareator	Flow				N/A			Yes	Input for Control
Deareator	Pressure				No			Yes	
Steam Drum	Level				N/A			Yes	Input for Control
Steam Drum	Pressure				No			Yes	
RC1	Flow				Yes			Yes	
RC1	Flow				Yes			Yes	
Aux. Boiler Oil	Flow				Yes			Yes	
Water to Evap.	Temp				Yes			Yes	

INSTRUMENTATION REQUIREMENTS

SYSTEM DESIGNATION: Steam Generation Table 4-15

Figure 4-18 Instrumentation Requirements for Steam Generation (continued)

NAME	TYPE	RANGE OF MEASUREMENT	ACCURACY	SAMPLE RATE	TRANSDUCER/CONDITION REQUIRED	SCS DISPL.	PRINT TABLE	ARCHIVE	REMARKS
Steam thru #10	Flow				Yes			Yes	
Salt to S/H	Temp				Yes			Yes	
Steam to S/H Attept	Temp Flow				Yes Yes			Yes Yes	
Throttle Valve (@1)	Press Temp				N/A Yes			Yes Yes	Input for Control
Feedwater Pump	Flow				N/A			Yes	Input for Control
Con. Pump CP1, CP2	Flow Flow				Yes Yes			Yes Yes	
Con. Hold-up Drum	Level				N/A			Yes	Input for Control
MED Steam Supply	Temp				N/A			Yes	Input for Control
Valves #1-8, 10,13, 16-18	Position				No			Yes	
Valves #9,11 12, 14,15	On-Off				No			Yes	

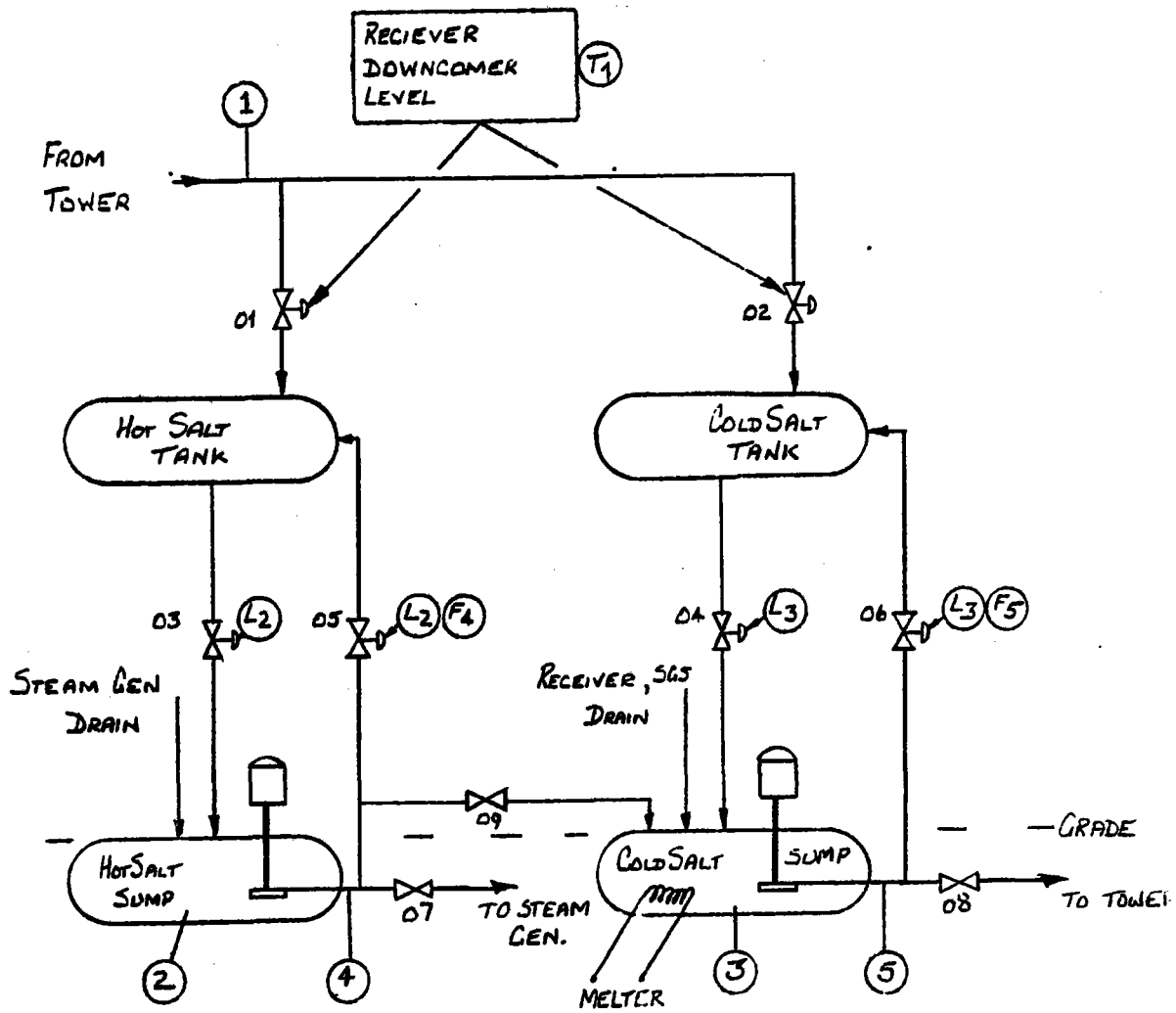


Figure 4-49 Thermal Storage

CONTROL REQUIREMENTS

SYSTEM DESIGNATION: Thermal Storage Figure 4-49

Table 4-19 Instrumentation Requirements for Thermal Storage

FUNCTION	TYPE	CONTROL	PROCESS VARIABLES	CONTROL FUNC. DIAGRAM	REMARKS
Valves #01 and #02	Position	Supervision and Regulation	i) Salt temperature from receiver ii) Downcomer Level	-	
Valve #03	Regulatory	Single PI loop	Hot salt sump level	-	Maintains salt level in sump.
Valve #04	Regulatory	Single PI loop	Cold salt sump level	-	Maintains salt level in sump.
Valve #05	Regulatory	Single PI loop	Salt flow through pump	-	Avoids overheating pump.
Valve #06	Regulatory	Single PI loop	Salt flow through pump	-	Avoids overheating pump.
Valve #07-09	Isolation	Supervisory			
Pumps (2 off)	-	On-Off	N/A	N/A	Hot and Cold Salt Sumps.

INSTRUMENTATION REQUIREMENTS

SYSTEM DESIGNATION: Thermal Storage Figure 4-49

Page 1 of 2

Figure 4-20 Instrumentation Requirements for Thermal Storage

NAME	TYPE	RANGE OF MEASUREMENT	ACCURACY	SAMPLE RATE	TRANSDUCER/ CONDITION. REQUIRED	SCS DISPL.	PRINT TABLE	ARCHIVE	REMARKS
Salt Outlet	Temp	200-800°F	+ 2°F	2 sec	LIN	Yes		2	
Heat Trace	Power			2 sec		Yes		Yes	
Hot Tank Shell (30 off)	Temp			2 sec	LIN	5		30	
Cold Tank Shell (30 off)	Temp			2 sec	LIN	5		30	
Salt Melter	On/Off					Yes		Yes	
Hot Sump Tank	Level					Yes		Yes	
Cold Sump Tank	Level					Yes		Yes	
Hot Tank Shut-Off Valve, #07	Position					Yes		Yes	
Cold Tank Shut-Off Valve, #08	Position					Yes		Yes	

INSTRUMENTATION REQUIREMENTS

SYSTEM DESIGNATION: Thermal Storage Figure 4-49

Table 4-20 Instrumentation Requirements for Thermal Storage (continued)

NAME	TYPE	RANGE OF MEASUREMENT	ACCURACY	SAMPLE RATE	TRANSDUCER/ CONDITION. REQUIRED	SCS DISPL.	PRINT TABLE	ARCHIVE	REMARKS
Hot Salt Diversion Valve, #09	On/Off Position								
Salt Diversion Valves, #05, 06	Position								
Hot Storage	Level					Yes		Yes	
Cold Storage	Level					Yes		Yes	

Individual control panels are provided in the control room for controlling the RO and MED subsystems.

The data acquisition requirements are listed in Tables 4-21 through 4-24 for the MED, RO, EPGS and balance of plant, respectively.

#### 4.11.5 Baseline MCS

The baseline MCS is the Foxboro system shown in Figure 4-50. The MCS requirements will be defined in greater detail in Phase II, and a final selection of the MCS hardware will be made.

In the system shown in Figure 4-50, the automatic control functions are implemented in the Unit Control Modules (UCM). The UCM includes the I/O equipment for the automatic control loops, dual redundant microprocessor based controllers and dual power supplies.

The Universal Field Multiplexer (UFM) provides the input capability for all of the data measurements that are not used in the automatic control loops.

The two color operator consoles and Videospec Processor provide the operator workstation. This workstation provides four levels of displays, alarm logging, data storage and a function keyboard for operator commands to the controlled subsystems.

The Fox 3 computer and Fox 3 graphics provide the capability for color graphic displays and additional display, sequential control and interlock logic functions.

The whole system is interconnected by a primary and redundant communications link such that full system operation is possible even if one communication link fails.

Manual control stations (not shown explicitly on Figure 4-50) provide the operator with the capability for direct control of critical valves, overriding the digital control system.

The CRT displays are constructed to provide the operator with overviews which focus his attention onto any control which is moving out of bounds. Dedicated buttons are provided which will enable him to immediately zero-in on any process, over which he can assume control and operate manually as required. The two operator control stations provide the means to startup and close down the plant. This can be achieved using software resident in the MCS to prompt the operator during either procedure and for the trip sequences.

#### 4.11.6 Other Candidate MCS Configurations

Taylor Instrument Company proposed a system that uses dual control minicomputers to perform all of the automatic control, sequencing, interlock logic and data acquisition functions.



INSTRUMENTATION REQUIREMENTS

SYSTEM DESIGNATION: MED

Table 4-21 Instrumentation Requirements for MED

NAME	TYPE	RANGE OF MEASUREMENT	ACCURACY	SAMPLE RATE	TRANSDUCER/ CONDITION REQUIRED	SCS DISPL.	PRINT TABLE	ARCHIVE	REMARKS
Raw Seawater	Pressure				No				
Raw Seawater	Flow				Yes				
Product Water	Flow				Yes				
Steam Feed	Pressure				No				
Distilled Water	Cond.				No				
Condensed Water	Cond.				No				
Raw Seawater	Temp.				Yes				
Product water	Pressure				Yes				
Produce Storage Tank	Level				No				
Steam Feed	Temp.				Yes				
Ejector Steam	Flow				Yes				
Steam Feed Condensate	Level				No				
Contingency (4 Off)					-				
Contingency (3 Off)	Temp				Yes				

131

INSTRUMENTATION REQUIREMENTS

SYSTEM DESIGNATION: RO

Table 4-22 Instrumentation Requirements for RO

NAME	TYPE	RANGE OF MEASUREMENT	ACCURACY	SAMPLE RATE	TRANSDUCER/ CONDITION REQUIRED	SCS DISPL.	PRINT TABLE	ARCHIVE	REMARKS
Raw Seawater	Flow				Yes				
Permeate	Flow				Yes				
Reject	Flow				Yes				
Feed	Press.				No				
Feed Chlorine Residual	4-20mA				Yes				
Permeate	Cond.				-				
Product Storage Tank	Level				No				
Contingency (2 Off)					-				
Contingency (2 Off)	Temp.				Yes				

INSTRUMENTATION REQUIREMENTS

SYSTEM DESIGNATION: EPGS

Table 4-23 Instrumentation Requirements for EPGS

NAME	TYPE	RANGE OF MEASUREMENT	ACCURACY	SAMPLE RATE	TRANSDUCER/ CONDITION REQUIRED	SCS DISPL.	PRINT TABLE	ARCHIVE	REMARKS
Gross Gener- ated	kW				No				
Gross Gener- ated	kW-hours				No				
Generator Winding (3 Off)	Temp.				Yes				
Generator Circuit Breaker Position	Contact				No				
Utility Cir- cuit Breaker Position	Contact				No				
Turbine Steam Inlet	Temp.				Yes				
Turbine Steam Inlet	Press.				No				
Turbine Steam Outlet	Temp.				Yes				

INSTRUMENTATION REQUIREMENTS

SYSTEM DESIGNATION: EPGS

Table 4-23 Instrumentation Requirements for EPGS (continued)

NAME	TYPE	RANGE OF MEASUREMENT	ACCURACY	SAMPLE RATE	TRANSDUCER/ CONDITION REQUIRED	SCS DISPL.	PRINT TABLE	ARCHIVE	REMARKS
Turbine Steam Outlet	Press.				No				
Turbine Steam	Flow				Yes				
Turbine Govenor Oil Supply	Press.				No				
Turbine Govenor Oil Supply	Temp.				Yes				
Turbine Casing Gland Seal	Press.				No				
Turbine Bearing Lube Oil	Press.				No				

INSTRUMENTATION REQUIREMENTS

SYSTEM DESIGNATION: EPGs

Table 4-23 Instrumentation Requirements for EPGs (continued)

NAME	TYPE	RANGE OF MEASUREMENT	ACCURACY	SAMPLE RATE	TRANSDUCER/ CONDITION REQUIRED	SCS DISPL.	PRINT TABLE	ARCHIVE	REMARKS
Turbine Bearing (3 Off)	Temp.				Yes				
Turbine Bearing Lube Oil Cooling Water	Temp.				Yes				
Turbine Vibration (2 Off)					No				
Feedwater PH					No				
Decerator	Level				No				
Feed Pump Discharge	Press.				No				
Steam to Deareator	Flow				Yes				

INSTRUMENTATION REQUIREMENTS

SYSTEM DESIGNATION: EPGs

Table 4-23 Instrumentation Requirements for EPGs (continued)

NAME	TYPE	RANGE OF MEASUREMENT	ACCURACY	SAMPLE RATE	TRANSDUCER/ CONDITION REQUIRED	SCS DISPL.	PRINT TABLE	ARCHIVE	REMARKS
Feedpump	Flow				Yes				
Condensate Pump	Flow				Yes				
Feedpump Motor	Temp.				Yes				
Desuperheater Condensate Pump Motor	Temp.				Yes				
Feedwater #1 Water Inlet	Temp.				Yes				
Feedwater Heater #1 Water Outlet	Temp.				Yes				
Desuperheater #1 Water Inlet	Temp.				Yes				

INSTRUMENTATION REQUIREMENTS

SYSTEM DESIGNATION: EPGS

Table 4-23 Instrumentation Requirements for EPGS (continued)

NAME	TYPE	RANGE OF MEASUREMENT	ACCURACY	SAMPLE RATE	TRANSDUCER/ CONDITION REQUIRED	SCS DISPL.	PRINT TABLE	ARCHIVE	REMARKS
Desuperheater #1 Steam Outlet	Temp.				Yes				
Feedwater Heater #1 Steam Inlet	Temp.				Yes				
Feedwater Heater #1 Drain Flow	Temp.				Yes				
Feedwater Heater #1 Drain	Flow				Yes				

INSTRUMENTATION REQUIREMENTS

SYSTEM DESIGNATION: BOP

Table 4-24 Instrumentation Requirements for BOP

138

NAME	TYPE	RANGE OF MEASUREMENT	ACCURACY	SAMPLE RATE	TRANSDUCER/ CONDITION REQUIRED	SCS DISPL.	PRINT TABLE	ARCHIVE	REMARKS
RO System Usage	kW				No				
MED System Usage	kW				No				
EPGS System Usage	kW				No				
Salt System Usage	kW				No				
Collector System Usage	kW				No				
Receiver System Usage	kW				No				
BOP Equipment Usage	kW				No				
RO System kW-hr Usage	Pulse				No				
MED System kW-hr Usage	Pulse				No				
EPGS System kW-hr Usage	Pulse				No				



INSTRUMENTATION REQUIREMENTS

SYSTEM DESIGNATION: BOP

Table 4-24 Instrumentation Requirements for BOP (continued)

NAME	TYPE	RANGE OF MEASUREMENT	ACCURACY	SAMPLE RATE	TRANSDUCER/ CONDITION REQUIRED	SCS DISPL.	PRINT TABLE	ARCHIVE	REMARKS
Salt System kW-hr Usage	Pulse				No				
Collector System kW-hr Usage	Pulse				No				
Receiver System kW-hr Usage	Pulse				No				
BOP System kW-hr Usage	Pulse				No				
Makeup Water	Flow				Yes				
Decerator	Press.				No				
Desuperheater #1	Flow				Yes				
Contingency (12 Off)	4-20 mA				No				
Contingency (2 Off)	Pulse				No				
Contingency (8 Off)	Temp.				Yes				
Contingency (8 Off)	Contact				No				
Contingency (2 Off)	RTD				No				

140

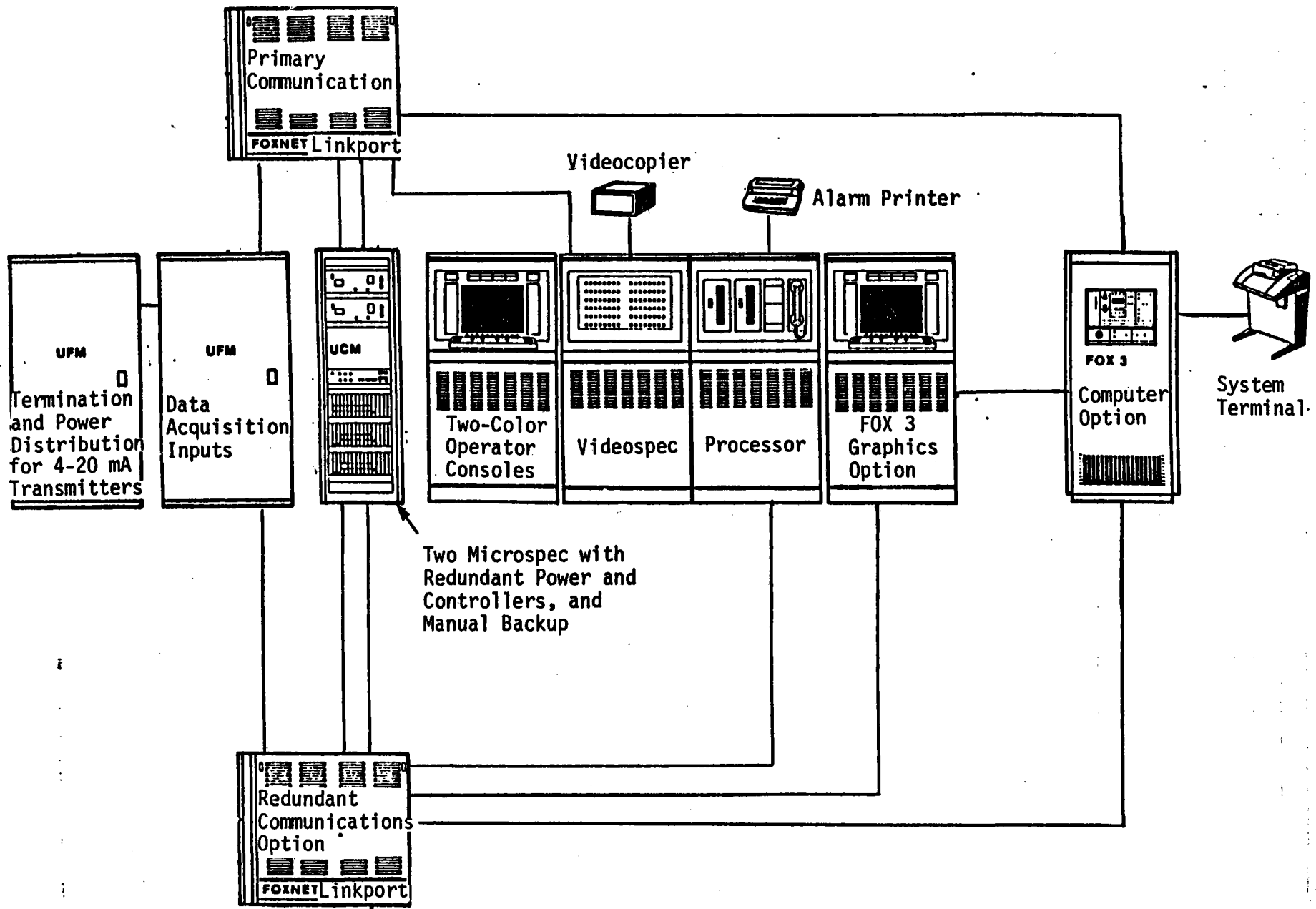


Figure 1V-50 Foxborough Spectrum Configuration

This system, as shown in Figure 4-51, consists of a dual MOD 3606 TMX-II system with a dual computer bus switch, a direct memory access (DMA) link and the associated computer peripherals and I/O equipment.

The two MOD 3606 computers each have 128K words of Error Checking and Correcting (ECC) semiconductor memory, an Automatic Bootstrap Load (ABL)/clock board, an I/O expansion chassis, a system typer, a dual floppy disk, and a 1.96M word fixed head drum. Two Priority Interrupt Modules are provided to give capability of 32 interrupts.

The computers are housed in a standard four bay computer cabinet which contains end bays for connections to remote termination cabinets. The computers are connected through a dual bus switch located in the center bay, allowing the second computer to automatically back up the first computer.

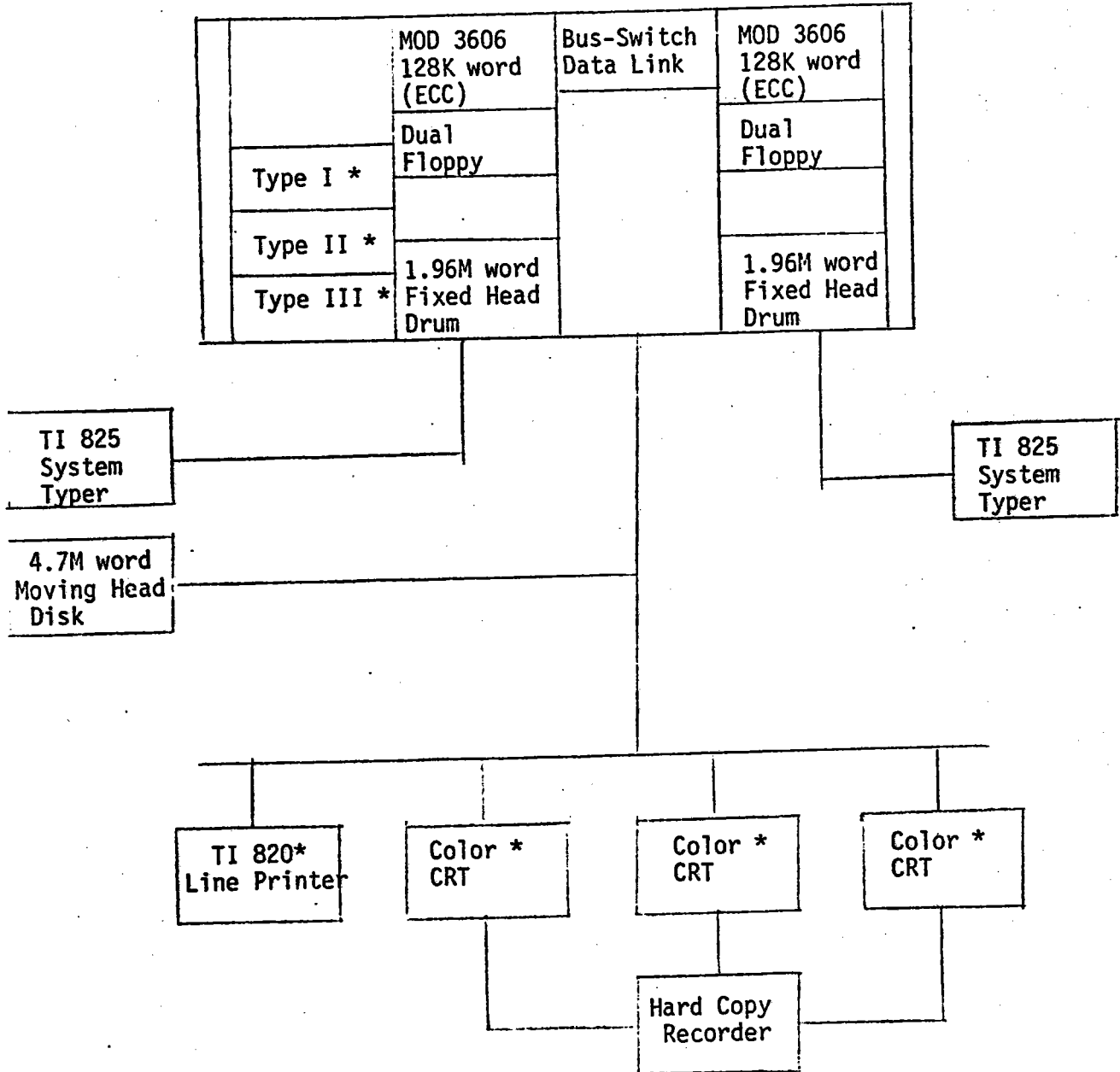
Downstream of the bus switch are a 4.7M word moving head disk, a line printer, three (3) color CRT's with hard copy capability, and input/output card files. In this way, the active computer, which is always connected to the process inputs/outputs, is accessible through the three (3) operator colorgraphic CRTs. The disk, which is located on the common bus, is available to both computer "A" and computer "B" for data storage. In addition, since each computer has its own system typer and the line printer is common, logs and reports will always be printed out for operator and management personnel.

To insure I/O subsystem integrity, system integrity modules are used to monitor the state-of-health of the I/O subsystem and to inform the processor when malfunctions in this subsystem occur.

Since the peripheral devices provide the interface between the human operator and the process control system, a failure of a peripheral can, in some cases, be nearly as critical as the failure of a central processing unit. For this reason, the system incorporates multiple operator interfaces devices. In many cases operator interface functions can take place at another terminal in the event of the malfunction of a given terminal.

Computer/manual stations are included in the system for all critical control functions and provide the capability for the operator to directly control valve position. This manual control overrides any command sent out by the digital control system.

In this system, all of the plant I/O and the color CRT terminals communicate with the minicomputers via a single data bus. A failure in this communication link would prevent commands from either the prime or backup computer from getting to the plant. A System Integrity Module is included in the system to monitor the integrity of the data bus and to provide failsafe commands to the I/O equipment in the event of loss of communications with the minicomputers. Nevertheless, this is a single-point failure that could shut down the entire plant; a dual redundant data bus appears to be a better technique.



\* Items downstream of Bus-switch

Figure 4-51 System Block Diagram

Bailey Controls Company proposed a configuration using their Network 90 system as illustrated in Figure 4-52. In this system, the Process Control Units (PCU's) include modules to perform the I/O, automatic control, sequencing and interlock logic functions. These modules all use microprocessors. The PCU's communicate with the operator consoles and with the minicomputers via dual redundant data buses. The operator consoles provide function keyboards and multiple levels of displays for operator control of the plant.

The minicomputer is a DEC PDP 11/24 and includes a magnetic tape unit; its function is to provide the data acquisition and archiving capability. The Network 90 system does not provide the capability for data storage except by adding the minicomputer; in the Foxboro system, on the other hand, data can be stored on a floppy disk.

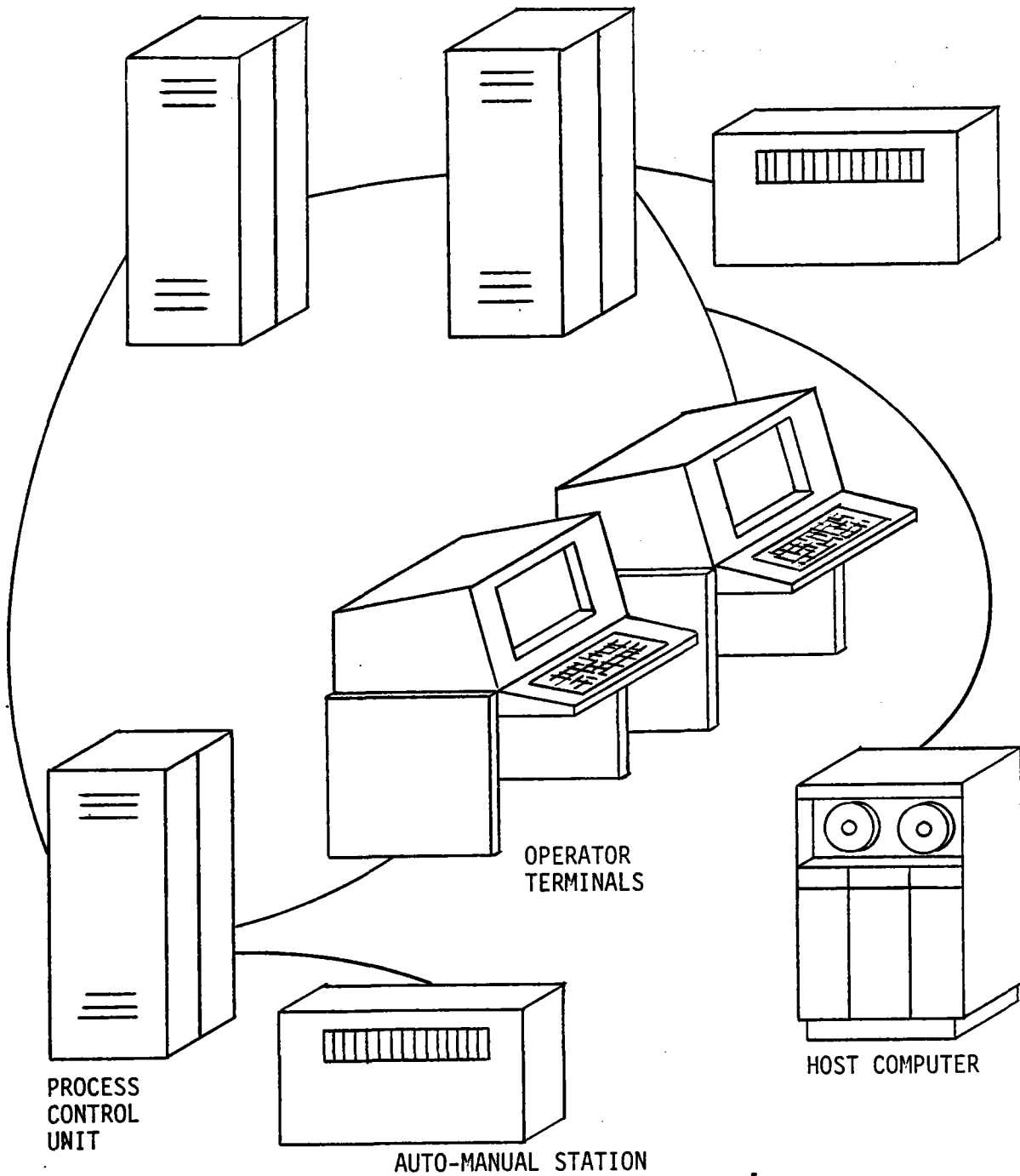
The Bailey system does not provide redundancy in the hardware that performs the automatic control and sequencing functions, as the two systems discussed previously do. In the Bailey system, several controller modules installed in the PCU's are used to perform the automatic control functions. In fact, one controller module can be used for each automatic control loop, so that the failure of a controller module would affect only that one control loop and not the whole plant. In the event of the failure of a controller module, the affected control valve would automatically be set to a predetermined fail-safe position. That control loop could then be controlled manually until the failed controller module could be replaced.

For the desalination plant, redundant controllers that perform more (or all) of the automatic control functions are probably preferable to nonredundant individual controllers.

#### 4.11.7 Electrical System

The electrical system design is based on supplying and distributing the electrical power to meet all system electrical demands during shutdown, start-up and different operating modes of the solar desalination plant. The voltage levels selected provide the most economic distribution and utilization of electrical energy, based on BVI engineering judgement.

The electrical system has two major categories of power supply: normal and uninterruptible. Normal power supply is for equipment whose power supply is not considered as critical; the interruption of normal power will not cause major plant disruption or loss of critical data. Uninterruptible power supply, on the other hand, is for loads such as the master control subsystem and data acquisition system computers, which are essential for the proper functioning of the plant equipment and which must remain in service under normal and/or abnormal operating conditions of the solar desalination plant. In addition, since the operation of the heliostats is considered as critical, the power for heliostats is fed from the uninterruptible power supply system. In the



**BAILEY NETWORK 90 CONFIGURATION**

*Figure 4-52 Bailey Network 90 Configuration*

event of overload or failure of the inverter, which is the source of the uninterruptible power, means will be provided to transfer the UPS load to the normal source with almost no time delay.

In addition to the two major categories described above, the electrical system design will include some minor but very important subsystems for the protection of the plant equipment and the safety of the operating personnel. These include lighting, grounding and lightning protection, cathodic protection, heat tracing, and communication.